Ph.D. DISSERTATION

AN ANALYTICAL MODEL FOR THE SCATTERING AND COUPLING OF ANTENNAS AND ITS APPLICATION TO WIRELESS ENERGY TRANSFER

안테나의 산란 및 결합 해석과
무선 에너지 전송에의 응용

BY

Yoon Goo Kim

AUGUST 2015

DEPARTMENT OF ELECTRICAL
AND COMPUTER ENGINEERING
COLLEGE OF ENGINEERING
SEOUL NATIONAL UNIVERSITY

Abstract

This dissertation proposes analytical models for scattering by an antenna and coupling among antennas. The scattering properties of an antenna are analyzed using the theory of characteristic modes. The current of an antenna terminated in a load is expanded into the characteristic currents of a short-circuited antenna. When an antenna is very small compared to the wavelength of the incident electromagnetic field, the antenna rarely scatters unless the load reactance is close to the negative of the input reactance, i.e., the antenna can be modeled as a minimum scattering antenna. When the current of an antenna and its input impedance are determined using only one characteristic mode, the open-circuited antenna rarely scatters the electromagnetic field, i.e., the antenna can be modeled as a canonical minimum scattering antenna.

The voltages and currents at the feed ports of coupled antennas can be calculated using impedance parameters. In this dissertation, three methods for calculating impedance parameters among coupled antennas are proposed. The first method is to use a generalized scattering matrix, the second is to use the current distributions of the antennas, and the third is to use the equivalent current that generates the same field as that generated by the antenna. A method is also proposed for calculating the electromagnetic fields generated by coupled antennas using a generalized scattering matrix when an electromagnetic field is incident on them or when sources are applied to their feed ports. These methods can be used both when the antennas are in free space and when they are near objects. If the

antennas are minimum scattering antennas, the calculations of the impedance parameters and electromagnetic field are simplified.

The models for scattering and coupling proposed in this dissertation are applied to the analysis of wireless energy transfer via the near field. Many antennas used in wireless energy transfer via the near field can be modeled as minimum scattering antennas because such wireless energy transfer generally operate at a frequency below or near the lowest resonant frequency of the antennas. In this dissertation, the maximum power transfer efficiency of a wireless energy transfer system and the load impedance that maximizes the power transfer efficiency are derived from the impedance parameters.

Keywords : Antenna coupling, Antenna scattering, Generalized scattering matrix, Theory of characteristic modes, Wireless energy transfer

Student Number : 2011 − 30221

Contents

List of Figures

List of Tables

Chapter 1

Introduction

1.1 Introduction

In antenna applications such as array antennas, near-field communication, and wireless energy transfer, multiple antennas are gathered in an electrically small area. In this case, the properties of the element antennas are different from those of an isolated antenna because the behavior of each element antenna is affected by the electromagnetic field scattered by the adjacent antennas. Therefore, in the investigation of such applications, the analysis of the mutual coupling among antennas is required.

It is important to determine the voltages and currents at the ports of coupled antennas and the electromagnetic fields generated by them. The relationship between the voltages and currents at the ports of coupled antennas can be described by impedance parameters, admittance parameters, or scattering parameters. One method to calculate these parameters and the electromagnetic fields is a full-wave simulation. Using a full-wave simulation, we

cannot understand factors that affect mutual coupling, so analytical methods are needed. In this dissertation, several analytical methods for mutual coupling among antennas are studied.

One analytical method for determining the impedance, admittance, and scattering parameters and electromagnetic fields is to use a generalized scattering matrix. In [1], scattering parameters between two antennas in free space were derived using a generalized scattering matrix and plane waves. In [2], scattering parameters between two antennas in free space were derived using a generalized scattering matrix and spherical waves. In [3], scattering parameters among multiple antennas in free space and electromagnetic fields generated by antennas were derived using a generalized scattering matrix and spherical waves. In [4], scattering parameters between two antennas in the presence of extraneous objects were derived using a generalized scattering matrix and spherical waves. In [5], impedance and admittance parameters between two antennas in free space were derived using a generalized scattering matrix and spherical waves when the characteristic impedances of the transmission lines are one. In the present dissertation, the impedance parameters, admittance parameters, and scattering parameters among multiple antennas are derived using a generalized scattering matrix and spherical waves. Additionally, electromagnetic fields generated by coupled antennas when an electromagnetic field is incident on them or sources are applied to their feed ports are derived using a generalized scattering matrix and spherical waves. The proposed method can be applied to antennas near objects as well as those in free space. Therefore, the method proposed in this dissertation is more general than those presented in [1]–[5].

One analytical method for determining impedance parameters is to use the current distribution of antennas [6]. Impedance parameters include self impedance[1] and mutual impedance. Self impedance is the same as the input impedance of an antenna when all other antennas are open-circuited. Therefore, the calculation of the self impedance is the same as the calculation of the input impedance of an antenna near objects. The method for calculating the mutual impedance presented in [6, Sec. 7.13] works well. However, the method for calculating the input impedance of an antenna presented in [6, Sec. 7.8] is valid only when the antennas are lossless, but not when they are lossy. This dissertation proposes a method for calculating the input impedance of an antenna near objects (or self impedance) using the current distribution. In addition, it proposes a method for calculating impedance parameters by simply using the equivalent current that generates the same field as that generated by an antenna.

If antennas are minimum scattering antennas, the determination of the impedance parameters among them is simplified (e.g., [7]). Many authors intuitively assume that antennas that are small compared with the wavelength of the incident field are minimum scattering antennas. The rigorous conditions under which an antenna becomes a minimum scattering antenna are not known. This dissertation identifies the conditions under which an antenna becomes a minimum scattering antenna. To do this, the scattering of antennas is analyzed using the theory of characteristic modes. The current of a loaded antenna illuminated by an electromagnetic field is expanded into the characteristic currents of a

[1] Some authors refer to the input impedance of an isolated antenna as self impedance. In this dissertation, self impedance refers to the input impedance of an antenna with all other antennas open-circuited.

short-circuited antenna. Using the current expressed in terms of the characteristic currents, the scattered power when an electromagnetic field is incident on an antenna is analyzed. In this way, the conditions under which it becomes a minimum scattering antenna are identified. The scattering model proposed in this dissertation can also be applied to the investigation of the scattering properties of antennas.

To calculate the impedance parameters, admittance parameters, and scattering parameters using a generalized scattering matrix, the determination of the values of the generalized scattering matrix is necessary. This dissertation proposes a method for determining the generalized scattering matrix using the theory of characteristic modes.

Wireless energy transfer is a technique through which electrical energy is transferred to a device that is not physically connected to a source. A wireless energy transfer system can be viewed as a coupled antenna system because energy is transferred from antenna to antenna through a coupling phenomenon. The models for the scattering and coupling presented in this dissertation are applied to the analysis of wireless energy transfer. One of the most important parameters in wireless energy transfer is the power transfer efficiency, which depends on the load impedance. This dissertation derives formulas for calculating the load impedance for which the power transfer efficiency is maximized and the maximum power transfer efficiency using impedance parameters.

This dissertation is organized as follows: In Chapter 2, the preliminary theory is provided. Spherical waves, power waves, and the generalized scattering matrix are introduced. Moreover, the theory of characteristic modes is explained. In Chapter 3, the transmitting and scattering properties of an antenna are analyzed from the perspective of

characteristic modes. Moreover, the author investigates under what conditions an antenna scatters large or small power. In addition, a formula for calculating the generalized scattering matrix of an antenna using characteristic modes is derived. In Chapter 4, three methods for determining the impedance parameters among antennas are proposed: the first uses a generalized scattering matrix and spherical waves, the second uses the current distribution of the antennas, and the third uses the equivalent current that generates the same field as that generated by the antenna. Moreover, formulas for calculating the admittance parameters among antennas and the electromagnetic fields generated by them are derived. In Chapter 5, a method for analyzing wireless energy transfer is presented. The author derives formulas for calculating the load impedance for which the power transfer efficiency of a wireless energy transfer system is maximized and the maximum power transfer efficiency for the system. The author also presents a method to increase the power transfer efficiency of a wireless energy transfer system.

1.2 Notation Used in This Dissertation

j is used to represent imaginary numbers, i.e., $j^2 = -1$. Scalars are denoted by non-bold letters, and vectors and matrices are denoted by bold letters. An asterisk * in a superscript denotes a complex conjugate. A superscript T denotes a transpose of a matrix. A dagger † in a superscript denotes the adjoint of an operator. Integrals are denoted by

$$\int_G f \, dv \tag{1.1}$$

where f is a function and G is a region in which f is defined. When f is defined only on a line, equation (1.1) is a path integral. When f is defined only on a surface, equation (1.1) is

an integral of a scalar function over a surface. When f is defined within a volume, equation (1.1) is a triple integral. If f is defined on a line, surface, and volume, equation (1.1) is the same as the sum of the path integral, integral of a scalar function over a surface, and triple integral. A surface integral is denoted by

$$\iint_A \mathbf{f} \cdot d\mathbf{s} \tag{1.2}$$

where $\mathbf{f}$ is a vector field and A is a surface on which $\mathbf{f}$ is defined. When a surface integral is evaluated over a closed surface, $\oiint$ is used instead of $\iint$ in equation (1.2). Throughout this dissertation, the time dependence $e^{j\omega t}$ is used. The absolute value of a phasor is the same as the peak value of the sinusoidal function of time.

Chapter 2

Generalized Scattering Matrix and Theory of Characteristic Modes

2.1 Generalized Scattering Matrix

2.1.1 Spherical Waves

Values of electric and magnetic fields satisfy Maxwell's equations. Solutions to Maxwell's equations include plane waves [1], [8, Ch.4], cylindrical waves [8, Ch.5], spherical waves [2], [8, Ch.6], and spheroidal waves [9]. In this dissertation, spherical waves are used.

A spherical wave is a solution to Maxwell's equations obtained by using a spherical coordinate system. Electric fields (**E**) and magnetic fields (**H**) in a source-free region can be expressed by a linear combination of spherical waves:

$$\mathbf{E}(\mathbf{r}) = \sum_{n=1}^{\infty} \sum_{m=-n}^{n} \sum_{s=1}^{2} Q_{s,m,n}^{(c)} \mathbf{E}_{s,m,n}^{(c)}(\mathbf{r}) \tag{2.1a}$$

$$\mathbf{H}(\mathbf{r}) = \sum_{n=1}^{\infty} \sum_{m=-n}^{n} \sum_{s=1}^{2} Q_{s,m,n}^{(c)} \mathbf{H}_{s,m,n}^{(c)}(\mathbf{r}) \tag{2.1b}$$

Here, $\mathbf{r}$ is the position of a field point and $Q_{s,m,n}^{(c)}$ is a coefficient. $\mathbf{E}_{s,m,n}^{(c)}$ and $\mathbf{H}_{s,m,n}^{(c)}$ are given by

$$\mathbf{E}_{s,m,n}^{(c)}(\mathbf{r}) = \begin{cases} k\sqrt{\eta}\mathbf{M}_{m,n}^{(c)} & \text{for } s=1 \\ k\sqrt{\eta}\mathbf{N}_{m,n}^{(c)} & \text{for } s=2 \end{cases} \tag{2.2a}$$

$$\mathbf{H}_{s,m,n}^{(c)}(\mathbf{r}) = \begin{cases} \dfrac{jk}{\sqrt{\eta}}\mathbf{N}_{m,n}^{(c)}(\mathbf{r}) & \text{for } s=1 \\ \dfrac{jk}{\sqrt{\eta}}\mathbf{M}_{m,n}^{(c)}(\mathbf{r}) & \text{for } s=2 \end{cases} \tag{2.2b}$$

where η is the intrinsic impedance and k is the wavenumber. The wave functions used in this dissertation are based on the wave functions used in [2]. $\mathbf{M}_{mn}^{(c)}$ and $\mathbf{N}_{mn}^{(c)}$ are given by the following:

$$\begin{aligned} \mathbf{M}_{mn}^{(c)}(\mathbf{r}) = & \left(-\frac{m}{|m|}\right)^{m} \sqrt{\frac{(2n+1)(n-|m|)!}{4\pi n(n+1)(n+|m|)!}} \cdot \\ & \left[\mathrm{z}_n^{(c)}(kr) \frac{jm\,\mathrm{P}_n^{|m|}(\cos\theta)}{\sin\theta} e^{jm\phi}\hat{\theta} \right. \\ & \left. - \mathrm{z}_n^{(c)}(kr) \frac{d\,\mathrm{P}_n^{|m|}(\cos\theta)}{d\theta} e^{jm\phi}\hat{\phi} \right] \end{aligned} \tag{2.3a}$$

$$\mathbf{N}_{mn}^{(c)}(\mathbf{r}) = \left(-\frac{m}{|m|}\right)^{m} \sqrt{\frac{(2n+1)(n-|m|)!}{4\pi n(n+1)(n+|m|)!}} \cdot \left[\frac{n(n+1)}{kr} \mathrm{z}_n^{(c)}(kr) \mathrm{P}_n^{|m|}(\cos\theta) e^{jm\phi} \hat{r} + \frac{1}{kr}\frac{d}{d(kr)}\left\{kr\,\mathrm{z}_n^{(c)}(kr)\right\} \frac{d\,\mathrm{P}_n^{|m|}(\cos\theta)}{d\theta} e^{jm\phi} \hat{\theta} + \frac{1}{kr}\frac{d}{d(kr)}\left\{kr\,\mathrm{z}_n^{(c)}(kr)\right\} \frac{jm\,\mathrm{P}_n^{|m|}(\cos\theta)}{\sin\theta} e^{jm\phi} \hat{\phi}\right] \quad (2.3b)$$

Here, [r, θ, ϕ] represents spherical coordinates, where r is the distance between a point and the origin, θ is an elevation angle, and ϕ is an azimuth angle; [$\hat{r}$, $\hat{\theta}$, $\hat{\phi}$] represents unit vectors for a spherical coordinate system. In equation (2.3), $(-m/|m|)^m$ is defined as 1 when m = 0. $\mathrm{P}_n^m(x)$ is the associated Legendre function; the sign of the associated Legendre function used in this dissertation is the same as that used in [8] and [10] but is different from that used in [2] and [11]. In $\mathrm{z}_n^{(c)}(kr)$, $\mathrm{z}_n^{(1)}$ denotes the spherical Bessel function, $\mathrm{z}_n^{(2)}$ denotes the spherical Neumann function, $\mathrm{z}_n^{(3)}$ denotes the spherical Hankel function of the first kind, and $\mathrm{z}_n^{(4)}$ denotes the spherical Hankel function of the second kind.

$\mathbf{E}_{s,m,n}^{(1)}$ and $\mathbf{H}_{s,m,n}^{(1)}$ are standing spherical waves. $\mathbf{E}_{s,m,n}^{(3)}$ and $\mathbf{H}_{s,m,n}^{(3)}$ are inward-propagating spherical waves (incoming spherical waves), and $\mathbf{E}_{s,m,n}^{(4)}$ and $\mathbf{H}_{s,m,n}^{(4)}$ are outward-propagating spherical waves (outgoing spherical waves) because the time dependence is $e^{j\omega t}$. The relationship between the standing spherical wave, inward-propagating spherical wave, and outward-propagating spherical wave is

$$\mathbf{E}_{s,m,n}^{(1)} = \frac{1}{2}\mathbf{E}_{s,m,n}^{(3)} + \frac{1}{2}\mathbf{E}_{s,m,n}^{(4)} \tag{2.4a}$$

$$\mathbf{H}_{s,m,n}^{(1)} = \frac{1}{2}\mathbf{H}_{s,m,n}^{(3)} + \frac{1}{2}\mathbf{H}_{s,m,n}^{(4)}. \tag{2.4b}$$

$\mathbf{E}_{s,m,n}^{(1)}$ and $\mathbf{H}_{s,m,n}^{(1)}$ are finite at the origin of a coordinate system, and $\mathbf{E}_{s,m,n}^{(3)}$, $\mathbf{H}_{s,m,n}^{(3)}$, $\mathbf{E}_{s,m,n}^{(4)}$ and $\mathbf{H}_{s,m,n}^{(4)}$ are infinite at the origin of a coordinate system. Therefore, a field that is finite at the origin of a coordinate system is expanded into standing spherical waves. A radiation field is expanded into outward-propagating spherical waves. Inward-propagating spherical waves do not physically exist, but they are needed for the mathematical representation of standing spherical waves.

s is the index to denote a mode type; $s = 1$ denotes the TE mode, and $s = 2$ denotes the TM mode. The ordering of spherical waves is arbitrary. In this dissertation, spherical waves are ordered as follows:

$$\mathrm{TE}_{-11},\ \mathrm{TE}_{01},\ \mathrm{TE}_{11},\ \mathrm{TM}_{-11},\ \mathrm{TM}_{01},\ \mathrm{TM}_{11},\ \mathrm{TE}_{-22},\ \mathrm{TE}_{-12},\ \mathrm{TE}_{02},\ \mathrm{TE}_{12},$$

$$\mathrm{TE}_{22},\ \mathrm{TM}_{-22},\ \mathrm{TM}_{-12},\ \mathrm{TM}_{02},\ \mathrm{TM}_{12},\ \mathrm{TM}_{22},\ \cdots,\ \mathrm{TE}_{mn},\ \cdots,\ \mathrm{TM}_{mn},\ \cdots$$

The *i*th spherical wave is the spherical wave with indices $\{s, m, n\}$ that satisfies the following equation:

$$i = (s-1)(2n+1) + (2n-1)(n+1) + m \tag{2.5}$$

In this dissertation, the single index *i* is sometimes used instead of indices $\{s, m, n\}$.

The total time-average power flowing through surface of a sphere centered at the origin of a coordinate system, P_r, can be calculated using the following equation:

$$P_r = \mathrm{Re}\left(\frac{1}{2} \oiint_{sphere} \mathbf{E}(\mathbf{r}) \times \mathbf{H}(\mathbf{r})^* \cdot d\mathbf{s} \right) = \frac{1}{2} \sum_{n=1}^{\infty} \sum_{m=-n}^{n} \sum_{s=1}^{2} \left(\left| Q_{s,m,n}^{(4)} \right|^2 - \left| Q_{s,m,n}^{(3)} \right|^2 \right) \tag{2.6}$$

If P_r is positive, the power leaves the sphere, and if P_r is negative, the power enters the sphere.

If all electric currents and magnetic currents exist inside a sphere with finite radius and there are no currents outside the sphere, the electromagnetic field outside the sphere is expanded into outward-propagating spherical waves (*i.e.*, c = 4 in equation (2.1)). In this case, the coefficients of the outward-propagating spherical waves can be determined using the current as follows [2, p. 333]:

$$Q_{s,m,n}^{(4)} = (-1)^{m+1} \int_G \left(\mathbf{E}_{s,-m,n}^{(1)} \cdot \mathbf{J} - \mathbf{H}_{s,-m,n}^{(1)} \cdot \mathbf{M} \right) dv \tag{2.7}$$

where **J** is the electric current density, **M** is the magnetic current density, and G is a region that contains all sources. If all electric and magnetic currents exist outside a sphere with finite radius and there are no currents inside the sphere, the electromagnetic field inside the sphere is expanded into standing spherical waves (*i.e.*, c =1 in equation (2.1)). In this case, the coefficients of the standing spherical waves can be determined using the current as follows [2, p. 334]:

$$Q_{s,m,n}^{(1)} = (-1)^{m+1} \int_G \left(\mathbf{E}_{s,-m,n}^{(4)} \cdot \mathbf{J} - \mathbf{H}_{s,-m,n}^{(4)} \cdot \mathbf{M} \right) dv \tag{2.8}$$

2.1.2 Power Waves

An electromagnetic field in a transmission line or waveguide can be expressed by the sum of the incident wave and reflected wave. There are several types of wave that express

electromagnetic fields in a transmission line or wave guide [12]. One convenient method is the use of a power wave.

Let *a* denote the coefficient of an incident power wave and *b* denote the coefficient of a reflected power wave. The coefficients of the incident and reflected power waves are, respectively, defined as [13], [14]

$$a = \frac{V + Z_R I}{2\sqrt{\mathrm{Re}(Z_R)}} \tag{2.9a}$$

$$b = \frac{V - Z_R^* I}{2\sqrt{\mathrm{Re}(Z_R)}} \tag{2.9b}$$

where V is the voltage at a reference plane and I is the current at a reference plane. Z_R is the reference impedance. The real part of the reference impedance should be positive. From equation (2.9), the voltage V and current I can be written as

$$V = \frac{(Z_R^* a + Z_R b)}{\sqrt{\mathrm{Re}(Z_R)}} \tag{2.10a}$$

$$I = \frac{a - b}{\sqrt{\mathrm{Re}(Z_R)}}\,. \tag{2.10b}$$

A reflection coefficient, Γ, is defined as the ratio of the coefficient of the reflected wave to the coefficient of the incident wave, and it can be calculated by [13], [14]

$$\Gamma = \frac{b}{a} = \frac{Z_i - Z_R^*}{Z_i + Z_R} \tag{2.11}$$

where Z_i is the impedance seen looking in the direction of the propagation of an incident wave at a reference plane. The time-average power that enters a reference plane, P_{in}, can be calculated by [13], [14]

$$P_{in} = \frac{1}{2}\mathrm{Re}\left(VI^*\right) = \frac{1}{2}|a|^2 - \frac{1}{2}|b|^2 . \tag{2.12}$$

If P_{in} is positive, power flows in the direction of the propagation of the incident wave, and if P_{in} is negative, power flows in the direction of the propagation of the reflected wave.

Power waves are convenient for the following reasons. First, an arbitrary reflection coefficient can be set by choosing an appropriate reference impedance. If a traveling wave is used and the input reactance at a reference plane is very large, the absolute value of the reflection coefficient is close to one, so that most of the power does not enter the reference plane. If a power wave is used, the reflection coefficient can be set to zero by setting the reference impedance to be the complex conjugate of the input impedance at a reference plane. Second, a power wave can be defined when there is no transmission line or waveguide. If a traveling wave is used, a characteristic impedance of a transmission line or waveguide is required. Third, the power that enters a reference plane can be calculated simply by using equation (2.12).

2.1.3 Generalized Scattering Matrix

The relation among the coefficients of waves at the feed ports of an antenna and the coefficients of the elements of basis for the vector space consisting of all electromagnetic fields in a source-free space can be expressed in matrix form:

$$\begin{bmatrix} \mathbf{w} \\ \mathbf{b} \end{bmatrix} = \left[\begin{array}{c|c} \boldsymbol{\Gamma} & \mathbf{R} \\ \hline \mathbf{T} & \mathbf{S} \end{array}\right] \begin{bmatrix} \mathbf{v} \\ \mathbf{a} \end{bmatrix} \tag{2.13}$$

where **v**, **w**, **a**, and **b** are column matrices[2]. In equation (2.13), the matrix composed of $\boldsymbol{\Gamma}$, **T**, **R**, and **S** is called the generalized scattering matrix.

The entries of **v** are the coefficients of incident waves at feed ports, and the entries of **w** are the coefficients of reflected waves at feed ports. In this dissertation, power waves are used. The generalized scattering matrix used in this dissertation is slightly different from the conventional generalized scattering matrix [2], in which **v** and **w** are the coefficients of traveling waves.

In equation (2.13), the entries of **a** are the coefficients of the elements of basis for the vector space consisting of all electromagnetic fields that propagate inward. The entries of **b** are the coefficients of the elements of basis for the vector space consisting of all electromagnetic fields that propagate outward. **a** and **b** are obtained from total field (i.e., the sum of the incident field and scattered field). There are several bases used in the generalized scattering matrix, including plane waves [1], cylindrical waves [15], spherical waves [2], and complex point source beams [16]. In this dissertation, spherical waves are used as a basis.

T, **R**, and **S** describe the transmitting, receiving, and scattering properties of an antenna, respectively. $\boldsymbol{\Gamma}$ represents the scattering parameters of a network whose ports are the feed ports of antennas. When the number of feed ports is one, $\boldsymbol{\Gamma}$ is a reflection coefficient. **T** is called a modal transmitting pattern, and **R** is called a modal receiving

[2] For some bases, the entries of **a**, **b**, **R**, **T**, and **S** are complex numbers. An example of this type of basis is a spherical wave. For some bases, the entries of **a** and **b** are functions, and the entries of **R**, **T**, and **S** are operators. Examples of this type of basis are plane waves and cylindrical waves. The entries of **v**, **w**, and $\boldsymbol{\Gamma}$ are typically complex numbers.

pattern [5], [7].

Modal receiving pattern **R** can be obtained from modal transmitting pattern **T**. For the case in which the spherical waves in (2.2) are used as a basis, **R** can be determined using the following equation [2, p. 36]:

$$R_{s,m,n} = (-1)^m T_{s,-m,n} \tag{2.14}$$

where $T_{s,m,n}$ and $R_{s,m,n}$ are the entries of **T** and **R**, respectively, and the subscript denotes the mode indices. That is, the ith entries of **T** and **R** are $T_{s,m,n}$ and $R_{s,m,n}$, with $\{s, m, n\}$ satisfying equation (2.5). In [2], (2.14) was derived for the case in which **v** and **w** are the coefficients of traveling waves and the feed waveguide is completely enclosed by a conductor except for a reference plane. Equation (2.14) is also valid when **v** and **w** are the coefficients of power waves[3] or when an antenna is excited at a gap.

[3] When the power wave is used, (v + w) in equation (2.81) in [2] is replaced by $(Z_R^* v + Z_R w)\big/\sqrt{Z_0 \,\mathrm{Re}(Z_R)}$, and (v – w) in equation (2.82) in [2] is replaced by $\sqrt{Z_0}\,(v - w)\big/\sqrt{\mathrm{Re}(Z_R)}$, where Z_0 is the real characteristic impedance of a feed waveguide and Z_R is the reference impedance. Then, the same result as that for the traveling wave is derived.

2.2 Theory of Characteristic Modes

Garbacz defined characteristic modes using a generalized scattering matrix [17]. Harrington redefined characteristic modes using an integral equation and showed that his characteristic modes were equivalent to those of Garbacz [18]. In this chapter, the author presents the theory of characteristic modes.

2.2.1 Characteristic Modes Based on a Generalized Scattering Matrix

When an object does not have a feed port, **v**, **w**, **Γ**, **R**, and **T** do not exist in the generalized-scattering-matrix equation (2.13), which becomes

$$\mathbf{b} = \mathbf{S}\mathbf{a}\,. \tag{2.15}$$

Although the number of spherical waves is infinite, we use a finite number of spherical waves. We use sufficiently large numbers of spherical waves so that an arbitrary electromagnetic field can be expanded into spherical waves. In this dissertation, the number of entries in **a** and **b** are the same; therefore, **S** is a square matrix. Garbarcz defined the characteristic modes as electromagnetic fields corresponding to the eigenvectors of **S** [17].

The coefficients of the *i*th outward-propagating spherical wave and the *i*th inward-propagating spherical wave (i = 1, 2, 3, ···) are the same when an incident field exists alone (i.e., when no obstacle is present). When an obstacle is present, there are no inward-propagating spherical waves in the scattered field. Therefore, the entries of **a** are the same as the coefficients of the outward-propagating spherical waves of the incident field. Therefore, **S** can be considered the matrix representation of a linear operator that

transforms an electromagnetic field that propagates outward. We denote this operator as *S*. That is, **S** is the matrix representation of *S*.

Throughout this dissertation, **S** is assumed to be diagonalizable. Further investigation is required to determine whether **S** of all types of antennas is diagonalizable. If **S** is diagonalizable, the set of all linearly independent eigenvectors of *S* is the basis of the vector space consisting of all outward-propagating fields. Therefore, arbitrary outward-propagating electromagnetic fields can be expressed as a linear combination of eigenvectors of *S*. An arbitrary incident field is the sum of outward-propagating spherical waves and inward-propagating spherical waves, and the coefficients of the outward-propagating spherical waves are the same as those of the inward-propagating spherical waves. Therefore, an arbitrary incident field can be calculated using eigenvectors of *S*.

In general, the current of an object cannot generate all of the eigenvectors of *S*. For example, consider a dipole antenna on the z-axis. Because the dipole antenna is symmetric about the z-axis, the current on the dipole antenna can only generate a field that is independent of the azimuth angle. Because arbitrary outward-propagating fields can be expanded into eigenvectors of *S*, the dipole antenna cannot generate all of the eigenvectors.

Let $\mathbf{E}_n^e$ and $\mathbf{H}_n^e$ be electric and magnetic fields, respectively, that correspond to the eigenvector of *S* that an object cannot generate. Let $\mathbf{E}_n^e$ and $\mathbf{H}_n^e$ be expanded as

$$\mathbf{E}_n^e(\mathbf{r}) = \sum_{i=1}^{J} B_i^n \mathbf{E}_i^{(4)}(\mathbf{r}) \tag{2.16a}$$

$$\mathbf{H}_n^e(\mathbf{r}) = \sum_{i=1}^{J} B_i^n \mathbf{H}_i^{(4)}(\mathbf{r}) \tag{2.16b}$$

where $\mathbf{E}_i^{(4)}$ and $\mathbf{H}_i^{(4)}$ are the electric and magnetic fields, respectively, that correspond to the *i*th outward-propagating spherical wave; $\mathbf{r}$ is the position of a field point; B_i^n is a coefficient; and J is the total number of spherical waves. Define $\tilde{\mathbf{E}}_n$ and $\tilde{\mathbf{H}}_n$ as

$$\tilde{\mathbf{E}}_n(\mathbf{r}) = \sum_{i=1}^{J} B_i^n \mathbf{E}_i^{(1)}(\mathbf{r}) \tag{2.17a}$$

$$\tilde{\mathbf{H}}_n(\mathbf{r}) = \sum_{i=1}^{J} B_i^n \mathbf{H}_i^{(1)}(\mathbf{r}) \tag{2.17b}$$

where $\mathbf{E}_i^{(1)}$ and $\mathbf{H}_i^{(1)}$ are the electric and magnetic fields, respectively, that correspond to the *i*th standing spherical wave and B_i^n is equal to the coefficient in (2.16).

If an object reacts to $\tilde{\mathbf{E}}_n$ and $\tilde{\mathbf{H}}_n$, the object should produce only $\mathbf{E}_n^e$ and $\mathbf{H}_n^e$ (with a coefficient) when only $\tilde{\mathbf{E}}_n$ and $\tilde{\mathbf{H}}_n$ are incident because $\mathbf{E}_n^e$ and $\mathbf{H}_n^e$ are an eigenvector of *S*. The object cannot generate $\mathbf{E}_n^e$ and $\mathbf{H}_n^e$. Therefore, the object does not interact with $\tilde{\mathbf{E}}_n$ and $\tilde{\mathbf{H}}_n$. The eigenvalue for the eigenvector $\mathbf{E}_n^e$ and $\mathbf{H}_n^e$ must be one because any other value would mean that the object produces $\mathbf{E}_n^e$ and $\mathbf{H}_n^e$.

2.2.2 Characteristic Modes Based on Integral Equations

In this section, materials are assumed to be linear and reciprocal. It is also assumed that all of the possible currents in an object radiate power. This assumption means that there are no non-radiating currents in an object.

A. Characteristic Modes for a Lossless Conductor

Consider a situation in which an electric field ($\mathbf{E}^i$) is incident on objects exclusively made of perfect electric conductors (PEC). The tangential component of the total electric field (incident electric field plus scattered electric field) on the surface of the PEC is zero. The electric current density ($\mathbf{J}$) on the PEC can be determined from the following integral equation:

$$\left[L\left(\mathbf{J}(\mathbf{r}')\right) + \mathbf{E}^i\left(\mathbf{r}'\right) \right]_{\tan} = \mathbf{0} \tag{2.18}$$

Here, $\mathbf{r}'$ is the position of a point in the current and the subscript "tan" denotes the tangential component to the surface of the conductors. $L(\mathbf{J})$ represents the electric field generated by the electric current density $\mathbf{J}$ (i.e., the scattered electric field). The linear transformation L is given by

$$L\left(\mathbf{J}(\mathbf{r}')\right) = -j\omega\mathbf{A}\left(\mathbf{J}(\mathbf{r}')\right) - \nabla\Phi\left(\mathbf{J}(\mathbf{r}')\right) \tag{2.19}$$

where

$$\mathbf{A}\left(\mathbf{J}(\mathbf{r}')\right) = \frac{\mu}{4\pi}\int_G \mathbf{J}(\mathbf{r}')\frac{e^{-jk|\mathbf{r}-\mathbf{r}'|}}{|\mathbf{r}-\mathbf{r}'|}dv' \tag{2.20}$$

$$\Phi\left(\mathbf{J}(\mathbf{r}')\right) = \frac{-1}{j4\pi\omega\varepsilon}\int_G \left(\nabla'\cdot\mathbf{J}(\mathbf{r}')\right)\frac{e^{-jk|\mathbf{r}-\mathbf{r}'|}}{|\mathbf{r}-\mathbf{r}'|}dv'. \tag{2.21}$$

Here, $\mathbf{r}$ denotes the position of a point in the space; ε, μ, and k denote the permittivity, permeability, and wavenumber, respectively; and G denotes the surface of the conductors. The superscript prime in ∇' and dv' indicates that the variables in $\mathbf{r}'$ are used for differentiation and integration. $L(\mathbf{J})$ in (2.19) represents the electric field at all points in the whole space. When solving integral equation (2.18), only $L(\mathbf{J})$ at $\mathbf{r}'$ is used. We define

the operator Z_P as

$$Z_P\left(\mathbf{J}(\mathbf{r}')\right)=\left[-L\left(\mathbf{J}(\mathbf{r}')\right)\right]_{\tan}. \tag{2.22}$$

The integral equation (2.18) is then written as

$$Z_P\left(\mathbf{J}(\mathbf{r}')\right)=\left[\mathbf{E}^i(\mathbf{r}')\right]_{\tan}. \tag{2.23}$$

We define $\langle\cdot,\cdot\rangle$ as

$$\langle\mathbf{A},\mathbf{B}\rangle=\int_G \mathbf{A}\cdot\mathbf{B}dv \tag{2.24}$$

where **A** and **B** are vectors, and G is the region in which **B** is defined. The inner product is defined as

$$\langle\mathbf{A},\mathbf{B}^*\rangle=\int_G \mathbf{A}\cdot\mathbf{B}^*dv \tag{2.25}$$

where the asterisk * denotes the complex conjugate.

The complex power (P_c) that a lossless conductor generates can be calculated using the following equation:

$$P_c=-\frac{1}{2}\int_G \mathbf{E}^r(\mathbf{r}')\cdot\mathbf{J}^*(\mathbf{r}')dv=\frac{1}{2}\left\langle Z_P\left(\mathbf{J}(\mathbf{r}')\right),\mathbf{J}^*(\mathbf{r}')\right\rangle \tag{2.26}$$

where $\mathbf{E}^r$ is the electric field generated by the current density **J**; i.e., $\mathbf{E}^r = L(\mathbf{J})$. The time-average power radiated or scattered by a conductor (P_r) can be calculated using the following equation:

$$P_r = \mathrm{Re}\left(\frac{1}{2}\left\langle Z_P\left(\mathbf{J}(\mathbf{r}')\right), \mathbf{J}^*(\mathbf{r}')\right\rangle\right) = \frac{1}{4}\left[\left\langle Z_P\left(\mathbf{J}\right), \mathbf{J}^*\right\rangle + \left(\left\langle Z_P\left(\mathbf{J}\right), \mathbf{J}^*\right\rangle\right)^*\right]$$
$$= \frac{1}{4}\left[\left\langle Z_P\left(\mathbf{J}\right), \mathbf{J}^*\right\rangle + \left\langle \mathbf{J}, \left(Z_P\left(\mathbf{J}\right)\right)^*\right\rangle\right] = \frac{1}{4}\left[\left\langle Z_P\left(\mathbf{J}\right), \mathbf{J}^*\right\rangle + \left\langle Z_P^\dagger\left(\mathbf{J}\right), \mathbf{J}^*\right\rangle\right] \tag{2.27}$$
$$= \frac{1}{4}\left\langle \left(Z_P\left(\mathbf{J}\right) + Z_P^\dagger\left(\mathbf{J}\right)\right), \mathbf{J}^*\right\rangle = \frac{1}{2}\left\langle R_P\left(\mathbf{J}\right), \mathbf{J}^*\right\rangle$$

Because it is assumed that all currents on the object radiate power, $\left\langle R_P\left(\mathbf{J}\right), \mathbf{J}^*\right\rangle > 0$ for all non-zero **J**.

Let R_P and X_P be the real and imaginary parts of Z_P, respectively; i.e.,

$$R_P = \frac{1}{2}\left(Z_P + Z_P^\dagger\right) \tag{2.28a}$$

$$X_P = \frac{1}{2j}\left(Z_P - Z_P^\dagger\right) \tag{2.28b}$$

where † denotes the adjoint of an operator. An eigenvalue equation that defines the characteristic modes is as follows:

$$X_P\left(\mathbf{J}_n(\mathbf{r}')\right) = \lambda_n R_P\left(\mathbf{J}_n(\mathbf{r}')\right) \tag{2.29}$$

Here, λ_n are the eigenvalues, and $\mathbf{J}_n$ are the eigenvectors. The eigenvectors $\mathbf{J}_n$ are called the characteristic currents [18]. An electromagnetic field generated by a characteristic current is called a characteristic field. In this dissertation, we call both a characteristic current and a characteristic field a characteristic mode.

The characteristic modes are ordered such that $|\lambda_1| \le |\lambda_2| \le |\lambda_3| \le \cdots$. If the shapes of two characteristic currents at different frequencies are similar, these two characteristic currents are considered to be the same mode. The order of the characteristic modes can be different at different frequencies.

The integral equation (2.29) can be transformed into a matrix equation using the method of moments. In the transformation, real functions are used as expansion functions, and the same functions are used as testing functions [19]. Let $\mathbf{R_P}$ and $\mathbf{X_P}$ be, respectively, the square matrices corresponding to R_P and X_P, and let $\boldsymbol{x}_n$ and $\boldsymbol{x}$ be, respectively, the column matrices containing the coordinates of $\mathbf{J}_n$ and $\mathbf{J}$ relative to the basis for the current. We then have the following matrix equation:

$$\mathbf{X_P}\boldsymbol{x}_n = \lambda_n \mathbf{R_P}\boldsymbol{x}_n \tag{2.30}$$

Here, $\mathbf{X_P}$ and $\mathbf{R_P}$ are real symmetric matrices. Because $\left\langle R_P\left(\mathbf{J}\right), \mathbf{J}^*\right\rangle > 0$ for all non-zero $\mathbf{J}$, $(\boldsymbol{x}^*)^T \mathbf{R_P}\boldsymbol{x} > 0$ for all non-zero $\boldsymbol{x}$ (where T denotes the transpose of a matrix). Therefore, $\mathbf{R_P}$ is a positive-definite matrix.

Because $\mathbf{X_P}$ and $\mathbf{R_P}$ are real symmetric matrices and $\mathbf{R_P}$ is a positive-definite matrix, the eigenvalues λ_n and the eigenvectors $\boldsymbol{x}_n$ in (2.30) have real values, and the $\boldsymbol{x}_n$ are orthogonal with respect to the inner product induced by $\mathbf{R_P}$ [20]. Therefore, the following equation is satisfied:

$$\boldsymbol{x}_n^T \mathbf{R_P}\boldsymbol{x}_m = (\boldsymbol{x}_n^*)^T \mathbf{R_P}\boldsymbol{x}_m = \delta_{mn} \tag{2.31}$$

where δ_{mn} is the Kronecker delta (0 if $m \neq n$ and 1 if $m = n$). In equation (2.31), the $\boldsymbol{x}_n$ are normalized such that (2.31) is satisfied. Because $\boldsymbol{x}_n^T \mathbf{R_P}\boldsymbol{x}_m = \left\langle R_P(\mathbf{J}_m), \mathbf{J}_n\right\rangle$ and $(\boldsymbol{x}^*)^T \mathbf{R_P}\boldsymbol{x} = \left\langle R_P\left(\mathbf{J}\right), \mathbf{J}^*\right\rangle$, $\mathbf{J}_n$ satisfy the following orthogonal relationships:

$$\left\langle R_P(\mathbf{J}_m), \mathbf{J}_n\right\rangle = \left\langle R_P(\mathbf{J}_m), \mathbf{J}_n^*\right\rangle = \delta_{mn} \tag{2.32a}$$

$$\left\langle X_P(\mathbf{J}_m), \mathbf{J}_n\right\rangle = \left\langle X_P(\mathbf{J}_m), \mathbf{J}_n^*\right\rangle = \lambda_n \delta_{mn} \tag{2.32b}$$

$$\left\langle Z_P(\mathbf{J}_m), \mathbf{J}_n \right\rangle = \left\langle Z_P(\mathbf{J}_m), \mathbf{J}_n^* \right\rangle = (1 + j\lambda_n)\delta_{mn} \tag{2.32c}$$

Equations (2.32b) and (3.32c) are obtained from (2.32a) and (2.29).

The total current **J** on a conductor can be derived using the orthogonal relationship (2.32c). **J** is represented by a linear combination of all of the characteristic currents as follows [18]:

$$\mathbf{J}(\mathbf{r}') = \sum_{n=1}^{\infty} \frac{V_n}{1 + j\lambda_n} \mathbf{J}_n(\mathbf{r}') \tag{2.33}$$

where V_n are the modal excitation coefficients and are determined by [18]

$$V_n = \left\langle \mathbf{E}^i, \mathbf{J}_n \right\rangle = \int_G \mathbf{E}^i(\mathbf{r}') \cdot \mathbf{J}_n(\mathbf{r}') dv \,. \tag{2.34}$$

B. Characteristic Modes for a Lossy Conductor

Consider a situation in which the electric field ($\mathbf{E}^i$) is incident on objects exclusively made of lossy conductors. The electric current density (**J**) on conductors is related to the total electric field on conductors by Ohm's law.

$$\mathbf{J}(\mathbf{r}') = \sigma \left[\mathbf{E}^i(\mathbf{r}') + \mathbf{E}^s(\mathbf{r}') \right]_{\tan} \tag{2.35}$$

where σ is the conductivity of a conductor and $\mathbf{E}^s$ is the scattered electric field. We define the operator Z_S as

$$Z_S\left(\mathbf{J}(\mathbf{r}')\right) = \frac{1}{\sigma} \mathbf{J}(\mathbf{r}') \,. \tag{2.36}$$

Let $Z_C = Z_P + Z_S$. Then, from equation (2.35), the following integral equation is obtained:

$$Z_C\left(\mathbf{J}(\mathbf{r}')\right) = \left[\mathbf{E}^i(\mathbf{r}') \right]_{\tan} \tag{2.37}$$

The time-average power dissipated by the conductors (P_d) can be calculated using the following equation:

$$P_d = \frac{1}{2}\mathrm{Re}\left(\int_G \left(\mathbf{E}^i + \mathbf{E}^s\right)\cdot \mathbf{J}^* dv\right) = \frac{1}{2}\mathrm{Re}\left(\left\langle Z_S\left(\mathbf{J}\right), \mathbf{J}^*\right\rangle\right) = \frac{1}{2}\left\langle R_S\left(\mathbf{J}\right), \mathbf{J}^*\right\rangle \tag{2.38}$$

where R_S is the real part of Z_S. The time-average radiated power plus the time-average dissipated power for the conductor can be calculated using the following equation:

$$P = \frac{1}{2}\left\langle R_P\left(\mathbf{J}\right), \mathbf{J}^*\right\rangle + \frac{1}{2}\left\langle R_S\left(\mathbf{J}\right), \mathbf{J}^*\right\rangle = \frac{1}{2}\left\langle R_C\left(\mathbf{J}\right), \mathbf{J}^*\right\rangle \tag{2.39}$$

where R_C is the real part of Z_C. Because it is assumed that all currents on the object radiate power, $\left\langle R_C\left(\mathbf{J}\right), \mathbf{J}^*\right\rangle > 0$ for all non-zero $\mathbf{J}$.

There are two types of eigenvalue equations that define the characteristic modes when the conductors are lossy. One eigenvalue equation is

$$\left(X_P - jZ_S\right)\left(\mathbf{J}_n(\mathbf{r}')\right) = \lambda_n R_P\left(\mathbf{J}_n(\mathbf{r}')\right). \tag{2.40}$$

The other eigenvalue equation is

$$X_C\left(\mathbf{J}'_n(\mathbf{r}')\right) = \lambda'_n R_C\left(\mathbf{J}'_n(\mathbf{r}')\right) \tag{2.41}$$

where R_C and X_C are the real and imaginary parts of Z_C, respectively; i.e.,

$$R_C = \frac{1}{2}\left(Z_C + Z_C^\dagger\right) \tag{2.42a}$$

$$X_C = \frac{1}{2j}\left(Z_C - Z_C^\dagger\right). \tag{2.42b}$$

Note that when conductors are lossless, the eigenvalue equations (2.40) and (2.41) become equation (2.29).

The integral equations (2.40) and (2.41) can be transformed into matrix equations using the method of moments. In this transformation, real functions are used as expansion functions, and the same functions are used as testing functions [19]. Let $\mathbf{R_C}$, $\mathbf{X_C}$ and $\mathbf{Z_S}$ be, respectively, the square matrices corresponding to R_C, X_C and Z_S, and let $\boldsymbol{x}_n$ and $\boldsymbol{x}_n'$ be, respectively, the column matrices containing the coordinates of $\mathbf{J}_n$ and $\mathbf{J}_n'$ relative to the basis for the currents. Then, we have the following matrix equations:

$$(\mathbf{X_P} - j\mathbf{Z_S})\boldsymbol{x}_n = \lambda_n \mathbf{R_P} \boldsymbol{x}_n \tag{2.43}$$

$$\mathbf{X_C} \boldsymbol{x}_n' = \lambda_n' \mathbf{R_C} \boldsymbol{x}_n' \tag{2.44}$$

Here, $\mathbf{R_C}$ and $\mathbf{X_C}$ are real symmetric matrices and $\mathbf{Z_S}$ is a complex symmetric matrix. Because $\left\langle R_C(\mathbf{J}), \mathbf{J}^* \right\rangle > 0$ for all non-zero $\mathbf{J}$, $(\boldsymbol{x}^*)^T \mathbf{R_C} \boldsymbol{x} > 0$ for all non-zero $\boldsymbol{x}$. Therefore, $\mathbf{R_C}$ is a positive-definite matrix.

Because $(\mathbf{X_P} - j\mathbf{Z_S})$ and $\mathbf{R_P}$ are symmetric matrices and $\mathbf{R_P}$ is a positive-definite matrix, the $\boldsymbol{x}_n$ in (2.43) satisfy the following equations [21]:

$$\boldsymbol{x}_n^T \mathbf{R_P} \boldsymbol{x}_m = \delta_{mn} \tag{2.45}$$

Here, the $\boldsymbol{x}_n$ are normalized such that (2.45) is satisfied. Because $\boldsymbol{x}_n^T \mathbf{R_P} \boldsymbol{x}_m = \left\langle R_P(\mathbf{J}_m), \mathbf{J}_n \right\rangle$, the $\mathbf{J}_n$ in (2.40) satisfy the following relationships:

$$\left\langle R_P(\mathbf{J}_m), \mathbf{J}_n \right\rangle = \delta_{mn} \tag{2.46a}$$

$$\left\langle (X_P - jZ_S)(\mathbf{J}_m), \mathbf{J}_n \right\rangle = \lambda_n \delta_{mn} \tag{2.46b}$$

$$\left\langle Z_C(\mathbf{J}_m), \mathbf{J}_n \right\rangle = (1 + j\lambda_n)\delta_{mn} \tag{2.46c}$$

Equations (2.46b) and (2.46c) are obtained from (2.46a) and (2.40). When the conductors

are lossy, ($\mathbf{X_P} - j\mathbf{Z_S}$) is not a Hermitian (self-adjoint) matrix. Therefore,

$$(\boldsymbol{x}_n^*)^T \mathbf{R_P} \boldsymbol{x}_m \neq \delta_{mn} \tag{2.47}$$

and, from (2.47),

$$\left\langle R_P(\mathbf{J}_m), \mathbf{J}_n^* \right\rangle \neq \delta_{mn} . \tag{2.48}$$

Because $\mathbf{X_C}$ and $\mathbf{R_C}$ are real symmetric matrices and $\mathbf{R_P}$ is a positive-definite matrix, the eigenvalues λ_n' and eigenvectors $\boldsymbol{x}_n'$ have real values, and the $\boldsymbol{x}_n'$ are orthogonal with respect to the inner product induced by $\mathbf{R_C}$ [20]. Therefore, the $\boldsymbol{x}_n'$ satisfy the following equation:

$$\boldsymbol{x}_n'^T \mathbf{R_C} \boldsymbol{x}_m' = (\boldsymbol{x}_n'^*)^T \mathbf{R_C} \boldsymbol{x}_m' = \delta_{mn} \tag{2.49}$$

Here, the $\boldsymbol{x}_n'$ are normalized such that (2.49) is satisfied. From (2.49), the $\mathbf{J}_n'$ satisfy the following orthogonal relationships.

$$\left\langle R_C(\mathbf{J}_m'), \mathbf{J}_n' \right\rangle = \left\langle R_C(\mathbf{J}_m'), \mathbf{J}_n'^* \right\rangle = \delta_{mn} \tag{2.50a}$$

$$\left\langle X_C(\mathbf{J}_m'), \mathbf{J}_n' \right\rangle = \left\langle X_C(\mathbf{J}_m'), \mathbf{J}_n'^* \right\rangle = \lambda_n \delta_{mn} \tag{2.50b}$$

$$\left\langle Z_C(\mathbf{J}_m'), \mathbf{J}_n' \right\rangle = \left\langle Z_C(\mathbf{J}_m'), \mathbf{J}_n'^* \right\rangle = (1 + j\lambda_n)\delta_{mn} \tag{2.50c}$$

Equations (2.50b) and (2.50c) are obtained from (2.50a) and (2.41).

The total current **J** on a conductor can be derived from equations (2.46c) and (2.50c). **J** is represented by a linear combination of all characteristic currents as follows:

$$\mathbf{J}(\mathbf{r}') = \sum_{n=1}^{\infty} \frac{V_n}{1 + j\lambda_n} \mathbf{J}_n(\mathbf{r}') = \sum_{n=1}^{\infty} \frac{V_n'}{1 + j\lambda_n'} \mathbf{J}_n'(\mathbf{r}') \tag{2.51}$$

where V_n and V_n' are determined by

$$V_n = \left\langle \mathbf{E}^i, \mathbf{J}_n \right\rangle = \int_G \mathbf{E}^i(\mathbf{r}') \cdot \mathbf{J}_n(\mathbf{r}') dv \tag{2.52a}$$

$$V_n' = \left\langle \mathbf{E}^i, \mathbf{J}_n' \right\rangle = \int_G \mathbf{E}^i(\mathbf{r}') \cdot \mathbf{J}_n'(\mathbf{r}') dv \,. \tag{2.52b}$$

C. Characteristic Modes for an Object Made of Conductors and Dielectrics

Consider a situation in which an electric field ($\mathbf{E}^i$) is incident on an object exclusively made of dielectrics. The equivalent electric current density (polarization current density) in dielectrics is

$$\mathbf{J}(\mathbf{r}') = \left(\sigma + j\omega(\varepsilon - \varepsilon_0)\right)\left(\mathbf{E}^i(\mathbf{r}') + \mathbf{E}^s(\mathbf{r}')\right) \tag{2.53}$$

where ω is the angular frequency, σ is the conductivity, and ε and ε_0 are the permittivities of the dielectric and of free space, respectively. We define the operator Z_M as

$$Z_M\left(\mathbf{J}(\mathbf{r}')\right) = \frac{1}{\sigma + j\omega(\varepsilon - \varepsilon_0)} \mathbf{J}(\mathbf{r}') \,. \tag{2.54}$$

Let $Z_D = -L + Z_M$. Then, from equation (2.53), the following integral equation is obtained:

$$Z_D\left(\mathbf{J}(\mathbf{r}')\right) = \mathbf{E}^i(\mathbf{r}') \tag{2.55}$$

Consider a situation where an electric field ($\mathbf{E}^i$) is incident on an object consisting of both conductors and dielectrics. On the surface of the conductors, equation (2.35) should be satisfied, and in the dielectrics, equation (2.54) should be satisfied. Therefore, the following integral equation should be satisfied:

$$Z\left(\mathbf{J}(\mathbf{r}')\right) = \left[\mathbf{E}^i(\mathbf{r}')\right]_{\tan \text{ or all}} \tag{2.56}$$

where

$$Z = Z_V + Z_M \tag{2.57}$$

Here, Z_V is defined to be

$$Z_V(\mathbf{J}) = \left[-L(\mathbf{J})\right]_{\tan \text{ or all}}. \tag{2.58}$$

The subscript "tan or all" means that the tangential component is used on the surface of the conductors and all the components are used in the dielectrics. If an object is exclusively made of conductors, Z is the same as Z_C, and if an object is exclusively made of dielectrics, Z is the same as Z_D.

The time-average power radiated or scattered by an object (P_r) can be calculated using the following equation:

$$\begin{aligned} P_r &= -\frac{1}{2}\mathrm{Re}\left(\int_G \mathbf{E}^r(\mathbf{r}')\cdot\mathbf{J}^*(\mathbf{r}')dv\right) = \frac{1}{2}\mathrm{Re}\left(\left\langle Z_V\left(\mathbf{J}(\mathbf{r}')\right),\mathbf{J}^*(\mathbf{r}')\right\rangle\right) \\ &= \frac{1}{2}\left\langle R_V\left(\mathbf{J}(\mathbf{r}')\right),\mathbf{J}^*(\mathbf{r}')\right\rangle \end{aligned} \tag{2.59}$$

where R_V is the real part of Z_V. Because it is assumed that all of the currents of the object radiate power, $\left\langle R_V(\mathbf{J}),\mathbf{J}^*\right\rangle > 0$ for all non-zero $\mathbf{J}$. The time-average power dissipated in an object (P_d) can be calculated using the following equation:

$$P_d = \frac{1}{2}\mathrm{Re}\left(\int_G\left(\mathbf{E}^i+\mathbf{E}^s\right)\cdot\mathbf{J}^*dv\right) = \frac{1}{2}\mathrm{Re}\left(\left\langle Z_M(\mathbf{J}),\mathbf{J}^*\right\rangle\right) = \frac{1}{2}\left\langle R_M(\mathbf{J}),\mathbf{J}^*\right\rangle \tag{2.60}$$

where R_M is the real part of Z_M. The time-average radiated power plus the time-average dissipated power can be calculated using the following equation:

$$\begin{aligned} P &= \frac{1}{2}\mathrm{Re}\left(\left\langle Z_V(\mathbf{J}),\mathbf{J}^*\right\rangle\right) + \frac{1}{2}\mathrm{Re}\left(\left\langle Z_M(\mathbf{J}),\mathbf{J}^*\right\rangle\right) \\ &= \frac{1}{2}\mathrm{Re}\left(\left\langle Z(\mathbf{J}),\mathbf{J}^*\right\rangle\right) = \frac{1}{2}\left\langle R(\mathbf{J}),\mathbf{J}^*\right\rangle \end{aligned} \tag{2.61}$$

where R is the real part of Z.

There are two types of eigenvalue equations that define the characteristic modes [22]. One eigenvalue equation is

$$\left(X_V - jZ_M\right)\left(\mathbf{J}_n(\mathbf{r}')\right) = \lambda_n R_V\left(\mathbf{J}_n(\mathbf{r}')\right). \tag{2.62}$$

where R_V and X_V are the real and imaginary parts of Z_V, respectively; i.e.,

$$R_V = \frac{1}{2}\left(Z_V + Z_V^{\dagger}\right) \tag{2.63a}$$

$$X_V = \frac{1}{2j}\left(Z_V - Z_V^{\dagger}\right). \tag{2.63b}$$

The other eigenvalue equation is

$$X\left(\mathbf{J}_n'(\mathbf{r}')\right) = \lambda_n' R\left(\mathbf{J}_n'(\mathbf{r}')\right) \tag{2.64}$$

where R and X are the real and imaginary parts of Z, respectively; i.e.,

$$R = \frac{1}{2}\left(Z + Z^{\dagger}\right) \tag{2.65a}$$

$$X = \frac{1}{2j}\left(Z - Z^{\dagger}\right). \tag{2.65b}$$

Note that when an object is lossless, eigenvalue equations (2.62) and (2.64) are the same.

The integral equations (2.62) and (2.64) can be transformed into matrix equations using the method of moments. In the transformation, real functions are used as expansion functions, and the same functions are used as testing functions [19]. Let $\mathbf{R_V}$, $\mathbf{X_V}$, $\mathbf{Z_M}$, $\mathbf{R}$, and $\mathbf{X}$ be the square matrices corresponding to R_V, X_V, Z_M, R, and X, respectively. We then have the following matrix equations:

$$(\mathbf{X_V} - j\mathbf{Z_M})\boldsymbol{x}_n = \lambda_n \mathbf{R_V}\boldsymbol{x}_n \tag{2.66}$$

$$\mathbf{X}\boldsymbol{x}'_n = \lambda'_n \mathbf{R}\boldsymbol{x}'_n \tag{2.67}$$

Here, $\mathbf{R_V}$, $\mathbf{X_V}$, $\mathbf{R}$, and $\mathbf{X}$ are real symmetric matrices, and $\mathbf{Z_M}$ is a complex symmetric matrix. Because $\left\langle R_V(\mathbf{J}), \mathbf{J}^* \right\rangle > 0$ and $\left\langle R(\mathbf{J}), \mathbf{J}^* \right\rangle > 0$ for all non-zero $\mathbf{J}$, $\mathbf{R_V}$ and $\mathbf{R}$ are positive-definite matrices.

Because ($\mathbf{X_V} - j\mathbf{Z_M}$) and $\mathbf{R_V}$ are symmetric matrices and $\mathbf{R_V}$ is a positive-definite matrix, the $\boldsymbol{x}_n$ in (2.66) satisfy the following equation [21]:

$$\boldsymbol{x}_n^T \mathbf{R_V} \boldsymbol{x}_m = \delta_{mn} \tag{2.68}$$

Here, the $\boldsymbol{x}_n$ are normalized such that (2.68) is satisfied. Because $\boldsymbol{x}_n^T \mathbf{R_V} \boldsymbol{x}_m = \left\langle R_V(\mathbf{J}_m), \mathbf{J}_n \right\rangle$, the $\mathbf{J}_n$ in (2.62) satisfy the following relationships:

$$\left\langle R_V(\mathbf{J}_m), \mathbf{J}_n \right\rangle = \delta_{mn} \tag{2.69a}$$

$$\left\langle (X_V - jZ_M)(\mathbf{J}_m), \mathbf{J}_n \right\rangle = \lambda_n \delta_{mn} \tag{2.69b}$$

$$\left\langle Z(\mathbf{J}_m), \mathbf{J}_n \right\rangle = (1 + j\lambda_n)\delta_{mn} \tag{2.69c}$$

Equations (2.69b) and (2.69c) are obtained from (2.69a) and (2.62). When the object is lossless, ($\mathbf{R_V} - j\mathbf{Z_M}$) is a real symmetric matrix. In this case, all of the eigenvalues λ_n and all of the eigenvectors $\boldsymbol{x}_n$ in (2.66) have real values, and the $\boldsymbol{x}_n$ are orthogonal with respect to the inner product induced by $\mathbf{R_v}$ [20]. Therefore, the $\boldsymbol{x}_n$ in (2.66) satisfy the following equation:

$$(\boldsymbol{x}_n^*)^T \mathbf{R_V} \boldsymbol{x}_m = \delta_{mn} \tag{2.70}$$

for a lossless object. From (2.70), the $\mathbf{J}_n$ in (2.62) satisfy the following orthogonal relationships when the object is lossless:

$$\left\langle R_V\left(\mathbf{J}_m\right), \mathbf{J}_n^*\right\rangle = \delta_{mn} \tag{2.71a}$$

$$\left\langle \left(X_V - jZ_M\right)\left(\mathbf{J}_m\right), \mathbf{J}_n^*\right\rangle = \lambda_n \delta_{mn} \tag{2.71b}$$

$$\left\langle Z\left(\mathbf{J}_m\right), \mathbf{J}_n^*\right\rangle = (1 + j\lambda_n)\delta_{mn} \tag{2.71c}$$

When the object is lossy, $(\mathbf{R_V} - j\mathbf{Z_M})$ is not a Hermitian (self-adjoint) matrix. Therefore,

$$(\boldsymbol{x}_n^*)^T \mathbf{R_V} \boldsymbol{x}_m \neq \delta_{mn} \tag{2.72}$$

and

$$\left\langle R_V\left(\mathbf{J}_m\right), \mathbf{J}_n^*\right\rangle \neq \delta_{mn}\,. \tag{2.73}$$

Because **X** and **R** are real symmetric matrices and **R** is a positive-definite matrix, the eigenvalues λ_n' and eigenvectors $\boldsymbol{x}_n'$ in (2.67) have real values, and the $\boldsymbol{x}_n'$ are orthogonal with respect to the inner product induced by **R** [20]. Therefore, the $\boldsymbol{x}_n'$ in (2.67) satisfy the following equation:

$$\boldsymbol{x}_n'^T \mathbf{R} \boldsymbol{x}_m' = (\boldsymbol{x}_n'^*)^T \mathbf{R} \boldsymbol{x}_m' = \delta_{mn} \tag{2.74}$$

where the $\boldsymbol{x}_n'$ are normalized such that this equation is satisfied. Hence, the $\mathbf{J}_n'$ in (2.64) satisfy the following orthogonal relationships:

$$\left\langle R(\mathbf{J}_m'), \mathbf{J}_n'\right\rangle = \left\langle R(\mathbf{J}_m'), \mathbf{J}_n'^*\right\rangle = \delta_{mn} \tag{2.75a}$$

$$\left\langle X(\mathbf{J}_m'), \mathbf{J}_n'\right\rangle = \left\langle X(\mathbf{J}_m'), \mathbf{J}_n'^*\right\rangle = \lambda_n' \delta_{mn} \tag{2.75b}$$

$$\left\langle Z(\mathbf{J}_m'), \mathbf{J}_n'\right\rangle = \left\langle Z(\mathbf{J}_m'), \mathbf{J}_n'^*\right\rangle = (1 + j\lambda_n')\delta_{mn} \tag{2.75c}$$

The total current **J** will now be derived. Assume that **J** is a linear combination of the characteristic currents:

$$\mathbf{J}(\mathbf{r}') = \sum_{n=1}^{\infty} \alpha_n \mathbf{J}_n(\mathbf{r}') \tag{2.76}$$

Substituting (2.76) into (2.56), and using the linearity of Z, we obtain

$$\sum_{n=1}^{\infty} \alpha_n Z\left(\mathbf{J}_n(\mathbf{r}')\right) = \left[\mathbf{E}^i(\mathbf{r}')\right]_{\tan \text{ or all}} . \tag{2.77}$$

Taking the inner products with $\mathbf{J}_m$ on the left- and right-hand sides of equation (2.77), we obtain

$$\sum_{n=1}^{\infty} \alpha_n \left\langle Z(\mathbf{J}_n), \mathbf{J}_m \right\rangle = \left\langle \mathbf{E}^i, \mathbf{J}_m \right\rangle . \tag{2.78}$$

From (2.69c), equation (2.78) reduces to

$$\alpha_n (1 + \lambda_n) = \left\langle \mathbf{E}^i, \mathbf{J}_n \right\rangle . \tag{2.79}$$

Let

$$V_n = \left\langle \mathbf{E}^i, \mathbf{J}_n \right\rangle = \int_G \mathbf{E}^i \cdot \mathbf{J}_n dv . \tag{2.80}$$

Then, the total current is represented by

$$\mathbf{J} = \sum_{n=1}^{\infty} \frac{V_n}{1 + j\lambda_n} \mathbf{J}_n . \tag{2.81}$$

Similarly, the total current $\mathbf{J}$ can be expressed in terms of the characteristic currents $\mathbf{J}'_n$

$$\mathbf{J} = \sum_{n=1}^{\infty} \frac{V'_n}{1 + j\lambda'_n} \mathbf{J}'_n \tag{2.82}$$

where

$$V'_n = \left\langle \mathbf{E}^i, \mathbf{J}'_n \right\rangle = \int_G \mathbf{E}^i \cdot \mathbf{J}'_n dv . \tag{2.83}$$

The time-average power radiated or scattered by a lossless object can be calculated

using the parameters for the characteristic mode defined in (2.62). This power (P_r) can be calculated using the following equation:

$$\begin{aligned} P_r &= \frac{1}{2}\left\langle R_V\left(\mathbf{J}\right), \mathbf{J}^*\right\rangle = \frac{1}{2}\left\langle R_V\left(\sum_{m=1}^{\infty}\alpha_m \mathbf{J}_m\right), \left(\sum_{m=1}^{\infty}\alpha_n \mathbf{J}_n\right)^*\right\rangle \\ &= \frac{1}{2}\sum_{n=1}^{\infty}\alpha_n^* \sum_{m=1}^{\infty}\alpha_m \left\langle R_V\left(\mathbf{J}_m\right), \mathbf{J}_n^*\right\rangle = \frac{1}{2}\sum_{n=1}^{\infty}\left|\alpha_n\right|^2 \end{aligned} \tag{2.84}$$

Theoretically, (2.84) is not exact when the materials are lossy because of (2.73). However, in Section 3.1.5, we present an example in which the power radiated by a lossy antenna is calculated using (2.84) with little error. The time-average radiated or scattered power plus the time-average dissipated power can be calculated using the parameters for the characteristic modes defined in (2.64). This power (P) can be calculated using the following equation:

$$P = \frac{1}{2}\left\langle R\left(\mathbf{J}\right), \mathbf{J}^*\right\rangle = \frac{1}{2}\sum_{n=1}^{\infty}\alpha_n'^* \sum_{m=1}^{\infty}\alpha_m' \left\langle R\left(\mathbf{J}_m'\right), \mathbf{J}_n'^*\right\rangle = \frac{1}{2}\sum_n |\,\alpha_n'\,|^2 \tag{2.85}$$

where $\alpha_n' = V_n'/(1+j\lambda_n')$.

D. Characteristic Modes for Magnetic Materials

Consider a situation in which a magnetic field ($\mathbf{H}^i$) is incident on an object exclusively made of magnetic materials. The magnetization current, **M**, in magnetic materials is

$$\mathbf{M}(\mathbf{r}') = j\omega(\mu-\mu_0)\left(\mathbf{H}^i(\mathbf{r}') + \mathbf{H}^s(\mathbf{r}')\right) \tag{2.86}$$

where μ and μ_0 are the permeabilities of the magnetic material and of free space, respectively. $\mathbf{H}^s$ is the magnetic field generated by the magnetization current **M** (i.e., the

scattered magnetic field). $\mathbf{H}^s$ can be calculated through the following linear transformation:

$$\mathbf{H}^s(\mathbf{r}) = -Y_V\left(\mathbf{M}(\mathbf{r}')\right) \tag{2.87}$$

where

$$Y_V\left(\mathbf{M}(\mathbf{r}')\right) = j\omega\mathbf{F}\left(\mathbf{M}(\mathbf{r}')\right) + \nabla\Psi\left(\mathbf{M}(\mathbf{r}')\right) \tag{2.88}$$

where

$$\mathbf{F}\left(\mathbf{M}(\mathbf{r}')\right) = \frac{\varepsilon}{4\pi}\int_G \mathbf{M}(\mathbf{r}')\frac{e^{jk|\mathbf{r}-\mathbf{r}'|}}{|\mathbf{r}-\mathbf{r}'|}dv' \tag{2.89}$$

$$\Psi\left(\mathbf{M}(\mathbf{r}')\right) = \frac{-1}{j4\pi\omega\mu}\int_G \left(\nabla'\cdot\mathbf{M}(\mathbf{r}')\right)\frac{e^{jk|\mathbf{r}-\mathbf{r}'|}}{|\mathbf{r}-\mathbf{r}'|}dv' \tag{2.90}$$

We define an operator Y_M as

$$Y_M\left(\mathbf{M}(\mathbf{r}')\right) = \frac{1}{j\omega(\mu-\mu_0)}\mathbf{M}(\mathbf{r}')\,. \tag{2.91}$$

Let $Y = Y_V + Y_M$. Then, from equation (2.86), the following integral equation is obtained:

$$Y\left(\mathbf{M}(\mathbf{r}')\right) = \mathbf{H}^i(\mathbf{r}') \tag{2.92}$$

There are two types of eigenvalue equations that define the characteristic modes. One eigenvalue equation is

$$\left(B_V - jY_M\right)\left(\mathbf{M}_n(\mathbf{r}')\right) = \lambda_n G_V\left(\mathbf{M}_n(\mathbf{r}')\right) \tag{2.93}$$

where G_V and B_V are the real and imaginary parts of Y_V, respectively; i.e.,

$$G_V = \frac{1}{2}\left(Y_V + Y_V^\dagger\right) \tag{2.94a}$$

$$B_V = \frac{1}{2j}\left(Y_V - Y_V^\dagger\right). \tag{2.94b}$$

The other eigenvalue equation is

$$B\left(\mathbf{M}_n(\mathbf{r}')\right) = \lambda_n G\left(\mathbf{M}_n(\mathbf{r}')\right) \tag{2.95}$$

where G and B are the real and imaginary parts of Y, respectively; i.e.,

$$G = \frac{1}{2}\left(Y + Y^{\dagger}\right) \tag{2.96a}$$

$$B = \frac{1}{2j}\left(Y - Y^{\dagger}\right). \tag{2.96b}$$

The eigenvector $\mathbf{M}_n$ is called the characteristic current, and the electromagnetic field generated by $\mathbf{M}_n$ is called the characteristic field.

The $\mathbf{M}_n$ in (2.93) satisfy the following relationship:

$$\left\langle G_V\left(\mathbf{M}_m\right), \mathbf{M}_n \right\rangle = \delta_{mn} \tag{2.97a}$$

$$\left\langle \left(B_V - jY_M\right)\left(\mathbf{M}_m\right), \mathbf{M}_n \right\rangle = \lambda_n \delta_{mn} \tag{2.97b}$$

$$\left\langle Y\left(\mathbf{M}_m\right), \mathbf{M}_n \right\rangle = (1 + j\lambda_n)\delta_{mn} \tag{2.97c}$$

where the $\mathbf{M}_n$ are normalized such that these equations are satisfied. The $\mathbf{M}_n$ in (2.95) satisfy the following orthogonal relationships:

$$\left\langle G(\mathbf{M}_m), \mathbf{M}_n \right\rangle = \left\langle G(\mathbf{M}_m), \mathbf{M}_n^* \right\rangle = \delta_{mn} \tag{2.98a}$$

$$\left\langle B(\mathbf{M}_m), \mathbf{M}_n \right\rangle = \left\langle B(\mathbf{M}_m), \mathbf{M}_n^* \right\rangle = \lambda_n \delta_{mn} \tag{2.98b}$$

$$\left\langle Y(\mathbf{M}_m), \mathbf{M}_n \right\rangle = \left\langle Y(\mathbf{M}_m), \mathbf{M}_n^* \right\rangle = (1 + j\lambda_n)\delta_{mn} \tag{2.98c}$$

where the $\mathbf{M}_n$ are normalized such that these equations are satisfied.

The total magnetization current $\mathbf{M}$ in the magnetic material can be derived from

equations (2.97c) and (2.98c). **M** is represented by a linear combination of all of the characteristic currents as follows:

$$\mathbf{M}(\mathbf{r}') = \sum_{n=1}^{\infty} \frac{V_n}{1+j\lambda_n} \mathbf{M}_n(\mathbf{r}') \tag{2.99}$$

where the V_n are determined by

$$V_n = \left\langle \mathbf{H}^i, \mathbf{M}_n \right\rangle = \int_G \mathbf{H}^i(\mathbf{r}') \cdot \mathbf{M}_n(\mathbf{r}') dv \tag{2.100}$$

Equations (2.99) and (2.100) are valid for the eigenvectors $\mathbf{M}_n$ in (2.93) and (2.95).

E. Characteristic Modes for Objects Both Dielectric and Magnetic

Consider a situation in which an electric field $\mathbf{E}^i$ and a magnetic field $\mathbf{H}^i$ are incident on an object composed of both dielectric and magnetic materials. The scattered electric field $\mathbf{E}^s$ and the scattered magnetic field $\mathbf{H}^s$ for an object can be calculated from the potential as follows:

$$\mathbf{E}^s(\mathbf{r}) = -j\omega\mathbf{A}\left(\mathbf{J}(\mathbf{r}')\right) - \nabla\Phi\left(\mathbf{J}(\mathbf{r}')\right) - \frac{1}{\varepsilon_0}\nabla\times\mathbf{F}\left(\mathbf{M}(\mathbf{r}')\right) \tag{2.101a}$$

$$\mathbf{H}^s(\mathbf{r}) = -j\omega\mathbf{F}\left(\mathbf{M}(\mathbf{r}')\right) - \nabla\Psi\left(\mathbf{M}(\mathbf{r}')\right) + \frac{1}{\mu_0}\nabla\times\mathbf{A}\left(\mathbf{J}(\mathbf{r}')\right) \tag{2.101b}$$

Here, **J** and **M** satisfy equations (2.53) and (2.86), respectively. From (2.53), (2.86) and (2.101), an integral equation to solve for the electric current density **J** and the magnetic current density **M** can be obtained as follows [22]:

$$\begin{bmatrix} Z_D & U \\ U & Y \end{bmatrix} \begin{bmatrix} \mathbf{J}(\mathbf{r}') \\ j\mathbf{M}(\mathbf{r}') \end{bmatrix} = \begin{bmatrix} \mathbf{E}^i(\mathbf{r}') \\ j\mathbf{H}^i(\mathbf{r}') \end{bmatrix} \tag{2.102}$$

where U is given by

$$U = \frac{-j}{\mu_0} \nabla \times \mathbf{A} = \frac{-j}{\varepsilon_0} \nabla \times \mathbf{F} \tag{2.103}$$

$jU(\mathbf{J})$ represents the magnetic field over the entire space that is generated by electric current **J**, and $-jU(\mathbf{M})$ represents electric field over the entire space generated by magnetic current **M**. When solving integral equation (2.102), $U(\mathbf{J})$ and $U(j\mathbf{M})$ only at $\mathbf{r}'$ are used. In equation (2.102), there are no points where ε is equal to ε_0 or μ is equal to μ_0. When the object is only made of dielectrics, U, Y, **M**, and $\mathbf{H}^i$ are eliminated, and when the object is only made of magnetic materials, U, Z_D, **J**, and $\mathbf{E}^i$ are eliminated in (2.102).

Define the operator T as

$$T = \begin{bmatrix} Z_D & U \\ U & Y \end{bmatrix}. \tag{2.104}$$

Define **f** as

$$\mathbf{f} = \begin{bmatrix} \mathbf{J}(\mathbf{r}') \\ j\mathbf{M}(\mathbf{r}') \end{bmatrix} \tag{2.105}$$

and define $\mathbf{g}^i$ as

$$\mathbf{g}^i = \begin{bmatrix} \mathbf{E}^i(\mathbf{r}') \\ j\mathbf{H}^i(\mathbf{r}') \end{bmatrix}. \tag{2.106}$$

Then, integral equation (2.102) is written as

$$T(\mathbf{f}) = \mathbf{g}^i. \tag{2.107}$$

Define the operators T_V and T_M as

$$T_V = \begin{bmatrix} -L & U \\ U & Y_V \end{bmatrix} \tag{2.108}$$

$$T_M = \begin{bmatrix} Z_M & T_0 \\ T_0 & Y_M \end{bmatrix} \tag{2.109}$$

where T_0 is the zero transformation (i.e., $T_0(\mathbf{J}) = 0$ for all $\mathbf{J}$). Then, $T = T_V + T_M$. Let T_R and T_I be the real and imaginary parts of T, respectively, and let T_V^R and T_V^I be the real and imaginary parts of T_V, respectively; i.e.,

$$T_R = \frac{1}{2}\left(T + T^\dagger\right) \tag{2.110a}$$

$$T_I = \frac{1}{2j}\left(T - T^\dagger\right) \tag{2.110b}$$

$$T_V^R = \frac{1}{2}\left(T_V + T_V^\dagger\right) \tag{2.111a}$$

$$T_V^I = \frac{1}{2j}\left(T_V - T_V^\dagger\right). \tag{2.111b}$$

Define vectors $\vec{\mathbf{A}}$ and $\vec{\mathbf{C}}$ to be

$$\vec{\mathbf{A}} = \begin{bmatrix} \mathbf{A} \\ j\mathbf{B} \end{bmatrix} \tag{2.112a}$$

$$\vec{\mathbf{C}} = \begin{bmatrix} \mathbf{C} \\ j\mathbf{D} \end{bmatrix} \tag{2.112b}$$

where **A**, **B**, **C**, and **D** are vectors. We define $\langle \cdot , \cdot \rangle$ to be

$$\left\langle \vec{\mathbf{A}}, \vec{\mathbf{C}} \right\rangle = \int_G \mathbf{A} \cdot \mathbf{C} - \mathbf{B} \cdot \mathbf{D} dv \tag{2.113}$$

where G is a region in which $\vec{\mathbf{C}}$ is defined. The inner product is defined as

$$\left\langle \vec{\mathbf{A}}, \vec{\mathbf{C}}^* \right\rangle = \int_G \mathbf{A} \cdot \mathbf{C}^* + \mathbf{B} \cdot \mathbf{D}^* dv. \tag{2.114}$$

When an antenna operates in transmitting mode (i.e., when there is no incident field and the input terminals of the antenna are excited), $\mathrm{Re}\left(\left\langle T_V(\mathbf{f}),\mathbf{f}^*\right\rangle\right)/2$ is equal to the time-average power radiated by an antenna and $\mathrm{Re}\left(\left\langle T(\mathbf{f}),\mathbf{f}^*\right\rangle\right)/2$ is equal to time-average power radiated by an antenna plus the time-average power dissipated in an antenna. $\mathrm{Im}\left(\left\langle T_V(\mathbf{f}),\mathbf{f}^*\right\rangle\right)/2$ and $\mathrm{Im}\left(\left\langle T(\mathbf{f}),\mathbf{f}^*\right\rangle\right)/2$ differ from the reactive power [22].

There are two types of eigenvalue equations that define the characteristic modes. One eigenvalue equation is

$$\left(T_V^I - jT_M\right)\left(\mathbf{f}_n\right) = \lambda_n T_V^R\left(\mathbf{f}_n\right). \tag{2.115}$$

The eigenvectors $\mathbf{f}_n$ are the characteristic currents and are written as

$$\mathbf{f}_n = \begin{bmatrix} \mathbf{J}_n \\ j\mathbf{M}_n \end{bmatrix}. \tag{2.116}$$

The $\mathbf{f}_n$ satisfy the following equations:

$$\left\langle T_V^R(\mathbf{f}_m),\mathbf{f}_n\right\rangle = \delta_{mn} \tag{2.117a}$$

$$\left\langle \left(T_V^I - jT_M\right)\left(\mathbf{f}_m\right),\mathbf{f}_n\right\rangle = \lambda_n\delta_{mn} \tag{2.117b}$$

$$\left\langle T(\mathbf{f}_m),\mathbf{f}_n\right\rangle = (1+j\lambda_n)\delta_{mn} \tag{2.117c}$$

When objects are lossy,

$$\left\langle T_V^R(\mathbf{f}_m),\mathbf{f}_n^*\right\rangle \neq \delta_{mn}. \tag{2.118}$$

The other eigenvalue equation is

$$T_I\left(\mathbf{f}_n'\right) = \lambda_n' T_R\left(\mathbf{f}_n'\right). \tag{2.119}$$

The eigenvectors $\mathbf{f}'_n$ are the characteristic currents and are written as

$$\mathbf{f}'_n = \begin{bmatrix} \mathbf{J}'_n \\ j\mathbf{M}'_n \end{bmatrix}. \tag{2.120}$$

The $\mathbf{f}'_n$ satisfy the following equation:

$$\left\langle T_R(\mathbf{f}'_m), \mathbf{f}'_n \right\rangle = \left\langle T_R(\mathbf{f}'_m), \mathbf{f}'^*_n \right\rangle = \delta_{mn} \tag{2.121a}$$

$$\left\langle T_I(\mathbf{f}'_m), \mathbf{f}'_n \right\rangle = \left\langle T_I(\mathbf{f}'_m), \mathbf{f}'^*_n \right\rangle = \lambda'_n \delta_{mn} \tag{2.121b}$$

$$\left\langle T(\mathbf{f}'_m), \mathbf{f}'_n \right\rangle = \left\langle T(\mathbf{f}'_m), \mathbf{f}'^*_n \right\rangle = (1 + j\lambda'_n)\delta_{mn} \tag{2.121c}$$

The total current **f** on objects can be derived from equations (2.117c) and (2.121c). **f** is represented by

$$\mathbf{f} = \sum_{n=1}^{\infty} \frac{V_n}{1 + j\lambda_n} \mathbf{f}_n = \sum_{n=1}^{\infty} \frac{V'_n}{1 + j\lambda'_n} \mathbf{f}'_n \tag{2.122}$$

where V_n and V'_n are given by

$$V_n = \left\langle \mathbf{g}^i, \mathbf{f}_n \right\rangle = \int_G \mathbf{E}^i \cdot \mathbf{J}_n - \mathbf{H}^i \cdot \mathbf{M}_n dv \tag{2.123a}$$

$$V'_n = \left\langle \mathbf{g}^i, \mathbf{f}'_n \right\rangle = \int_G \mathbf{E}^i \cdot \mathbf{J}'_n - \mathbf{H}^i \cdot \mathbf{M}'_n dv\,. \tag{2.123b}$$

Therefore, the total electric current **J** and the total magnetic current **M** are represented by

$$\begin{bmatrix} \mathbf{J} \\ \mathbf{M} \end{bmatrix} = \sum_{n=1}^{\infty} \frac{V_n}{1 + \lambda_n} \begin{bmatrix} \mathbf{J}_n \\ \mathbf{M}_n \end{bmatrix} = \sum_{n=1}^{\infty} \frac{V'_n}{1 + \lambda'_n} \begin{bmatrix} \mathbf{J}'_n \\ \mathbf{M}'_n \end{bmatrix}. \tag{2.124}$$

2.2.3 Modal Excitation Coefficient

In this section, objects are assumed to be composed of conductors or dielectrics. That

is, there is no magnetic material in the objects. Let $\mathbf{E}_n$ and $\mathbf{H}_n$ be the characteristic electric and magnetic fields, respectively, generated by the characteristic currents $\mathbf{J}_n$ in equation (2.62); i.e., $\mathbf{E}_n = L(\mathbf{J}_n)$ and $\mathbf{H}_n = jU(\mathbf{J}_n)$. Let $\mathbf{E}'_n$ and $\mathbf{H}'_n$ be the characteristic electric and magnetic fields, respectively, generated by the characteristic currents $\mathbf{J}'_n$ in equation (2.64); i.e., $\mathbf{E}'_n = L(\mathbf{J}'_n)$ and $\mathbf{H}'_n = jU(\mathbf{J}'_n)$. Expanding the characteristic fields $\mathbf{E}_n$ and $\mathbf{H}_n$ into spherical waves,

$$\mathbf{E}_n(\mathbf{r}) = \sum_{i=1}^{J} A_i^n \mathbf{E}_i^{(4)}(\mathbf{r}) \tag{2.125a}$$

$$\mathbf{H}_n(\mathbf{r}) = \sum_{i=1}^{J} A_i^n \mathbf{H}_i^{(4)}(\mathbf{r}). \tag{2.125b}$$

Let $\bar{\mathbf{E}}_n$ and $\bar{\mathbf{H}}_n$ be defined as

$$\bar{\mathbf{E}}_n = L^{\dagger}(\mathbf{J}_n(\mathbf{r}')) \tag{2.126a}$$

$$\bar{\mathbf{H}}_n = jU^{\dagger}\left(\mathbf{J}_n(\mathbf{r}')\right). \tag{2.126b}$$

$L^{\dagger}(\mathbf{J})$ and $jU^{\dagger}(\mathbf{J})$ satisfy Maxwell's equations and represent the inward-propagating electric and magnetic fields, respectively. If we determine the coefficients of the incoming spherical waves for $\bar{\mathbf{E}}_n$ and $\bar{\mathbf{H}}_n$,

$$\bar{\mathbf{E}}_n(\mathbf{r}) = \sum_{i=1}^{J} A_i^n \mathbf{E}_i^{(3)}(\mathbf{r}) \tag{2.127a}$$

$$\bar{\mathbf{H}}_n(\mathbf{r}) = \sum_{i=1}^{J} A_i^n \mathbf{H}_i^{(3)}(\mathbf{r}) \tag{2.127b}$$

where $\mathbf{E}_i^{(3)}$ and $\mathbf{H}_i^{(3)}$ are the electric and magnetic fields, respectively, corresponding to

the *i*th inward-propagating spherical wave and A_i^n is equal to the coefficient in (2.125)[4]. $\left(\mathbf{E}_n(\mathbf{r})+\bar{\mathbf{E}}_n(\mathbf{r})\right)$ and $\left(\mathbf{H}_n(\mathbf{r})+\bar{\mathbf{H}}_n(\mathbf{r})\right)$ are able to become the incident fields[5].

Let $a_n\left(\mathbf{E}_n+\bar{\mathbf{E}}_n\right)$ and $a_n\left(\mathbf{H}_n+\bar{\mathbf{H}}_n\right)$ be incident on an object. In this case, the *m*th modal excitation coefficient V_m is as follows:

$$\begin{aligned} V_m &= \left\langle a_n\left(\mathbf{E}_n+\bar{\mathbf{E}}_n\right),\mathbf{J}_m\right\rangle = a_n\left(\left\langle L(\mathbf{J}_n),\mathbf{J}_m\right\rangle+\left\langle L^{\dagger}(\mathbf{J}_n),\mathbf{J}_m\right\rangle\right) \\ &= -a_n\left(\left\langle Z_V(\mathbf{J}_n),\mathbf{J}_m\right\rangle+\left\langle Z_V^{\dagger}(\mathbf{J}_n),\mathbf{J}_m\right\rangle\right) = -2a_n\left\langle R_V(\mathbf{J}_n),\mathbf{J}_m\right\rangle = -2a_n\delta_{mn} \end{aligned} \tag{2.128}$$

From (2.128), we know that when $\left(\mathbf{E}_n+\bar{\mathbf{E}}_n\right)$ and $\left(\mathbf{H}_n+\bar{\mathbf{H}}_n\right)$ are incident on an object the object generates only $\mathbf{E}_n$ and $\mathbf{H}_n$ with a coefficient. Therefore, the characteristic fields $\mathbf{E}_n$ and $\mathbf{H}_n$ are an eigenvector of *S*. When an object is lossless, the characteristic fields $\mathbf{E}_n'$ and $\mathbf{H}_n'$ are an eigenvector of *S* because $\mathbf{E}_n\left(\mathbf{H}_n\right)$ and $\mathbf{E}_n'\left(\mathbf{H}_n'\right)$ are the same. When an object is lossy, $\mathbf{E}_n'$ and $\mathbf{H}_n'$ are not an eigenvector of *S*.

An arbitrary incident field can be expanded into eigenvectors of *S* as follows[6]:

---

[4] A_i^n in (2.125) can be calculated using equation (2.7). Equation (2.7) is derived from the reciprocity theorem [2, p. 333]. Because $\bar{\mathbf{E}}_n$ and $\bar{\mathbf{H}}_n$ satisfy Maxwell's equations, the reciprocity theorem can be used to determine the incoming spherical wave coefficients of $\bar{\mathbf{E}}_n$ and $\bar{\mathbf{H}}_n$. If we use the reciprocity theorem, we find that the coefficients of the incoming spherical waves can also be calculated using the right-hand side of equation (2.7).

[5] At the origin of the coordinate system, the magnitudes of $\mathbf{E}_n$, $\bar{\mathbf{E}}_n$, $\mathbf{H}_n$, and $\bar{\mathbf{H}}_n$ are infinite. We define $\left(\mathbf{E}_n(\mathbf{0})+\bar{\mathbf{E}}_n(\mathbf{0})\right)$ as $\sum_i A_i^n\mathbf{E}_i^{(1)}(\mathbf{0})$ and $\left(\mathbf{H}_n(\mathbf{0})+\bar{\mathbf{H}}_n(\mathbf{0})\right)$ as $\sum_i A_i^n\mathbf{H}_i^{(1)}(\mathbf{0})$.

[6] Harrington omitted $\sum_{n=1}^{M} b_n\tilde{\mathbf{E}}_n(\mathbf{r})$ in [18]. However, the results in [18] and in the present dissertation are the same.

$$\mathbf{E}^i(\mathbf{r}) = \sum_{n=1}^{N} a_n \left(\mathbf{E}_n(\mathbf{r}) + \bar{\mathbf{E}}_n(\mathbf{r}) \right) + \sum_{n=1}^{M} b_n \tilde{\mathbf{E}}_n(\mathbf{r}) \tag{2.129a}$$

$$\mathbf{H}^i(\mathbf{r}) = \sum_{n=1}^{N} a_n \left(\mathbf{H}_n(\mathbf{r}) + \bar{\mathbf{H}}_n(\mathbf{r}) \right) + \sum_{n=1}^{M} b_n \tilde{\mathbf{H}}_n(\mathbf{r}) \tag{2.129b}$$

where $\tilde{\mathbf{E}}_n$ and $\tilde{\mathbf{H}}_n$ are defined in (2.17), a_n and b_n are coefficients, N is the number of eigenvectors that an antenna can generate ($\mathbf{E}_n$ and $\mathbf{H}_n$), and M is the number of eigenvectors that an antenna cannot generate ($\mathbf{E}_n^e$ and $\mathbf{H}_n^e$). When $\mathbf{E}^i$ and $\mathbf{H}^i$ are incident on an object, the modal excitation coefficient is, from (2.128), as follows:

$$V_n = \left\langle \mathbf{E}^i, \mathbf{J}_n \right\rangle = \left\langle \sum_{m=1}^{N} a_m \left(\mathbf{E}_m + \bar{\mathbf{E}}_m \right) + \sum_{m=1}^{M} b_m \tilde{\mathbf{E}}_m, \mathbf{J}_n \right\rangle = -2a_n \tag{2.130}$$

Because the antenna does not react to $\tilde{\mathbf{E}}_m$, $\tilde{\mathbf{E}}_m$ is ignored in the calculation of V_n.

Chapter 3

Analysis of Scattering by an Antenna

3.1 Analysis of the Transmitting and Scattering Properties of an Antenna Using the Theory of Characteristic Modes

3.1.1 Current Distribution of a Loaded Antenna

In this chapter, it is assumed that a source or load is connected at an infinitesimal gap on a conducting wire, and there is only one feed gap. The current of a loaded antenna illuminated by an electromagnetic field is the superposition of a current component for a short-circuited antenna and a current component for a transmitting antenna [23]–[25]:

$$\mathbf{J}^r(\mathbf{r}') = \mathbf{J}^s(\mathbf{r}') + \frac{I^{sc}Z_L}{Z_A + Z_L}\frac{\mathbf{J}^t(\mathbf{r}')}{I^t} \tag{3.1}$$

where $\mathbf{J}^r$ is the current density of a loaded antenna; $\mathbf{J}^s$ is the current density of the short-circuited antenna when the same field as that incident on a loaded antenna is incident; $\mathbf{J}^t$ is the current density of the antenna operating in the transmitting mode; I^t is the total current at the feed point of the transmitting antenna when the current density is $\mathbf{J}^t$; Z_A is the input

impedance of an antenna; Z_L is the load impedance; I^{sc} is the short-circuit current in the Norton equivalent circuit for the receiving antenna (see Section 4.2). Let I^s be the total current at the feed point of a short-circuited antenna when the current density of the short-circuited antenna is $\mathbf{J}^s$. Then, $I^{sc} = -I^s$.

When objects are near the antenna, I^{sc} and $\mathbf{J}^s$ are calculated from the sum of the incident field and the field generated by the objects (excluding the field generated by $\mathbf{J}^r$). The current distribution of the objects is calculated in the presence of the antenna and the objects.

3.1.2 Representation of the Current of an Antenna in Term of Characteristic Currents

Equation (3.1) can be expressed in terms of the characteristic current. $\mathbf{J}^s$ can be represented, from (2.81), as follows:

$$\mathbf{J}^s(\mathbf{r}') = \sum_{n=1}^{N} \frac{V_n}{1 + j\lambda_n} \mathbf{J}_n(\mathbf{r}') \tag{3.2}$$

where N is the number of characteristic modes. From (3.2), the total current at the feed point of a short-circuited antenna, I^s, is written as

$$I^s = \sum_{n=1}^{N} \frac{V_n}{1 + j\lambda_n} I_n^{ch} \tag{3.3}$$

where I_n^{ch} is the total current at the feed point for the nth characteristic current.

When the input terminals (the feed point) are excited with V volts and there is no incident field, using (2.80) and the delta gap model, the modal excitation coefficient V_n becomes

$$V_n = VI_n^{ch} . \tag{3.4}$$

Therefore, $\mathbf{J}^t$ can be written as follows:

$$\mathbf{J}^t(\mathbf{r}') = \sum_{n=1}^{N} \frac{VI_n^{ch}}{1+j\lambda_n} \mathbf{J}_n(\mathbf{r}') \tag{3.5}$$

From (3.5), $\mathbf{J}^t / I^t$ is written as

$$\frac{\mathbf{J}^t}{I^t} = Z_A \sum_{n=1}^{N} \frac{I_n^{ch}}{1+j\lambda_n} \mathbf{J}_n . \tag{3.6}$$

Substituting (3.2) and (3.6) into (3.1) and rearranging, the following equation is obtained:

$$\begin{aligned} \mathbf{J}^r(\mathbf{r}') &= \sum_{n=1}^{N} \frac{1}{1+j\lambda_n} \left(V_n - \frac{Z_L Z_A I^s I_n^{ch}}{Z_L + Z_A} \right) \mathbf{J}_n(\mathbf{r}') \\ &= \sum_{n=1}^{N} \frac{1}{1+j\lambda_n} \left(V_n - \frac{Z_L Z_A I_n^{ch}}{Z_L + Z_A} \left(\sum_{m=1}^{N} \frac{V_m I_m^{ch}}{1+j\lambda_m} \right) \right) \mathbf{J}_n(\mathbf{r}') \end{aligned} \tag{3.7}$$

From (3.5), the total current at the feed point of a transmitting antenna I^t is written as

$$I^t = \sum_{n=1}^{N} \frac{V(I_n^{ch})^2}{1+j\lambda_n} . \tag{3.8}$$

The input impedance can be calculated using the parameters of the characteristic modes. From (3.8), the input impedance is

$$Z_A = \frac{1}{\sum_{n=1}^{N} \frac{(I_n^{ch})^2}{1+j\lambda_n}} . \tag{3.9}$$

3.1.3 Scattering Properties of an Antenna

In this section, we investigate the scattering properties of antennas. First, consider a short-circuited antenna (*i.e.*, Z_L = 0). Let $\mathbf{E}^s$ and $\mathbf{H}^s$ be the electric and magnetic fields

scattered by the antenna, respectively. The electromagnetic field scattered by a short-circuited antenna is, from (3.7) and (2.130),

$$\mathbf{E}^s = \sum_{n=1}^{N} \frac{-2a_n}{1+j\lambda_n} \mathbf{E}_n \tag{3.10a}$$

$$\mathbf{H}^s = \sum_{n=1}^{N} \frac{-2a_n}{1+j\lambda_n} \mathbf{H}_n \,. \tag{3.10b}$$

In general, when the size of the antenna is much smaller than the wavelength (smaller than approximately the wavelength/10), the absolute values of all the eigenvalues λ_n are very large (larger than 50). In this case, the magnitudes of $\mathbf{E}^s$ and $\mathbf{H}^s$ are very small compared with the magnitudes of the incident field (2.129)[7]. Therefore, short-circuited antennas rarely scatter fields when the size of the antenna is much smaller than the wavelength of the incident field.

The absolute values of the eigenvalues decrease as the frequency increases up to a certain frequency. At a certain frequency, one eigenvalue or a few eigenvalues are close to zero. In this case, the magnitudes of $\mathbf{E}^s$ and $\mathbf{H}^s$ when one or several eigenvalues are close to zero are relatively large compared with those when the absolute values of all the eigenvalues are large. Therefore, short-circuited antennas scatter well when some eigenvalues are close to zero. A series resonant frequency is an example of this effect.

The scattered power, P^s, is defined as

---

[7] In general, $\sum_{n=1}^{M} b_n \tilde{\mathbf{E}}_n(\mathbf{r})$ and $\sum_{n=1}^{M} b_n \tilde{\mathbf{H}}_n(\mathbf{r})$ do not substantially decrease the magnitudes of $\sum_{n=1}^{N} a_n \left(\mathbf{E}_n(\mathbf{r}) + \bar{\mathbf{E}}_n(\mathbf{r})\right)$ and $\sum_{n=1}^{N} a_n \left(\mathbf{H}_n(\mathbf{r}) + \bar{\mathbf{H}}_n(\mathbf{r})\right)$, respectively, in (2.129).

$$P^s = \frac{1}{2}\mathrm{Re}\left(\oiint \mathbf{E}^s \times \mathbf{H}^{s*} \cdot d\mathbf{s}\right). \tag{3.11}$$

Figure 3.1 shows the scattered power of a short-circuited dipole antenna illuminated by a linearly polarized plane wave and its eigenvalues as a function of frequency. The length of the dipole antenna is 30 cm, the diameter of the cross-section of wire is 1 mm, and the dipole antenna is made of PEC. The dipole antenna is aligned with the *z*-axis, and the input terminals are located at the center of the dipole. The plane wave propagates in the direction of [0, −1, −1] in rectangular coordinates, the polarization of the electric field lies in the *yz*-plane, and the magnitude of the electric field is 1 V/m. Figure 3.2 shows the scattered power of a short-circuited loop antenna illuminated by a linearly polarized plane wave and its eigenvalues as a function of frequency. The radius of the loop antenna is 4.8 cm, the diameter of the cross-section of the wire is 1 mm, and the loop antenna is made of PEC. The loop antenna lies in the *xy*-plane, and the center of the loop is located at the origin of the coordinate system. The input terminals are located at [0.048 m, 0 m, 0 m] in rectangular coordinates. The plane wave propagates in the direction of [0, −1, −1] in rectangular coordinates, the polarization of the electric field lies in the *xy*-plane, and the magnitude of the electric field is 1 V/m. In Figure 3.1 and Figure 3.2, we can see that the scattered power is small at lower frequencies and is large near the series resonant frequency when the antennas are short-circuited.

Next consider an open-circuited antenna (*i.e.*, $Z_L = \infty$). The electromagnetic field scattered by an open-circuited antenna is, from (3.7) and (2.130),

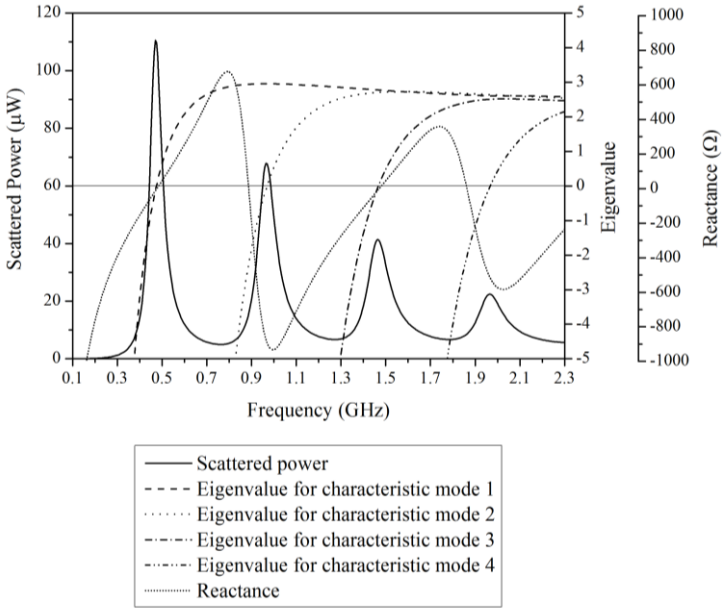

Figure 3.1 Scattered power and eigenvalues for a short-circuited 30 cm dipole antenna and the reactance of the center-fed dipole antenna.

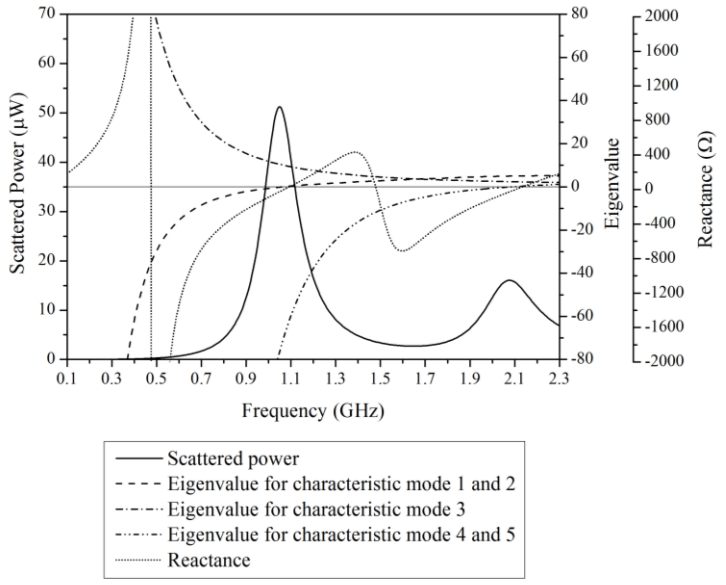

Figure 3.2 Scattered power and eigenvalues for a short-circuited loop antenna with a radius of 4.8 cm and the reactance of the loop antenna.

$$\mathbf{E}^s = \sum_{n=1}^{N} \frac{-1}{1+j\lambda_n}\left(2a_n + Z_A I^s I_n^{ch}\right)\mathbf{E}_n$$
$$= \sum_{n=1}^{N}\left(\frac{-2a_n}{1+j\lambda_n} + \sum_{m=1}^{N}\left(\frac{2Z_A I_n^{ch} I_m^{ch} a_m}{(1+j\lambda_n)(1+j\lambda_m)}\right)\right)\mathbf{E}_n \tag{3.12a}$$

$$\mathbf{H}^s = \sum_{n=1}^{N} \frac{-1}{1+j\lambda_n}\left(2a_n + Z_A I^s I_n^{ch}\right)\mathbf{H}_n . \tag{3.12b}$$

In general, $\left|Z_A I_n^{ch} I_m^{ch}\right|$ is much smaller than $\left|(1+j\lambda_n)(1+j\lambda_m)\right|$ when the antenna is much smaller than the wavelength. Therefore, an open-circuited antenna rarely scatters when an antenna is much smaller than the wavelength of the incident field.

We assume that the moduli of the eigenvalues of the higher order modes are much larger than the modulus of the eigenvalue of the first mode, and the current and the input impedance of the antenna are determined using only the single characteristic mode; i. e., $\left|\lambda_1\right| << \left|\lambda_n\right|$, $\left|a_1/(1+\lambda_1)\right| >> \left|a_n/(1+\lambda_n)\right|$, $\left|I_1^{ch}/(1+j\lambda_1)\right| >> \left|I_n^{ch}/(1+j\lambda_n)\right|$, $\left|(I_1^{ch})^2/(1+j\lambda_1)\right| >> \left|(I_n^{ch})^2/(1+j\lambda_n)\right|$ (n = 2, 3, 4, ⋯). In this case, Z_A and I^s are approximated by

$$Z_A \approx \frac{1+j\lambda_1}{(I_1^{ch})^2} \tag{3.13}$$

$$I^s \approx \frac{-2a_1}{1+j\lambda_1} I_1^{ch} . \tag{3.14}$$

Substituting (3.13) and (3.14) into (3.12) and calculating, $\mathbf{E}^s$ and $\mathbf{H}^s$ become zero. For the same case, the behavior of the antenna is determined using only the single characteristic mode. An example of this case is a center-fed dipole antenna near its lowest resonant

frequency (In fact, there is a small error between the exact current and the current calculated using only one characteristic mode).

For some classes of antennas, the modulus of the eigenvalue of the first mode is much smaller than the moduli of the eigenvalues of the higher order modes ($|\lambda_1| < |\lambda_2|/10$) and there are no degenerate modes (modes whose eigenvalues are the same and whose current distributions are different) at frequencies smaller than the lowest resonant frequency. In this case, the current of a short-circuited antenna $\mathbf{J}^s$ can be determined using one characteristic current with a small error. In this case, several characteristic modes are required to determine the current of a transmitting antenna and the input impedance because of the term I_n^{ch} in (3.5) and (3.9). The shape of the current of a transmitting antenna is slightly different from the shape of the current of a short-circuited antenna. For this class of antenna, the magnitude of the current of an open-circuited antenna is much smaller than the magnitude of the current of a short-circuited antenna at frequencies smaller than the lowest resonant frequency, because the current of an open-circuited antenna is the sum of the current components for a transmitting antenna and a short-circuited antenna and the difference between the phases of the two current components is 180°. Therefore, an open-circuited antenna scatters much less than a short-circuited antenna below the lowest resonant frequency for this class of antennas. A dipole antenna is an example of this case. Figure 3.3 shows the scattered power of an open-circuited dipole antenna illuminated by a linearly polarized plane wave and shows the eigenvalues as a function of frequency. The dipole antenna and the plane wave are the same as those used in Figure 3.1. In Figure 3.3, we can note that the open-circuited dipole antenna rarely scatters

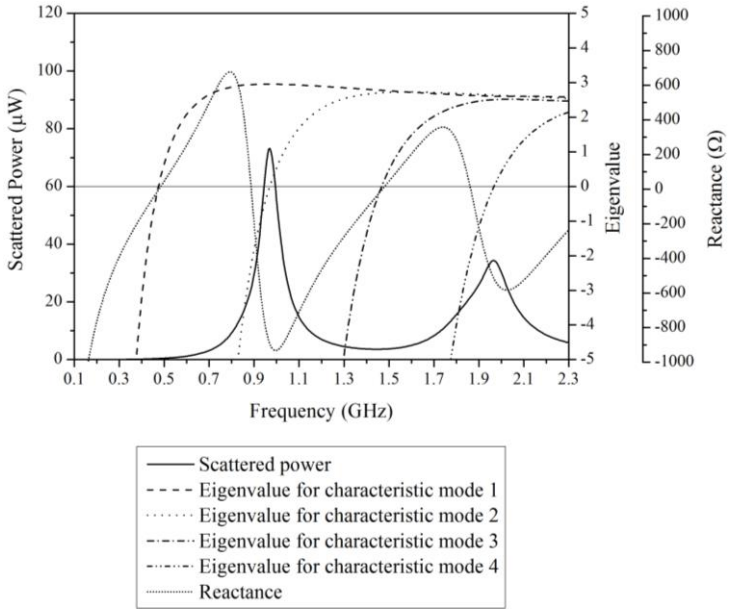

Figure 3.3 Scattered power for an open-circuited 30 cm dipole antenna, eigenvalues for the short-circuited dipole antenna and reactance of the center-fed dipole antenna.

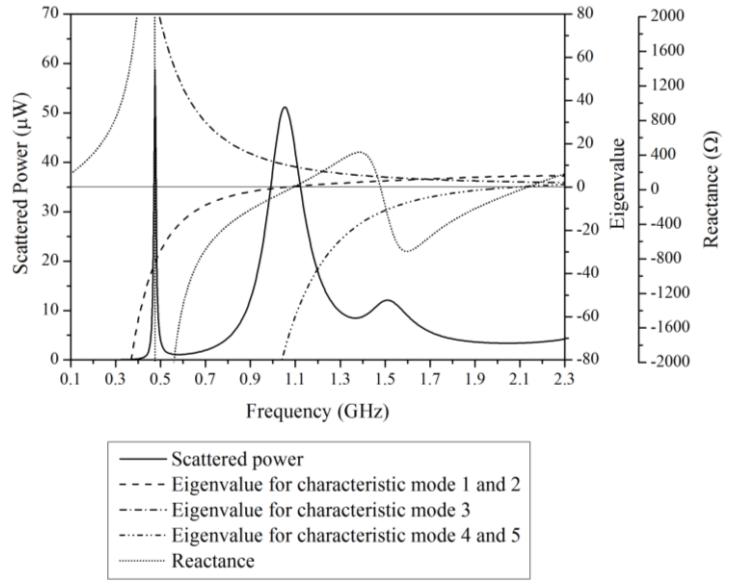

Figure 3.4 Scattered power for an open-circuited loop antenna with a radius of 4.8 cm, eigenvalues for the short-circuited loop antenna and reactance of the loop antenna.

near or below the lowest resonant frequency.

If an antenna is not dominated by a single characteristic mode and if the modulus of the input impedance of the antenna is very large compared with the modulus of the eigenvalue of the lowest order mode, an open-circuited antenna scatters well (see equation (3.12)). An example of this case is a loop antenna at its lowest antiresonant frequency. Figure 3.4 shows the scattered power of an open-circuited loop antenna illuminated by a linearly polarized plane wave and shows the eigenvalues as a function of frequency. The loop antenna and the plane wave are the same as those used in Figure 3.2. In Figure 3.4, we can see that an open-circuited loop antenna scatters much at the lowest antiresonant frequency. Note that a short-circuited loop antenna does not scatter well at the lowest antiresonant frequency because the absolute values of the eigenvalues are large.

If the imaginary part of the load impedance is the same as the negative of the imaginary part of the input impedance and if the real parts of the load and input impedances are small, the antenna scatters well even if the antenna is much smaller than the wavelength. This effect occurs because the absolute value of $Z_L/(Z_L + Z_A)$ in (3.7) is very large. In this case, a current component for a transmitting antenna is the dominant term in the total current distribution.

3.1.4 Transmitting Properties of a Small Antenna near Objects

Suppose that objects are present near an antenna. Suppose that the feed port of the antenna is excited with a source and that there is no incident field. Then, the total current (**J**) in the antenna is

$$\mathbf{J} = \mathbf{J}^t + \mathbf{J}^r \tag{3.15}$$

Here, $\mathbf{J}^t$ is the current density of a transmitting antenna in free-space, which is represented by (3.5); $\mathbf{J}^r$ is represented by (3.1). $\mathbf{J}^t$ in equation (3.1) is arbitrary. Let $\mathbf{J}^t$ in equation (3.1) be the same as $\mathbf{J}^t$ in equation (3.15). Then, equation (3.15) can be written as

$$\mathbf{J} = \left(1 - \frac{I^s Z_L}{(Z_A + Z_L) I^t}\right) \mathbf{J}^t + \mathbf{J}^s \tag{3.16}$$

where $\mathbf{J}^s$ is represented by (3.2). V_n in (3.2) is calculated from only the field generated by the objects.

When the antenna is much smaller than the wavelength, the magnitude of $\mathbf{J}^s$ is much smaller than the magnitude of $\mathbf{J}^t$ in equation (3.16) because $|V_n|$ in (3.2) is smaller than $\left|VI_n^{ch}/(1+j\lambda_n)\right|$ in (3.5) for most n[8] and the moduli of all the eigenvalues λ_n are very large. In this case, $\mathbf{J}^s$ in (3.16) can be ignored. Therefore, when an antenna is much smaller than the wavelength, the shape of the current of a transmitting antenna near objects is almost the same as the shape of current of a transmitting antenna in free space.

When there is only one dominant characteristic mode, the shapes of the currents of a transmitting antenna in free space and near objects are the same because the shapes of $\mathbf{J}^t$ and $\mathbf{J}^s$ are the same.

[8] For some n, $|V_n|$ may be larger than $\left|VI_n^{ch}/(1+j\lambda_n)\right|$. For most n, $|V_n|$ is smaller than $\left|VI_n^{ch}/(1+j\lambda_n)\right|$. This difference arises because the magnitude of the field scattered by the objects is smaller than the magnitude of the field transmitted by an excited antenna.

3.1.5 Validation

To verify the theory presented in this paper, we numerically calculated the current on a dipole antenna and the radiated power for a dipole antenna. The dipole antenna was aligned with the z axis, and the center of the dipole was located at the origin of the coordinate system. The length of the dipole antenna was 30 cm, the radius of the cross section of the wire was 1 mm, and the conductivity was 10000 S/m. We chose a very small conductivity so that the losses in the antenna were large. The input terminals were at the center of the dipole antenna. We determined that the generalized scattering matrix of this dipole antenna was diagonalizable.

The author calculated the impedance matrix ($\mathbf{R_C} + j\,\mathbf{X_C}$) using the method of moments. In the calculation with the method of moments, a pulse function was used for an expansion function, and point matching was used for testing [26]. We calculated the current distribution on the dipole antenna terminated with 50 Ω at 1.5 GHz when a linearly polarized plane wave was incident on the dipole antenna. The plane wave propagated in the direction of [−1, 0, −1] in rectangular coordinates, the polarization of the electric field lay in the *xz*-plane, and the magnitude of the electric field was 1 V/m. We calculated the current using two methods. In the first method, the current was calculated directly from (2.37), and in the second method, the current was calculated from the characteristic currents using (3.7). Figure 3.5 shows the current on the dipole antenna. The results obtained by the two methods agree well.

We calculated the power radiated by the 30 cm dipole antenna when the input terminals were excited with 1 V. The radiated power was calculated from 100 MHz to 1

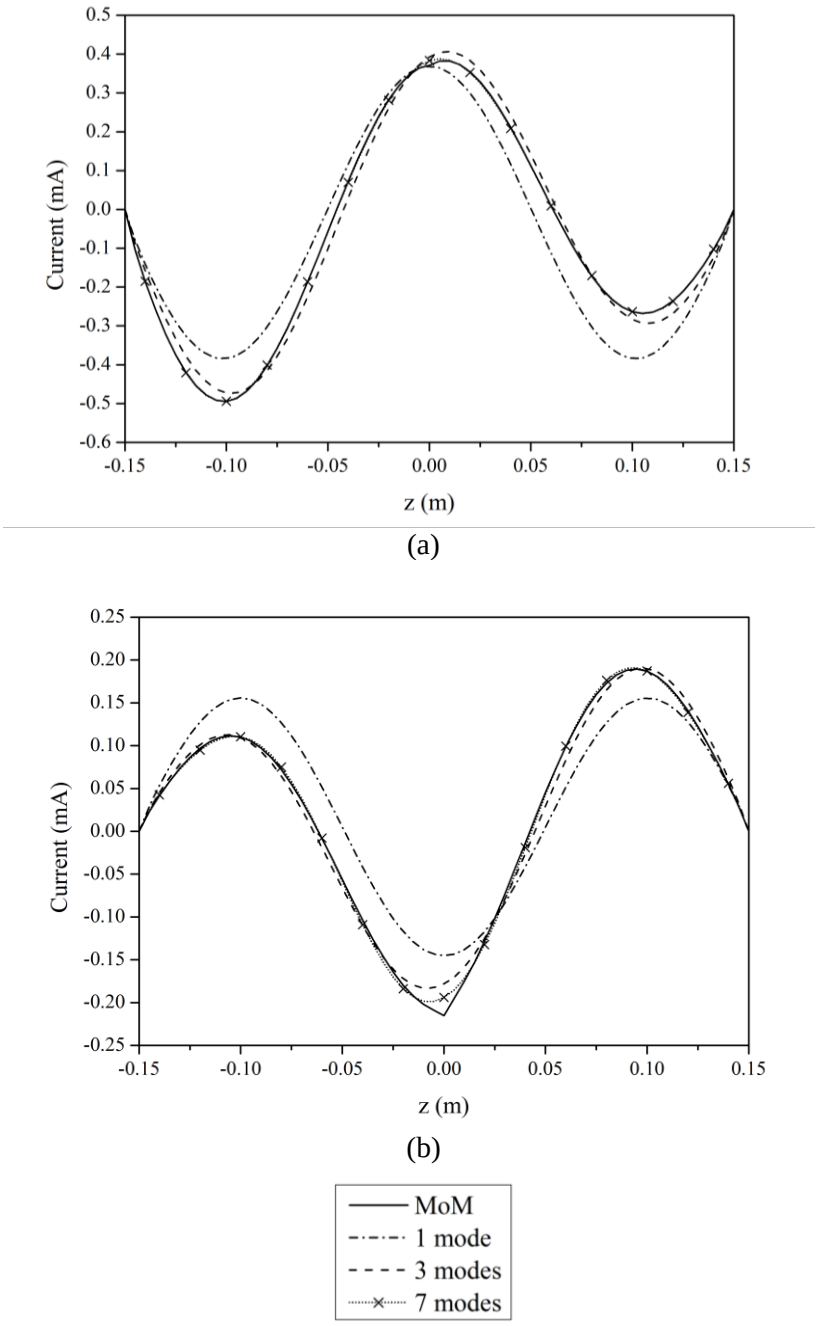

Figure 3.5 Current distribution on the 30 cm dipole antenna terminated with 50 Ω at 1.5 GHz. The graph for "MoM" is that obtained by the method of moments. The graph for "*n* modes" is that obtained by using *n* characteristic modes (*n* = 1, 3, 7). (a) Real part of the current (b) Imaginary part of the current.

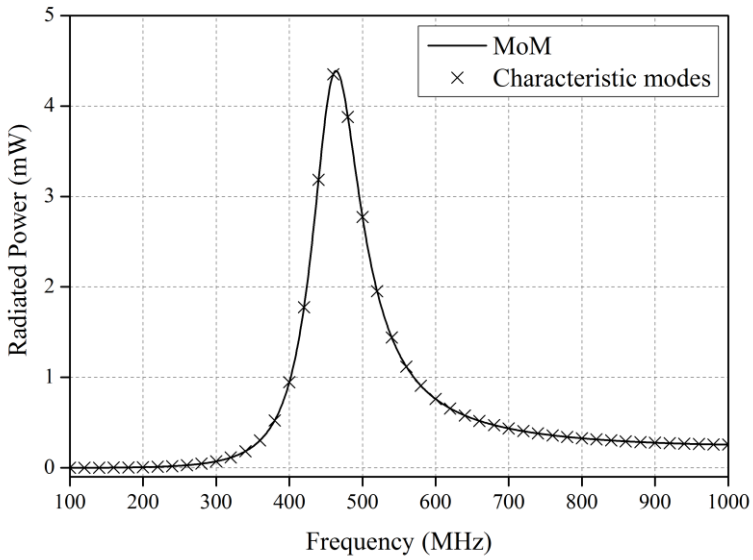

Figure 3.6 Radiated power for the 30 cm dipole antenna.

GHz. The radiation efficiency of the dipole antenna is 13% at 100 MHz and is 83% at 1 GHz. We calculated the radiated power using two methods. In one method, the radiated power was calculated using equation (2.27). In the other method, we calculated the radiated power using (2.84). Figure 3.6 shows the radiated powers calculated with the two methods. Although the dipole antenna has large losses, the results obtained by the two methods agree well. The maximum error is 0.07%. This phenomenon occurred because

$$\left\langle R_V(\mathbf{J}_n), \mathbf{J}_n^* \right\rangle >> \left\langle R_V(\mathbf{J}_m), \mathbf{J}_i^* \right\rangle \ (m \neq i). \tag{3.17}$$

3.1.6 Minimum Scattering Antenna

A minimum scattering (MS) antenna is one that does not scatter electromagnetic fields when its feed ports are terminated in suitable reactive loads [27]. The minimum

scattering antenna that does not scatter when its feed ports are open-circuited is called a canonical minimum scattering (CMS) antenna [27]. As explained in Section 3.1.3, an antenna much smaller than the wavelength of the incident field rarely scatters unless an antenna is terminated in a load whose reactance is close to the negative of the input reactance. If we assume such an antenna to be a minimum scattering antenna, we can calculate the network parameters (e.g., the impedance parameters, admittance parameters, and scattering parameters) among antennas and the electromagnetic fields generated by antennas with small errors. Therefore, an antenna much smaller than the wavelength can be modeled as a minimum scattering antenna. As explained in Section 3.1.3, an antenna whose input impedance and current distribution can be determined using only one characteristic mode rarely scatters when the antenna is open-circuited. If we assume such an antenna to be a canonical minimum scattering antenna, we can calculate the network parameters among the antennas and the electromagnetic fields generated by the antennas with small errors. Therefore, an antenna dominated by a single characteristic mode can be modeled as a canonical minimum scattering antenna.

Here, the **S** matrix in equation (2.13) for two types of minimum scattering antenna will be derived. One type is a canonical minimum scattering antenna, and the other type is a minimum scattering antenna that does not scatter when short-circuited. From (2.13), we have the following equations:

$$\mathbf{w} = \boldsymbol{\Gamma}\mathbf{v} + \mathbf{R}\mathbf{a} \tag{3.18}$$

$$\mathbf{b} = \mathbf{T}\mathbf{v} + \mathbf{S}\mathbf{a} \tag{3.19}$$

Let $\mathbf{w} = \boldsymbol{\xi}\mathbf{v}$. Then, equation (3.18) is written as

$$\mathbf{v} = \left(\boldsymbol{\xi} - \boldsymbol{\Gamma}\right)^{-1} \mathbf{R}\mathbf{a} \,. \tag{3.20}$$

Substituting (3.20) into (3.19), we obtain

$$\mathbf{b} = \left(\mathbf{T}\left(\boldsymbol{\xi} - \boldsymbol{\Gamma}\right)^{-1} \mathbf{R} + \mathbf{S}\right)\mathbf{a} \,. \tag{3.21}$$

If an antenna does not scatter the electromagnetic field at all, **b** = **a**. Therefore, when an antenna does not scatter the electromagnetic field at all under the condition of $\mathbf{w} = \boldsymbol{\xi}\mathbf{v}$, **S** is as follows:

$$\mathbf{S} = \mathbf{I} - \mathbf{T}\left(\boldsymbol{\xi} - \boldsymbol{\Gamma}\right)^{-1} \mathbf{R} \tag{3.22}$$

where **I** is the identity matrix in which the number of rows (or columns) is equal to the number of row in **T**.

Let $\mathbf{I}_p$ be the identity matrix in which the number of rows (or columns) is equal to the number of rows of **v** (or **w**). When all of the feed ports of an antenna are open-circuited, all of the currents at the feed ports are zero. In this case, from equation (2.10b), **v** = **w**; i.e., $\boldsymbol{\xi} = \mathbf{I}_p$. Therefore, **S** for a canonical minimum scattering antenna is

$$\mathbf{S} = \mathbf{I} - \mathbf{T}\left(\mathbf{I}_p - \boldsymbol{\Gamma}\right)^{-1} \mathbf{R} \,. \tag{3.23}$$

Let the reference impedance of the *i*th feed port be Z_i^R. Let $\boldsymbol{\chi}$ be a diagonal matrix whose entry in the *i*th row and *i*th column is $-(Z_i^R)^* / Z_i^R$. When all of the feed ports of an antenna are short-circuited, all of the voltages at the feed ports are zero. In this case, from equation (2.10a), $\mathbf{w} = \boldsymbol{\chi}\mathbf{v}$; i.e., $\boldsymbol{\xi} = \boldsymbol{\chi}$. Therefore, **S** for a minimum scattering antenna that does not scatter when short-circuited is

$$\mathbf{S} = \mathbf{I} - \mathbf{T}\left(\mathbf{I}_p - \boldsymbol{\chi}\right)^{-1} \mathbf{R} \,. \tag{3.24}$$

3.2 Determination of the Generalized Scattering Matrix of an Antenna Using the Theory of Characteristic Modes

As explained in Section 2.2.1, a column matrix containing the spherical wave coefficients of a characteristic field are an eigenvector of matrix **S**. If we know all eigenvectors of matrix **S**, we can calculate **S** using the following:

$$\mathbf{S} = \mathbf{Q}\mathbf{D}\mathbf{Q}^{-1} \tag{3.25}$$

where the *i*th column of **Q** is the *i*th eigenvector of **S** and **D** is the diagonal matrix whose entry in the *i*th row and *i*th column is the eigenvalue corresponding to the *i*th eigenvector of **S**.

This method has several disadvantages. First, we need to know all eigenvectors of matrix **S**. Objects that are not significantly larger than the wavelength can be described using a few characteristic modes, so we may not know all the characteristic modes. Second, equation (3.25) includes the inverse of a matrix, which makes it inconvenient. Third, when objects are lossy, a column matrix containing the spherical wave coefficients of a characteristic field may not be an eigenvector of matrix **S**.

In this section, a formula for calculating the generalized scattering matrix of an antenna using characteristic modes is derived.

3.2.1 Determination of the Generalized Scattering Matrix of an Antenna from Characteristic Modes

Figure 3.7 shows a representation of the type of antenna addressed in this dissertation. The material of an antenna is composed of conductors, dielectrics, or magnetic materials. The material can be lossy. It is assumed that the material is linear and reciprocal. Moreover,

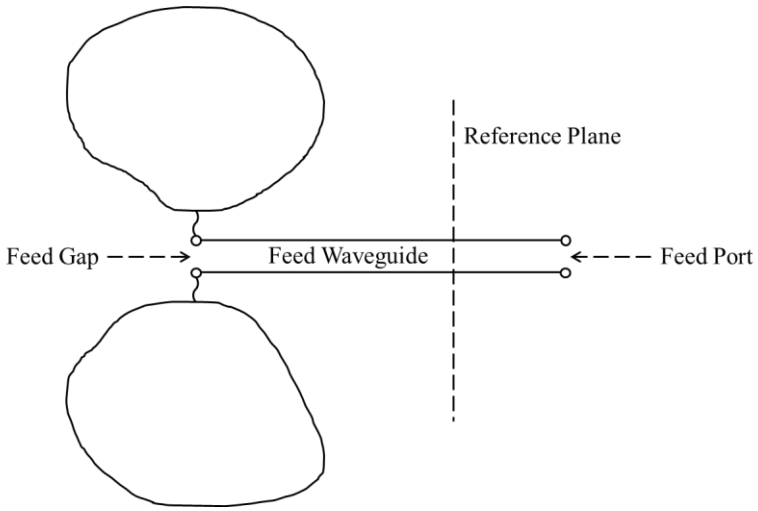

Figure 3.7 Material body, feed gap, feed waveguide, reference plane, and feed port for an antenna.

it is assume that the antenna is excited at an infinitesimal gap on the conducting wire and that the number of feed gaps is one. A transmission line or waveguide are connected to a feed gap, and a feed port is connected to the end of the waveguide (Figure 3.7). A load or source is connected to a feed port. A balun may exist between a feed gap and feed waveguide (or transmission line), but this is not considered in this dissertation. In this section, we assume that a reference plane is at a feed gap and that only one mode exists in a feed waveguide.

We first consider the generalized scattering matrix of an object that does not have a feed gap. In this case, the generalized scattering matrix equation is represented by equation (2.15). Because the incident wave is finite at the origin of the coordinate system, it can be expanded into standing spherical waves. Let a standing spherical wave with indices {s, m, n} be incident on a body, and let its amplitude be $2a_{s,m,n}$, i.e., let $2a_{s,m,n}\mathbf{E}^{(1)}_{s,m,n}$ and

$2a_{s,m,n}\mathbf{H}^{(1)}_{s,m,n}$ be incident on a body. Using (2.123), the modal excitation coefficient for the *p*th characteristic current is given by

$$V_p = 2a_{s,m,n}\int_G \left(\mathbf{J}_p \cdot \mathbf{E}^{(1)}_{s,m,n} - \mathbf{M}_p \cdot \mathbf{H}^{(1)}_{s,m,n}\right) dv\,. \tag{3.26}$$

Let the coefficient of the outgoing spherical wave with indices {*s*, *m*, *n*} produced by the *p*th characteristic current $\mathbf{f}_p$ be $T^p_{s,m,n}$, i.e.,

$$T^p_{s,m,n} = -(-1)^m \int_G \left(\mathbf{J}_p \cdot \mathbf{E}^{(1)}_{s,-m,n} - \mathbf{M}_p \cdot \mathbf{H}^{(1)}_{s,-m,n}\right) dv\,. \tag{3.27}$$

Comparing (3.26) with (3.27), we note that

$$V_p = -2(-1)^m T^p_{s,-m,n} a_{s,m,n}\,. \tag{3.28}$$

Let $\mathbf{T}^p$ be a column matrix whose *i*th entry is $T^p_{s,m,n}$, with {*s*, *m*, *n*} satisfying equation (2.5).

When multiple spherical waves are incident, the modal excitation coefficient for the *p*th characteristic current is, from (3.28),

$$V_p = -2\mathbf{R}^p\mathbf{a} \tag{3.29}$$

where *i*th entry of **a** is $a_{s,m,n}$, with {*s*, *m*, *n*} satisfying equation (2.5); $\mathbf{R}^p$ is a row matrix, and the *i*th entry of $\mathbf{R}^p$ is $R^p_{s,m,n}$, which is defined by

$$R^p_{s,m,n} = (-1)^m T^p_{s,-m,n} \tag{3.30}$$

where subscripts {*s*, *m*, *n*} satisfy equation (2.5).

When the incoming and outgoing waves with coefficients **a** are incident, the coefficients of the outgoing spherical waves for the scattered field ($\mathbf{b}^s$) are, from (2.124)

and (3.29),

$$\mathbf{b}^s = \sum_{p=1}^{\infty} \frac{-2\mathbf{R}^p\mathbf{a}}{1+j\lambda_p}\mathbf{T}^p \ . \tag{3.31}$$

Therefore, the coefficients of the outgoing spherical waves for the total field (**b**) when **a** is incident are as follows:

$$\mathbf{b} = \mathbf{a} - 2\sum_{p=1}^{\infty} \frac{1}{1+j\lambda_p}\mathbf{T}^p\mathbf{R}^p\mathbf{a} \tag{3.32}$$

Next, we consider the generalized scattering matrix of an antenna that has a feed gap. An antenna whose feed gap is short-circuited (i.e., the feed gap is filled with a conductor) can be considered an object without a feed gap. If a feed gap is short-circuited, from equation (3.21),

$$\mathbf{b} = \left(\frac{-Z_R}{Z_R^* + Z_R\Gamma}\mathbf{TR} + \mathbf{S} \right)\mathbf{a} \, . \tag{3.33}$$

Comparing (3.33) with (3.32), we obtain

$$\mathbf{S} = \mathbf{I} + \frac{Z_R}{Z_R^* + Z_R\Gamma}\mathbf{TR} - 2\sum_{p=1}^{\infty} \frac{1}{1+j\lambda_p}\mathbf{T}^p\mathbf{R}^p \tag{3.34}$$

where **I** is the identity matrix.

If the feed gap of an antenna is excited with V volts and there is no incident field, the modal excitation coefficient for the pth characteristic current is $V_p = VI_p^{ch}$ (equation (3.4)). In this case, the coefficients of the outgoing spherical waves that the antenna transmits ($\mathbf{b}^t$) are, from (2.124),

$$\mathbf{b}^t = \sum_{p=1}^{\infty} \frac{VI_p^{ch}}{1+j\lambda_p}\mathbf{T}^p \ . \tag{3.35}$$

If an incident power wave with a coefficient of 1 is excited at a feed gap, the voltage at the feed gap is

$$V = \frac{Z_R^* + \Gamma Z_R}{\sqrt{\mathrm{Re}(Z_R)}} \tag{3.36}$$

where Z_R is a reference impedance. Therefore, the modal transmitting pattern is represented by, from (3.35) and (3.36),

$$\mathbf{T} = \frac{Z_R^* + \Gamma Z_R}{\sqrt{\mathrm{Re}(Z_R)}} \sum_{p=1}^{\infty} \frac{I_p^{ch}}{1 + j\lambda_p} \mathbf{T}^p \tag{3.37}$$

The reflection coefficient can also be determined from the characteristic modes. From (3.9), the input admittance of the antenna, Y_A, is

$$Y_A = \frac{1-\Gamma}{Z_R^* + \Gamma Z_R} = \sum_{p=1}^{\infty} \frac{(I_p^{ch})^2}{1 + j\lambda_p}. \tag{3.38}$$

From this equation or equation (3.9), we can obtain the reflection coefficient.

In summary, the generalized scattering matrix can be obtained from the characteristic currents at a feed point, the coefficients of the spherical waves produced by the characteristic currents, and the eigenvalues.

3.2.3 Minimum Scattering Antenna

We assume that the absolute values of the eigenvalues of higher-order modes are very large compared with the absolute value of the eigenvalue of the lowest-order mode, so that the currents of the antenna and the input admittance are determined only from the lowest-order mode, i.e., $|\lambda_1| << |\lambda_n|$, $|a_1/(1+\lambda_1)| >> |a_n/(1+\lambda_n)|$, $|I_1^{ch}/(1+j\lambda_1)| >> |I_n^{ch}/(1+j\lambda_n)|$, and

$\left|(I_1^{ch})^2/(1+j\lambda_1)\right| >> \left|(I_n^{ch})^2/(1+j\lambda_n)\right|$ (p = 2, 3, 4, ···). In this case, from (3.37), **T** becomes

$$\mathbf{T} \approx \frac{Z_R^* + \Gamma Z_R}{\sqrt{\mathrm{Re}(Z_R)}} \frac{I_1^{ch}}{1+j\lambda_1} \mathbf{T}^1 \tag{3.39}$$

from (2.14), **R** becomes

$$\mathbf{R} \approx \frac{Z_R^* + \Gamma Z_R}{\sqrt{\mathrm{Re}(Z_R)}} \frac{I_1^{ch}}{1+j\lambda_1} \mathbf{R}^1 \tag{3.40}$$

and from (3.34), **S** becomes

$$\mathbf{S} \approx \mathbf{I} + \frac{Z_R}{Z_R^* + Z_R\Gamma}\mathbf{TR} - \frac{2}{1+j\lambda_1}\mathbf{T}^1\mathbf{R}^1 . \tag{3.41}$$

After substituting (3.39) and (3.40) into (3.41) and rearranging the result,

$$\mathbf{S} \approx \mathbf{I} + \frac{Z_R}{Z_R^* + Z_R\Gamma}\mathbf{TR} - \frac{2\,\mathrm{Re}(Z_R)}{(Z_R^* + \Gamma Z_R)^2}\frac{1+j\lambda_1}{(I_1^{ch})^2}\mathbf{TR} . \tag{3.42}$$

From (3.38), the input impedance of the antenna, Z_A, is

$$Z_A = \frac{Z_R^* + \Gamma Z_R}{1-\Gamma} \approx \frac{1+j\lambda_1}{(I_1^{ch})^2} . \tag{3.43}$$

Substituting (3.43) into (3.42) and rearranging the result, we obtain

$$\mathbf{S} \approx \mathbf{I} - \frac{1}{1-\Gamma}\mathbf{TR} . \tag{3.44}$$

Equation (3.44) is the same as equation (3.23), which is the equation for **S** of a CMS antenna. Therefore, an antenna whose behavior is dominated by a single characteristic mode becomes a CMS antenna when a load impedance is observed at the feed gap. If a load impedance is observed at a position separate from a feed gap in the feed waveguide (or transmission line), an antenna dominated by a single characteristic mode becomes an

MS antenna because a reactive load should be connected to the antenna port for the impedance seen looking into a load to be the impedance of an open-circuit.

3.2.4 Validation

To verify the theory, we calculated the **S**-matrix in (2.13) using two different methods and compared the two results. In one method, each spherical wave was incident on an antenna with a load whose impedance value was the same as the characteristic impedance of a feed waveguide. Next, we calculated the amplitudes of the scattered spherical waves generated by currents induced on an antenna and used this to determine **S**. In another method, we calculated **S** from the characteristic modes using the formula presented in this paper.

We simulated two antennas. The first example is a dipole antenna with a length of 300 mm and diameter of 1 mm. The conductivity of the wire was 10^5 S/m. The wire was on the *z* axis, and the center of the dipole was located at the origin of the coordinate system. The feed gap was at the center of the dipole antenna, and a waveguide with a characteristic impedance of 500 Ω was connected to the feed gap. The frequency was 2 GHz, which gave a dipole length of 2 wavelengths. The second example is a bow-tie antenna. The bow-tie antenna was made of copper, and its dimensions are shown in Figure 5.2. The bow-tie antenna was fed at its center, and the characteristic impedance of the feed waveguide was 100 Ω. The frequency was 3 GHz.

We calculated the impedance matrix ($\mathbf{R_C} + j\,\mathbf{X_C}$) for the dipole antenna using a pulse function for the expansion and point matching for testing [26]. For the bow-tie antenna, we

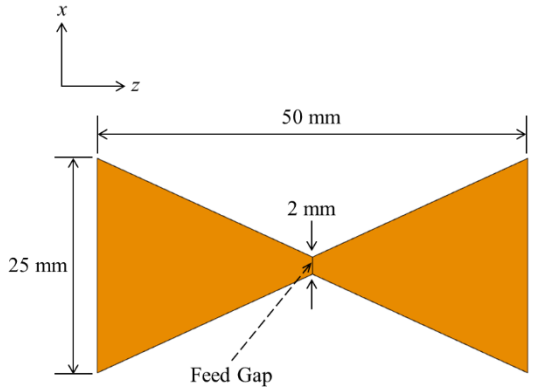

Figure 3.8 Bow-tie antenna. The origin of the coordinate system is at the center of the bow-tie antenna.

extracted the impedance matrix using the EM simulator FEKO, which uses an RWG basis function [28]. When we calculated **S** using the first method, we connected loads of 500 Ω and 100 Ω to the feed gaps of the dipole antenna and the bow-tie antenna, respectively. When we calculated **S** using (3.34), we used the characteristic modes defined in (2.64). We truncated the number of characteristic modes so that **S** was convergent. We used eight dominant characteristic modes for the dipole antenna and six dominant characteristic modes for the bow-tie antenna.

Tables 3.1 and 3.2 show the eigenvalues of several low-order characteristic modes and the complex amplitudes of the dominant spherical waves that each characteristic mode generates. Figure 3.3 shows the **S** calculated using the two methods for the dipole antenna, and Figure 3.4 shows the **S** calculated using the two methods for the bow-tie antenna. We show the dominant spherical waves in **S** in Figures 3.3 and 3.4. The two results are almost the same, which shows the validity of the proposed method to determine the generalized scattering matrix.

Table 3.1 Eigenvalues of characteristic modes and coefficients of dominant spherical waves generated by the characteristic currents for a dipole antenna

Mode Number	Eigenvalue	Dominant Spherical Wave	Amplitude
1	0.427	TM_{02}	− 0.398
		TM_{04}	0.769
		TM_{06}	0.376
2	2.358	TM_{03}	0.874
		TM_{05}	0.430
3	2.452	TM_{01}	− 0.980
4	2.475	TM_{02}	− 0.880
		TM_{04}	− 0.429
5	− 18.364	TM_{03}	− 0.331
		TM_{05}	0.695
		TM_{07}	0.285

Table 3.2 Eigenvalues of characteristic modes and coefficients of dominant spherical waves generated by the characteristic currents for a bow-tie antenna

Mode Number	Eigenvalue	Dominant Spherical Wave	Amplitude
1	1.511	TM_{01}	0.998
2	− 9.028	TM_{-11}	− 0.670
		TM_{11}	0.670
		TE_{-12}	$-0.195\,j$
		TE_{12}	$-0.195\,j$
3	− 14.908	TE_{-11}	$-0.396\,j$
		TE_{11}	$-0.396\,j$
		TM_{-12}	− 0.582
		TM_{12}	0.582
4	− 28.245	TM_{02}	0.994
5	35.691	TE_{-11}	$-0.575\,j$
		TE_{11}	$-0.575\,j$
		TM_{-12}	0.389
		TM_{12}	− 0.389

	5 (TM_{01})	14 (TM_{02})	27 (TM_{03})	44 (TM_{04})	65 (TM_{05})	90 (TM_{06})	119 (TM_{07})	152 (TM_{08})
5 (TM_{01})	$0.3708+0.5109j$	0	$0.0906+0.1072j$	0	$0.2252-0.0103j$	0	$0.0674-0.0072j$	0
14 (TM_{02})	0	$0.5461+0.6628j$	0	$0.3707+0.0080j$	0	$0.2081-0.0643j$	0	$0.0419-0.0161j$
27 (TM_{03})	$0.0906+0.1072j$	0	$0.7418+0.5052j$	0	$-0.1723+0.2660j$	0	$-0.0421+0.0608j$	0
44 (TM_{04})	0	$0.3707+0.0080j$	0	$0.0175+0.6138j$	0	$-0.4662+0.2676j$	0	$-0.0899+0.0504j$
65 (TM_{05})	$0.2252-0.0103j$	0	$-0.1723+0.2660j$	0	$0.8273+0.0803j$	0	$-0.0469+0.0085j$	0
90 (TM_{06})	0	$0.2081-0.0643j$	0	$-0.4662+0.2676j$	0	$0.7754+0.1188j$	0	$-0.0435+0.0221j$
119 (TM_{07})	$0.0674-0.0072j$	0	$-0.0421+0.0608j$	0	$-0.0469+0.0085j$	0	$0.9870-0.0021j$	0
152 (TM_{08})	0	$0.0419-0.0161j$	0	$-0.0899+0.0504j$	0	$-0.0435+0.0221j$	0	$0.9916+0.0040j$

Figure 3.9 **S**-matrix of the dipole antenna obtained using the two methods, providing almost the same results. The numbers to the left of the matrix indicate the row numbers and the numbers on top of the matrix indicate the column numbers. The letters in the parentheses indicate the mode type.

	1 (TE_{-11})	3 (TE_{11})	4 (TM_{-11})	5 (TM_{01})	6 (TM_{11})	8 (TE_{-12})	10 (TE_{12})	13 (TM_{-12})	14 (TM_{02})	15 (TM_{12})
1 (TE_{-11})	$0.9981-0.0024j$	$-0.0019-0.0024j$	$0.0000-0.0000j$	$-0.0001-0.0000j$	$-0.0000+0.0000j$	$-0.0000+0.0000j$	$-0.0000+0.0000j$	$0.0434-0.0017j$	$-0.0000+0.0000j$	$-0.0434+0.0017j$
3 (TE_{11})	$-0.0019-0.0024j$	$0.9981-0.0024j$	$0.0000-0.0000j$	$-0.0001-0.0000j$	$-0.0000+0.0000j$	$-0.0000+0.0000j$	$-0.0000+0.0000j$	$0.0434-0.0017j$	$-0.0000+0.0000j$	$-0.0434+0.0017j$
4 (TM_{-11})	$-0.0000+0.0000j$	$-0.0000+0.0000j$	$0.9891-0.0972j$	$0.0001+0.0001j$	$0.0109+0.0972j$	$-0.0316+0.0031j$	$-0.0316+0.0031j$	$-0.0000-0.0000j$	$-0.0000-0.0000j$	$0.0000+0.0000j$
5 (TM_{01})	$0.0001+0.0000j$	$0.0001+0.0000j$	$0.0001+0.0001j$	$0.2722+0.3965j$	$-0.0001-0.0001j$	$-0.0000-0.0000j$	$-0.0000-0.0000j$	$-0.0001+0.0001j$	$0.0001-0.0002j$	$0.0001-0.0001j$
6 (TM_{11})	$0.0000-0.0000j$	$0.0000-0.0000j$	$0.0109+0.0972j$	$-0.0001-0.0001j$	$0.9891-0.0972j$	$0.0316-0.0031j$	$0.0316-0.0031j$	$0.0000+0.0000j$	$0.0000+0.0000j$	$-0.0000-0.0000j$
8 (TE_{-12})	$-0.0000+0.0000j$	$-0.0000+0.0000j$	$0.0316-0.0031j$	$0.0000+0.0000j$	$-0.0316+0.0031j$	$0.9990+0.0019j$	$-0.0010+0.0019j$	$-0.0000+0.0000j$	$-0.0000+0.0000j$	$0.0000-0.0000j$
10 (TE_{12})	$-0.0000+0.0000j$	$-0.0000+0.0000j$	$0.0316-0.0031j$	$0.0000+0.0000j$	$-0.0316+0.0031j$	$-0.0010+0.0019j$	$0.9990+0.0019j$	$-0.0000+0.0000j$	$-0.0000+0.0000j$	$0.0000-0.0000j$
13 (TM_{-12})	$-0.0434+0.0017j$	$-0.0434+0.0017j$	$-0.0000-0.0000j$	$-0.0001+0.0001j$	$0.0000+0.0000j$	$0.0000-0.0000j$	$0.0000-0.0000j$	$0.9967-0.0368j$	$0.0000+0.0000j$	$0.0033+0.0368j$
14 (TM_{02})	$0.0000-0.0000j$	$0.0000-0.0000j$	$-0.0000-0.0000j$	$0.0001-0.0002j$	$0.0000+0.0000j$	$0.0000-0.0000j$	$0.0000-0.0000j$	$0.0000+0.0000j$	$0.9975-0.0699j$	$-0.0000-0.0000j$
15 (TM_{12})	$0.0434-0.0017j$	$0.0434-0.0017j$	$0.0000+0.0000j$	$0.0001-0.0001j$	$-0.0000-0.0000j$	$-0.0000+0.0000j$	$-0.0000+0.0000j$	$0.0033+0.0368j$	$-0.0000-0.0000j$	$0.9967-0.0368j$

Figure 3.10 **S**-matrix of the bow-tie antenna obtained using the two methods, providing almost the same results. The numbers to the left of the matrix indicate the row numbers and the numbers on top of the matrix indicate the column numbers. The letters in the parentheses indicate the mode type.

Chapter 4

Analysis of Coupling among Antennas

It is important to determine the voltages and currents at the feed ports of coupled antennas. Coupled antennas can be considered a network whose ports are the feed ports of antennas. Let the total number of ports of a network be N. Let V_m be the voltage at the mth port and I_n be the current at the nth port. A relation between V_m and I_n can be described in terms of the impedance parameters as follows:

$$V_m = \sum_{n=1}^{N} Z_{mn} I_n \tag{4.1}$$

Z_{mn} is called the impedance parameter or Z-parameter. A relation between V_m and I_n can also be described in terms of admittance parameters as follows:

$$I_m = \sum_{n=1}^{N} Y_{mn} V_n \tag{4.2}$$

Y_{mn} is called the admittance parameter or Y-parameter. Let a_n be the coefficient of an incident wave at the nth port and b_m be the coefficient of a reflected wave at the mth port. A

relation between a_n and b_m can be described in terms of scattering parameters as follows:

$$b_m = \sum_{n=1}^{N} S_{mn} a_n \tag{4.3}$$

S_{mn} is called the scattering parameter or S-parameter. In this chapter, several methods for calculating impedance parameters, admittance parameters and scattering parameters for coupled antennas are studied.

4.1 Analysis of Coupling among Antennas using a Generalized Scattering Matrix

4.1.1 Analysis of Coupling between Two Antennas in Free Space

A. Network Representation of Coupled Antennas

Consider a situation in which two antennas are present in free space. It is assumed that the two minimum spheres, one enclosing each antenna, do not overlap. We place the origin of coordinate system 1 (x_1, y_1, z_1 axes) at the position of antenna 1 and the origin of coordinate system 2 (x_2, y_2, z_2 axes) at the position of antenna 2, as shown in Figure 4.1. Coordinate system 3 (x_3, y_3, z_3 axes) is obtained by translating coordinate system 1, and coordinate system 2 is obtained by rotating coordinate system 3. The origin of coordinate system 3 is located at [r, θ, ϕ] in the spherical coordinates of coordinate system 1, and the rotation of the coordinates is expressed as the Euler angles [χ_0, θ_0, ϕ_0][2, Appendix A2]. The voltage and current at the feed port of antenna 1 are denoted by V_1 and I_1, respectively, and the voltage and current at the feed port of antenna 2 are denoted by V_2 and I_2, respectively.

The coupling of the two antennas can be considered as a cascade of three networks, as

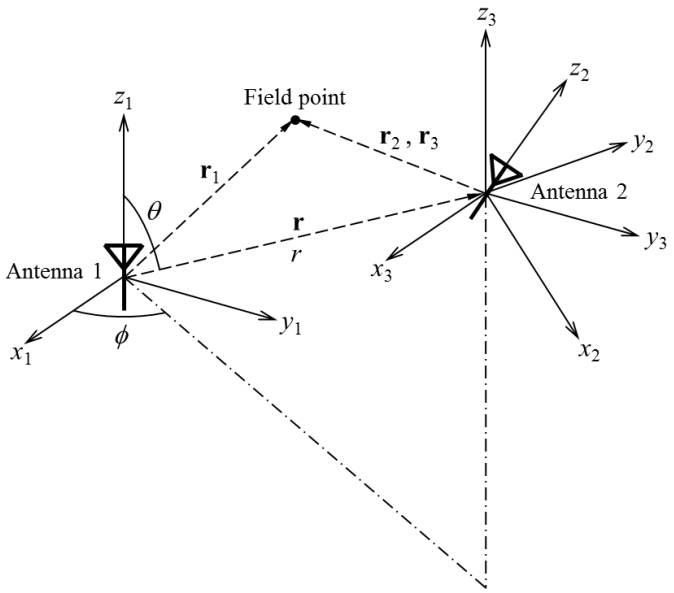

Figure 4.1 Coordinate systems and antennas.

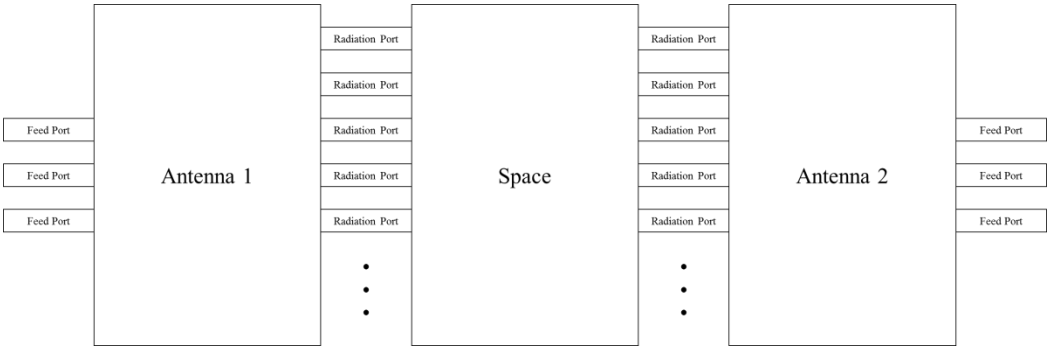

Figure 4.2 Network representation of coupled two antennas.

shown in Figure 4.2. Two of the networks are antenna networks described by a generalized scattering matrix, and the intermediate network represents the space outside the two spheres that surround antenna 1 and antenna 2. The intermediate network will be called a space network. The left side ports of the space network represent radiation ports with

respect to coordinate system 1, and the right side ports of the space network represent radiation ports with respect to coordinate system 2.

A radiation port (spherical wave port) is a virtual port. In one radiation port, one inward-propagating spherical wave and one outward-propagating spherical wave exist. Radiation ports can be addressed by considering them as physical ports. In the radiation port, the coefficient of the incoming spherical wave is considered the coefficient of the incident wave, and the coefficient of the outgoing spherical wave is considered the coefficient of the reflected wave.

B. Conversion of Spherical Wave Coefficients

To determine the impedance and admittance parameters between two antennas, an equation to relate the coefficients at the radiation ports of the space network is required. In this section, the relation between the coefficients at the radiation ports of a space network is determined.

Let the coefficient of the qth incoming spherical wave with respect to coordinate system p be $a_q^{(p)}$ and the coefficient of the qth outgoing spherical wave with respect to coordinate system p be $b_q^{(p)}$. Let $\mathbf{a}_p$ and $\mathbf{b}_p$ be column matrices and let the qth entries of $\mathbf{a}_p$ and $\mathbf{b}_p$ be $a_q^{(p)}$ and $b_q^{(p)}$, respectively. The total field is the superposition of the field generated by antenna 1 and the field generated by antenna 2 when there is no incident field outside the two antennas. In the sphere that is centered at the origin of coordinate system 1 and has radius r, the field generated by antenna 2 is composed of incoming and outgoing spherical waves with respect to coordinate system 1, and the coefficients of the incoming

and outgoing spherical waves are equal. The coefficient of the qth incoming spherical wave in coordinate system 1, $a_q^{(1)}$, is purely due to the current of antenna 2. Therefore, the coefficient of the qth outgoing spherical wave generated by antenna 1 alone is $b_q^{(1)} - a_q^{(1)}$ with respect to coordinate system 1. The coefficient of the pth incoming spherical wave in coordinate system 3, $a_p^{(3)}$, can be expanded in terms of $b_q^{(1)} - a_q^{(1)}$ using the translational addition theorem:

$$a_p^{(3)} = \sum_{q=1}^{\infty} \frac{1}{2} G_{pq}^T \left(r, \theta, \phi\right)\left(b_q^{(1)} - a_q^{(1)}\right) \tag{4.4}$$

where G_{pq}^T is defined by

$$G_{pq}^T \left(r, \theta, \phi\right) = \begin{cases} A_{\mu\nu,mn}^{(4)} \left(r, \theta, \phi\right) & \text{when } s = \sigma \\ B_{\mu\nu,mn}^{(4)} \left(r, \theta, \phi\right) & \text{when } s \neq \sigma \end{cases} \tag{4.5}$$

where $A_{\mu\nu,mn}^{(4)} \left(r, \theta, \phi\right)$ and $B_{\mu\nu,mn}^{(4)} \left(r, \theta, \phi\right)$ are functions defined in the Appendix. $\{\sigma, \mu, \nu\}$ are the indices for spherical waves. p and q satisfy the following equations:

$$p = (\sigma - 1)(2\nu + 1) + (2\nu - 1)(\nu + 1) + \mu \tag{4.6a}$$

$$q = (s - 1)(2n + 1) + (2n - 1)(n + 1) + m \tag{4.6b}$$

Equation (4.4) can be written in matrix form:

$$\mathbf{a}_3 = \frac{1}{2} \mathbf{G}^T \left(r, \theta, \phi\right)\left(\mathbf{b}_1 - \mathbf{a}_1\right) \tag{4.7}$$

where the entry in the pth row and qth column of $\mathbf{G}^T$ is G_{pq}^T. The coefficient of the pth incoming spherical wave in coordinate system 2, $a_p^{(2)}$, can be expanded in terms of $a_q^{(3)}$ using the rotational addition theorem:

$$a_p^{(2)} = \sum_{q=1}^{\infty} G_{pq}^R \left(\chi_0, \theta_0, \phi_0\right) a_q^{(3)} \tag{4.8}$$

where G_{pq}^R is defined as

$$G_{pq}^R \left(\chi_0, \theta_0, \phi_0\right) = \begin{cases} D_{\mu m}^n \left(\chi_0, \theta_0, \phi_0\right) & \text{when } s = \sigma \text{ and } n = \nu \\ 0 & \text{otherwise} \end{cases} \tag{4.9}$$

where $D_{\mu m}^n \left(\chi_0, \theta_0, \phi_0\right)$ is a function defined in the Appendix, and p and q are given by (4.6a) and (4.6b), respectively. Equation (4.8) can be written in matrix form:

$$\mathbf{a}_2 = \mathbf{G}^R \left(\chi_0, \theta_0, \phi_0\right) \mathbf{a}_3 \tag{4.10}$$

where the entry in the pth row and qth column of $\mathbf{G}^R$ is G_{pq}^R. Therefore, the relation between $\mathbf{b}_1 - \mathbf{a}_1$ and $\mathbf{a}_2$ can be written as

$$\mathbf{a}_2 = \frac{1}{2} \mathbf{G}^R \left(\chi_0, \theta_0, \phi_0\right) \mathbf{G}^T \left(r, \theta, \phi\right) \left(\mathbf{b}_1 - \mathbf{a}_1\right). \tag{4.11}$$

Likewise, the relation between $\mathbf{b}_3 - \mathbf{a}_3$ and $\mathbf{a}_1$ can be written as

$$\mathbf{a}_1 = \frac{1}{2} \mathbf{G}^T \left(r, \pi - \theta, \pi + \phi\right) \mathbf{G}^R \left(-\phi_0, -\theta_0, -\chi_0\right) \left(\mathbf{b}_2 - \mathbf{a}_2\right). \tag{4.12}$$

$\mathbf{G}^R \left(\chi_0, \theta_0, \phi_0\right) \mathbf{G}^T \left(r, \theta, \phi\right)$ will be denoted by $\mathbf{G}^+$, and $\mathbf{G}^T \left(r, \pi - \theta, \pi + \phi\right) \mathbf{G}^R \left(-\phi_0, -\theta_0, -\chi_0\right)$ will be denoted by $\mathbf{G}^-$, that is,

$$\mathbf{a}_2 = \frac{1}{2} \mathbf{G}^+ \left(\mathbf{b}_1 - \mathbf{a}_1\right) \tag{4.13a}$$

$$\mathbf{a}_1 = \frac{1}{2} \mathbf{G}^- \left(\mathbf{b}_2 - \mathbf{a}_2\right). \tag{4.13b}$$

C. Impedance Parameters and Admittance Parameters between Two Antennas

In this section, it is assumed that an antenna has one feed port and that one set of power waves (one incident power wave and one reflected power wave) exist at the feed port. Let the generalized-scattering-matrices of antenna 1 and antenna 2 be, respectively,

$$\mathbf{S}^{(1)} = \left[\begin{array}{c:c} \Gamma_1 & \mathbf{R}_1 \\ \hdashline \mathbf{T}_1 & \mathbf{S}_1 \end{array}\right], \qquad \mathbf{S}^{(2)} = \left[\begin{array}{c:c} \Gamma_2 & \mathbf{R}_2 \\ \hdashline \mathbf{T}_2 & \mathbf{S}_2 \end{array}\right] \tag{4.14}$$

where $\mathbf{S}^{(1)}$ and $\mathbf{S}^{(2)}$ refer to coordinate system 1 and coordinate system 2, respectively. Let the reference impedances of the feed ports of antenna 1 and antenna 2 be Z_{R1} and Z_{R2}, respectively. The generalized-scattering-matrix equations of antenna 1 and antenna 2 can be expressed as follows:

$$\left[\begin{array}{c} \left(V_1 - Z_{R1}^* I_1\right)\big/ 2\sqrt{\mathrm{Re}(Z_{R1})} \\ \hdashline \mathbf{b}_1 \end{array}\right] = \left[\begin{array}{c:c} \Gamma_1 & \mathbf{R}_1 \\ \hdashline \mathbf{T}_1 & \mathbf{S}_1 \end{array}\right] \left[\begin{array}{c} \left(V_1 + Z_{R1} I_1\right)\big/ 2\sqrt{\mathrm{Re}(Z_{R1})} \\ \hdashline \mathbf{a}_1 \end{array}\right] \tag{4.15a}$$

$$\left[\begin{array}{c} \left(V_2 - Z_{R2}^* I_2\right)\big/ 2\sqrt{\mathrm{Re}(Z_{R2})} \\ \hdashline \mathbf{b}_2 \end{array}\right] = \left[\begin{array}{c:c} \Gamma_2 & \mathbf{R}_2 \\ \hdashline \mathbf{T}_2 & \mathbf{S}_2 \end{array}\right] \left[\begin{array}{c} \left(V_2 + Z_{R2} I_2\right)\big/ 2\sqrt{\mathrm{Re}(Z_{R2})} \\ \hdashline \mathbf{a}_2 \end{array}\right] \tag{4.15b}$$

The impedance parameter for the two coupled antennas can be obtained by solving (4.13) and (4.15) and is given by the following:

$$Z_{11} = \frac{Z_{R1}^* + Z_{R1}\Gamma_1}{1-\Gamma_1} + \frac{\mathrm{Re}(Z_{R1})}{2\left(1-\Gamma_1\right)^2} \mathbf{R}_1 \mathbf{G}^- \left[\mathbf{I} - \frac{1}{4}\mathbf{P}_2^O \mathbf{G}^+ \mathbf{P}_1^O \mathbf{G}^-\right]^{-1} \mathbf{P}_2^O \mathbf{G}^+ \mathbf{T}_1 \tag{4.16a}$$

$$Z_{12} = \frac{\sqrt{\mathrm{Re}(Z_{R1})\,\mathrm{Re}(Z_{R2})}}{\left(1-\Gamma_1\right)\left(1-\Gamma_2\right)} \mathbf{R}_1 \mathbf{G}^- \left[\mathbf{I} - \frac{1}{4}\mathbf{P}_2^O \mathbf{G}^+ \mathbf{P}_1^O \mathbf{G}^-\right]^{-1} \mathbf{T}_2 \tag{4.16b}$$

$$Z_{21} = \frac{\sqrt{\mathrm{Re}(Z_{R1})\,\mathrm{Re}(Z_{R2})}}{\left(1-\Gamma_1\right)\left(1-\Gamma_2\right)} \mathbf{R}_2 \mathbf{G}^+ \left[\mathbf{I} - \frac{1}{4}\mathbf{P}_1^O \mathbf{G}^- \mathbf{P}_2^O \mathbf{G}^+\right]^{-1} \mathbf{T}_1 \tag{4.16c}$$

$$Z_{22} = \frac{Z_{R2}^{*} + Z_{R2}\Gamma_2}{1-\Gamma_2} + \frac{\mathrm{Re}(Z_{R2})}{2(1-\Gamma_2)^2}\mathbf{R}_2\mathbf{G}^{+}\left[\mathbf{I} - \frac{1}{4}\mathbf{P}_1^{O}\mathbf{G}^{-}\mathbf{P}_2^{O}\mathbf{G}^{+}\right]^{-1}\mathbf{P}_1^{O}\mathbf{G}^{-}\mathbf{T}_2 \qquad (4.16d)$$

where

$$\mathbf{P}_1^{O} = \mathbf{S}_1 + \frac{1}{1-\Gamma_1}\mathbf{T}_1\mathbf{R}_1 - \mathbf{I} \qquad (4.17a)$$

$$\mathbf{P}_2^{O} = \mathbf{S}_2 + \frac{1}{1-\Gamma_2}\mathbf{T}_2\mathbf{R}_2 - \mathbf{I} \qquad (4.17b)$$

The detailed procedure for the derivation of (4.16) is presented in Section 4.1.2.B. When the antennas are canonical-minimum-scattering antennas, $\mathbf{P}_1^{O}$ and $\mathbf{P}_2^{O}$ become zero from equation (3.23). Therefore, the impedance parameters between CMS antennas are as follows:

$$Z_{11} = \frac{Z_{R1}^{*} + Z_{R1}\Gamma_1}{1-\Gamma_1} = Z_{A1} \qquad (4.18a)$$

$$Z_{12} = \frac{\sqrt{\mathrm{Re}(Z_{R1})\,\mathrm{Re}(Z_{R2})}}{(1-\Gamma_1)(1-\Gamma_2)}\mathbf{R}_1\mathbf{G}^{-}\mathbf{T}_2 \qquad (4.18b)$$

$$Z_{21} = \frac{\sqrt{\mathrm{Re}(Z_{R1})\,\mathrm{Re}(Z_{R2})}}{(1-\Gamma_1)(1-\Gamma_2)}\mathbf{R}_2\mathbf{G}^{+}\mathbf{T}_1 \qquad (4.18c)$$

$$Z_{22} = \frac{Z_{R2}^{*} + Z_{R2}\Gamma_2}{1-\Gamma_2} = Z_{A2} \qquad (4.18d)$$

where Z_{A1} and Z_{A2} are the input impedances of antenna 1 and antenna 2, respectively.

Using the identity

$$(\mathbf{I}-\mathbf{A})^{-1} = \mathbf{I} + \mathbf{A} + \mathbf{A}^2 + \mathbf{A}^3 + \cdots, \qquad (4.19)$$

equations (4.16a) and (4.16c) are written as

$$Z_{11} = Z_{A1} + \frac{\mathrm{Re}(Z_{R1})}{2(1-\Gamma_1)^2}\Big[\mathbf{R}_1\mathbf{G}^{-}\mathbf{P}_2^{O}\mathbf{G}^{+}\mathbf{T}_1 + \frac{1}{4}\mathbf{R}_1\mathbf{G}^{-}\mathbf{P}_2^{O}\mathbf{G}^{+}\mathbf{P}_1^{O}\mathbf{G}^{-}\mathbf{P}_2^{O}\mathbf{G}^{+}\mathbf{T}_1 + \frac{1}{16}\mathbf{R}_1\mathbf{G}^{-}\left(\mathbf{P}_2^{O}\mathbf{G}^{+}\mathbf{P}_1^{O}\mathbf{G}^{-}\right)^2\mathbf{P}_2^{O}\mathbf{G}^{+}\mathbf{T}_1 + \cdots\Big] \quad (4.20a)$$

$$Z_{21} = \frac{\sqrt{\mathrm{Re}(Z_{R1})\mathrm{Re}(Z_{R2})}}{(1-\Gamma_1)(1-\Gamma_2)}\cdot \Big[\mathbf{R}_2\mathbf{G}^{+}\mathbf{T}_1 + \frac{1}{4}\mathbf{R}_2\mathbf{G}^{+}\mathbf{P}_1^{O}\mathbf{G}^{-}\mathbf{P}_2^{O}\mathbf{G}^{+}\mathbf{T}_1 + \frac{1}{16}\mathbf{R}_2\mathbf{G}^{+}\left(\mathbf{P}_1^{O}\mathbf{G}^{-}\mathbf{P}_2^{O}\mathbf{G}^{+}\right)^2\mathbf{T}_1 + \cdots\Big]. \quad (4.20b)$$

$\mathbf{P}_n^{O}\mathbf{a}_n$ represents the outgoing spherical wave coefficients for a scattered field by an open-circuited antenna *n*. Therefore, the higher-order terms (terms except for the first term) in the parentheses [] in (4.20a) and (4.20b) represent multiple reflections. The higher-order terms decay more rapidly than the first term as the distance between the two antennas increases [5]. Therefore, when the distance between two antennas is large, the higher-order terms can be neglected. Note that when the distance between two antennas is large, the mutual impedance between them is approximated by the mutual impedance between two CMS antennas.

The admittance parameters for two coupled antennas can be obtained from (4.13) and (4.15) and is given by the following:

$$Y_{11} = \frac{1-\Gamma_1}{Z_{R1}^{*}+Z_{R1}\Gamma_1} - \frac{\mathrm{Re}(Z_{R1})}{2\left(Z_{R1}^{*}+Z_{R1}\Gamma_1\right)^2}\mathbf{R}_1\mathbf{G}^{-}\left[\mathbf{I}-\frac{1}{4}\mathbf{P}_2^{S}\mathbf{G}^{+}\mathbf{P}_1^{S}\mathbf{G}^{-}\right]^{-1}\mathbf{P}_2^{S}\mathbf{G}^{+}\mathbf{T}_1 \quad (4.21a)$$

$$Y_{12} = \frac{-\sqrt{\mathrm{Re}(Z_{R1})\mathrm{Re}(Z_{R2})}}{\left(Z_{R1}^{*}+Z_{R1}\Gamma_1\right)\left(Z_{R2}^{*}+Z_{R2}\Gamma_2\right)}\mathbf{R}_1\mathbf{G}^{-}\left[\mathbf{I}-\frac{1}{4}\mathbf{P}_2^{S}\mathbf{G}^{+}\mathbf{P}_1^{S}\mathbf{G}^{-}\right]^{-1}\mathbf{T}_2 \quad (4.21b)$$

$$Y_{21} = \frac{-\sqrt{\mathrm{Re}(Z_{R1})\mathrm{Re}(Z_{R2})}}{\left(Z_{R1}^{*}+Z_{R1}\Gamma_1\right)\left(Z_{R2}^{*}+Z_{R2}\Gamma_2\right)}\mathbf{R}_2\mathbf{G}^{+}\left[\mathbf{I}-\frac{1}{4}\mathbf{P}_1^{S}\mathbf{G}^{-}\mathbf{P}_2^{S}\mathbf{G}^{+}\right]^{-1}\mathbf{T}_1 \quad (4.21c)$$

$$Y_{22} = \frac{1-\Gamma_2}{Z_{R2}^* + Z_{R2}\Gamma_2} - \frac{\mathrm{Re}(Z_{R2})}{2\left(Z_{R2}^* + Z_{R2}\Gamma_2\right)^2}\mathbf{R}_2\mathbf{G}^+\left[\mathbf{I} - \frac{1}{4}\mathbf{P}_1^S\mathbf{G}^-\mathbf{P}_2^S\mathbf{G}^+\right]^{-1}\mathbf{P}_1^S\mathbf{G}^-\mathbf{T}_2 \quad (4.21d)$$

where

$$\mathbf{P}_1^S = \mathbf{S}_1 - \frac{Z_{R1}}{Z_{R1}^* + Z_{R1}\Gamma_1}\mathbf{T}_1\mathbf{R}_1 - \mathbf{I} \quad (4.22a)$$

$$\mathbf{P}_2^S = \mathbf{S}_2 - \frac{Z_{R2}}{Z_{R2}^* + Z_{R2}\Gamma_2}\mathbf{T}_2\mathbf{R}_2 - \mathbf{I} \quad (4.22b)$$

When antennas are minimum-scattering antennas that do not scatter when short-circuited, $\mathbf{P}_1^S$ and $\mathbf{P}_2^S$ become zero from equation (3.24). In this case, the admittance parameters becomes as follows:

$$Y_{11} = \frac{1-\Gamma_1}{Z_{R1}^* + Z_{R1}\Gamma_1} = \frac{1}{Z_{A1}} \quad (4.23a)$$

$$Y_{12} = \frac{-\sqrt{\mathrm{Re}(Z_{R1})\,\mathrm{Re}(Z_{R2})}}{\left(Z_{R1}^* + Z_{R1}\Gamma_1\right)\left(Z_{R2}^* + Z_{R2}\Gamma_2\right)}\mathbf{R}_1\mathbf{G}^-\mathbf{T}_2 \quad (4.23b)$$

$$Y_{21} = \frac{-\sqrt{\mathrm{Re}(Z_{R1})\,\mathrm{Re}(Z_{R2})}}{\left(Z_{R1}^* + Z_{R1}\Gamma_1\right)\left(Z_{R2}^* + Z_{R2}\Gamma_2\right)}\mathbf{R}_2\mathbf{G}^+\mathbf{T}_1 \quad (4.23c)$$

$$Y_{22} = \frac{1-\Gamma_2}{Z_{R2}^* + Z_{R2}\Gamma_2} = \frac{1}{Z_{A2}} \quad (4.23d)$$

D. Electromagnetic Field Generated by Coupled Two Antennas

As explained in Section 4.1.2.B, the spherical wave coefficients produced by antenna 1 alone are $\mathbf{b}_1 - \mathbf{a}_1$ in coordinate system 1, and the spherical wave coefficients produced by antenna 2 alone are $\mathbf{b}_2 - \mathbf{a}_2$ in coordinate system 2. Solving (4.13) and (4.15), $\mathbf{b}_1 - \mathbf{a}_1$ and

$\mathbf{b}_2 - \mathbf{a}_2$ are obtained:

$$\mathbf{b}_1 - \mathbf{a}_1 = \left[\mathbf{I} - \frac{1}{4}\mathbf{P}_1^O \mathbf{G}^- \mathbf{P}_2^O \mathbf{G}^+\right]^{-1}\left[\frac{\sqrt{\mathrm{Re}(Z_{R1})}}{1-\Gamma_1} I_1 \mathbf{T}_1 + \frac{\sqrt{\mathrm{Re}(Z_{R2})}}{2(1-\Gamma_2)} I_2 \mathbf{P}_1^O \mathbf{G}^- \mathbf{T}_2\right] \tag{4.24a}$$

$$\mathbf{b}_2 - \mathbf{a}_2 = \left[\mathbf{I} - \frac{1}{4}\mathbf{P}_2^O \mathbf{G}^+ \mathbf{P}_1^O \mathbf{G}^-\right]^{-1}\left[\frac{\sqrt{\mathrm{Re}(Z_{R2})}}{1-\Gamma_2} I_2 \mathbf{T}_2 + \frac{\sqrt{\mathrm{Re}(Z_{R1})}}{2(1-\Gamma_1)} I_1 \mathbf{P}_2^O \mathbf{G}^+ \mathbf{T}_1\right] \tag{4.24b}$$

An alternative formula is

$$\mathbf{b}_1 - \mathbf{a}_1 = \left[\mathbf{I} - \frac{1}{4}\mathbf{P}_1^S \mathbf{G}^- \mathbf{P}_2^S \mathbf{G}^+\right]^{-1}\left[\frac{\sqrt{\mathrm{Re}(Z_{R1})}}{Z_{R1}^* + Z_{R1}\Gamma_1} V_1 \mathbf{T}_1 + \frac{\sqrt{\mathrm{Re}(Z_{R2})}}{2(Z_{R2}^* + Z_{R2}\Gamma_2)} V_2 \mathbf{P}_1^S \mathbf{G}^- \mathbf{T}_2\right] \tag{4.25a}$$

$$\mathbf{b}_2 - \mathbf{a}_2 = \left[\mathbf{I} - \frac{1}{4}\mathbf{P}_2^S \mathbf{G}^+ \mathbf{P}_1^S \mathbf{G}^-\right]^{-1}\left[\frac{\sqrt{\mathrm{Re}(Z_{R2})}}{Z_{R2}^* + Z_{R2}\Gamma_2} V_2 \mathbf{T}_2 + \frac{\sqrt{\mathrm{Re}(Z_{R1})}}{2(Z_{R1}^* + Z_{R1}\Gamma_1)} V_1 \mathbf{P}_2^S \mathbf{G}^+ \mathbf{T}_1\right]. \tag{4.25b}$$

A detailed derivation of (4.24) and (4.25) is presented in Section 4.1.2.B. If the antennas are canonical-minimum-scattering antennas, equation (4.24) becomes

$$\mathbf{b}_1 - \mathbf{a}_1 = \frac{\sqrt{\mathrm{Re}(Z_{R1})}}{1-\Gamma_1} I_1 \mathbf{T}_1 \tag{4.26a}$$

$$\mathbf{b}_2 - \mathbf{a}_2 = \frac{\sqrt{\mathrm{Re}(Z_{R2})}}{1-\Gamma_2} I_2 \mathbf{T}_2 . \tag{4.26b}$$

If the antennas are minimum-scattering antennas that do not scatter when short-circuited, equation (4.25) becomes

$$\mathbf{b}_1 - \mathbf{a}_1 = \frac{\sqrt{\mathrm{Re}(Z_{R1})}}{Z_{R1}^* + Z_{R1}\Gamma} V_1 \mathbf{T}_1 \tag{4.27a}$$

$$\mathbf{b}_2 - \mathbf{a}_2 = \frac{\sqrt{\mathrm{Re}(Z_{R2})}}{Z_{R2}^* + Z_{R2}\Gamma} V_2 \mathbf{T}_2 . \tag{4.27b}$$

V_1, V_2, I_1, and I_2 in equations (4.24) – (4.27) can be determined from the impedance parameters or admittance parameters. From (4.24) or (4.25) and the spherical wave functions in Section 2.1.1, we can calculate the electromagnetic field generated by two antennas in free space when they are excited by sources.

When antenna 2 is open-circuited and antenna 1 is excited with a current of 1 A, the spherical wave coefficients produced by antenna 1 alone are denoted by $\mathbf{b}_1^{o2}$, and the spherical wave coefficients produced by antenna 2 alone are denoted by $\mathbf{b}_2^{o2}$. When antenna 1 is open-circuited and antenna 2 is excited with a current of 1 A, the spherical wave coefficients produced by antenna 2 alone are denoted by $\mathbf{b}_2^{o1}$, and the spherical wave coefficients produced by antenna 1 alone are denoted by $\mathbf{b}_1^{o1}$. Then, (4.16) can be written as follows:

$$Z_{11} = \frac{Z_{R1}^* + Z_{R1}\Gamma_1}{1-\Gamma_1} + \frac{\sqrt{\mathrm{Re}(Z_{R1})}}{1-\Gamma_1} \mathbf{R}_1 \mathbf{G}^{-} \mathbf{b}_2^{o2} \tag{4.28a}$$

$$Z_{12} = \frac{\sqrt{\mathrm{Re}(Z_{R1})}}{1-\Gamma_1} \mathbf{R}_1 \mathbf{G}^{-} \mathbf{b}_2^{o1} \tag{4.28b}$$

$$Z_{21} = \frac{\sqrt{\mathrm{Re}(Z_{R2})}}{1-\Gamma_2} \mathbf{R}_2 \mathbf{G}^{+} \mathbf{b}_1^{o2} \tag{4.28c}$$

$$Z_{22} = \frac{Z_{R2}^* + Z_{R2}\Gamma_2}{1-\Gamma_2} + \frac{\sqrt{\mathrm{Re}(Z_{R2})}}{1-\Gamma_2} \mathbf{R}_2 \mathbf{G}^{+} \mathbf{b}_1^{o1} \tag{4.28d}$$

E. Validation

To verify the formula, we calculated the Z-parameters, Y-parameters and electromagnetic fields near coupled antennas using the formulas presented in this dissertation and compared the results with those obtained using the EM simulator FEKO. We designed four helical antennas, which will be termed as antenna 1, antenna 2, antenna 3, and antenna 4. For antenna 1, the radius was 30 cm, the height was 20 cm, the number of turns was 4.5, and the diameter of the cross-section of the wire was 4 mm. For antenna 2, the radius was 24 cm, the height was 25 cm, the number of turns was 5.5, and the diameter of the cross-section of the wire was 4 mm. For antenna 3, the radius was 8 cm, the height was 10 cm, the number of turns was 8, and the diameter of the cross-section of the wire

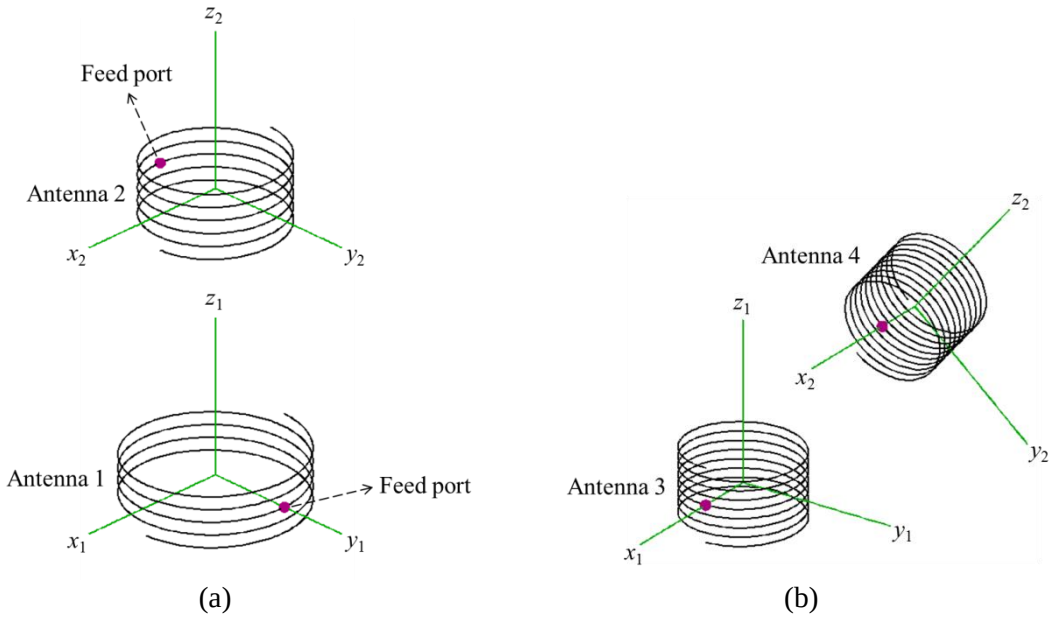

Figure 4.3 Antenna configurations and coordinate systems. (a) antenna 1 and antenna 2 (b) antenna 3 and antenna 4.

was 1 mm. For antenna 4, the radius was 7 cm, the height was 12 cm, the number of turns was 10, and the diameter of the cross-section of the wire was 1 mm. The wire used in all the antennas was made of copper, and all the antennas were fed at the center of the wire. The centers of antennas 1 and 3 were located at the origin of coordinate system 1, and their axes coincided with the z_1 axis. The centers of antennas 2 and 4 were located at the origin of coordinate system 2, and their axes coincided with the z_2 axis. For antenna 1, the coordinates for positions of the ends of the wire are [0.3, 0, −0.1] and [−0.3, 0, 0.1], and the coordinates for the position of the feed port is [0, 0.3, 0]. For antenna 2, the coordinates for the positions of the ends of the wire are [0.24, 0, −0.125] and [−0.24, 0, 0.125], and the coordinates for the position of the feed port is [0, −0.24, 0]. For antenna 3, the coordinates for the positions of the ends of the wire are [0.08, 0, −0.05] and [0.08, 0, 0.05], and the coordinates for the position of the feed port is [0.08, 0, 0]. For antenna 4, the coordinates for the positions of ends of the wire are [0.07, 0, −0.06] and [0.07, 0, 0.06], and the coordinates for the position of the feed port is [0.07, 0, 0]. Here, the coordinates are rectangular coordinates, and the unit is m. The resonant frequencies of antenna 1, antenna 2, antenna 3, and antenna 4 are 12.7 MHz, 13.9 MHz, 29.4 MHz, and 28.9 MHz, respectively. The four antennas operated at a frequency of 13.56 MHz.

The author extracted the current distributions of the helical antennas using FEKO. Using equation (2.7), the author calculated the modal transmitting pattern **T** at a frequency of 13.56 MHz, with the reference impedances being the complex conjugates of the input impedances of the antennas. Table 4.1 and Table 4.2 show the input impedance and the dominant spherical wave coefficients in the modal transmitting pattern for each antenna.

Table 4.1 Coefficients of dominant spherical waves
and input impedances for antenna 1 and antenna 2

	Antenna 1	Antenna 2
TE_{01} mode coefficient	− 0.448	− 0.359
TM_{01} mode coefficient	− 0.248	− 0.318
Input impedance (Ω)	$0.546 + j102$	$0.427 - j42.25$

Table 4.2 Coefficients of dominant spherical waves
and input impedances for antenna 3 and antenna 4

	Antenna 3	Antenna 4
TE_{01} mode coefficient	− 0.0439	− 0.0400
TM_{01} mode coefficient	− 0.0969	− 0.111
Input impedance (Ω)	$0.341 - j1187$	$0.351 - j1252$

Antenna 1 and antenna 2 are dominated by a single characteristic mode, so the author assumed them to be canonical-minimum-scattering antennas. The resonant frequencies of antennas 3 and 4 are quite higher than 13.56 MHz, so we assumed them to be minimum-scattering antennas that do not scatter when short-circuited.

The author calculated the Z-parameters between antenna 1 and antenna 2 at 13.56 MHz. In this case, r varied from 60 cm to 150 cm, and θ, ϕ, ϕ_0, θ_0, and χ_0 were all equal to 0. The Z-parameters were calculated with (4.18) using 6 spherical waves (maximum n is 1) and 30 spherical waves (maximum n is 3)[9]. We calculated the Y-parameters between antenna 3 and antenna 4 at 13.56 MHz. In this case, θ and ϕ were fixed at 40° and 90°,

[9] The number of spherical waves referenced in this section indicates the number of all the spherical waves for which the index n is not larger than the maximum value. In all the calculations in this section, many of the spherical waves do not contribute to the results.

respectively, and r varied from 20 cm to 110 cm. $\phi_0 = 90°$, $\theta_0 = \theta$, and $\chi_0 = -90°$, such that the line connecting the centers of the helices coincided with the z_2 axis, and the x_1 and x_2 axes were parallel. The Y-parameters were calculated with (4.23) using 6 spherical waves (maximum n of 1) and 30 spherical waves (maximum n of 3). Figure 4.4 and Figure 4.5 show the Z-parameter and Y-parameter values calculated using spherical waves and with FEKO. The Z- and Y- parameter values obtained using spherical waves agree well with those obtained using FEKO. When the two antennas are very close together, there are small errors between the result obtained with FEKO and the result obtained with spherical waves. If the exact generalized scattering matrices and the exact formulae (equations (4.16) and (4.21)) are used, the errors are reduced.

We calculated the electromagnetic field at 13.56 MHz for two configurations. Configuration 1 consists of antenna 1 and antenna 2, with r = 1 m and $\theta = \phi = \phi_0 = \theta_0 = \chi_0 = 0°$. A load of 10.8 + j45.0 Ω was connected to the feed port of antenna 2, and 10 V was applied to the feed port of antenna 1. The field was calculated using (4.26) at r_1 = 0.5 m, $\phi_1 = 0°$, and $\theta_1 = 0°$ to 360°, with the two antennas stationary. $\theta_1 = 180°$ to 360° and $\phi_1 = 0°$ corresponds to $\theta_1 = 180°$ to 0° and $\phi_1 = 180°$. [r_1, θ_1, ϕ_1] are the spherical coordinates for coordinate system 1. Configuration 2 consists of antenna 3 and antenna 4, with r = 30 cm, $\theta = 40°$, $\phi = 90°$, $\phi_0 = 90°$, $\theta_0 = 40°$, and $\chi_0 = -90°$. A load of 41.4 + j1251 Ω was connected to the feed port of antenna 4, and 10 V was applied to the feed port of antenna 3. The field was calculated using (4.27) at r_1 = 15 cm, $\phi_1 = 90°$, and $\theta_1 = 0°$ to 360°, with the two antennas stationary. $\theta_1 = 180°$ to 360° and $\phi_1 = 90°$ corresponds to $\theta_1 = 180°$ to 0° and

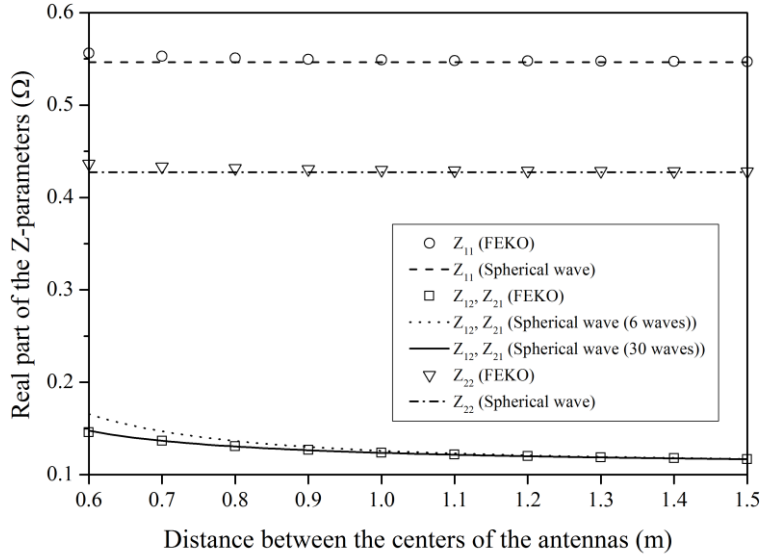

(a)

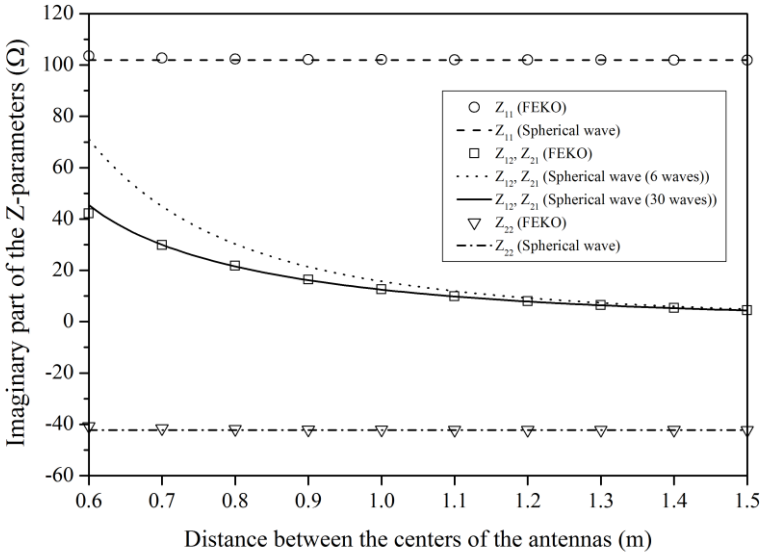

(b)

Figure 4.4 Z-parameters between antenna 1 and antenna 2. (a) real part (b) imaginary part.

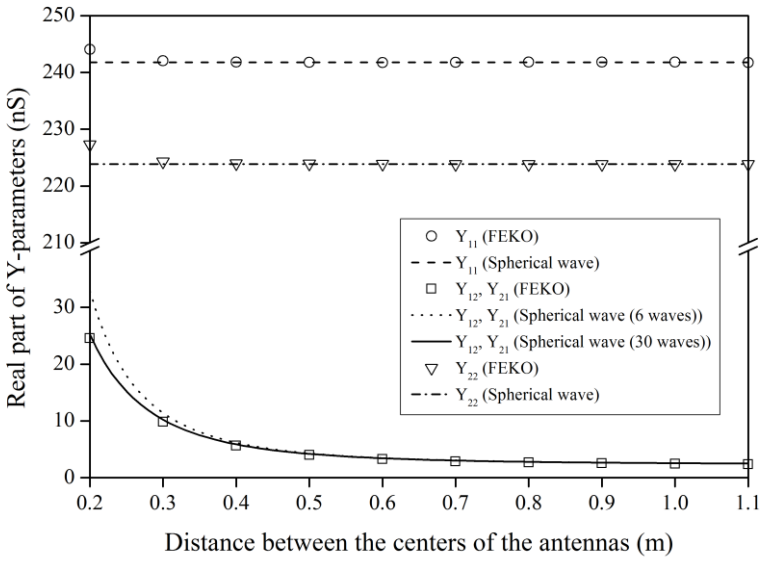

(a)

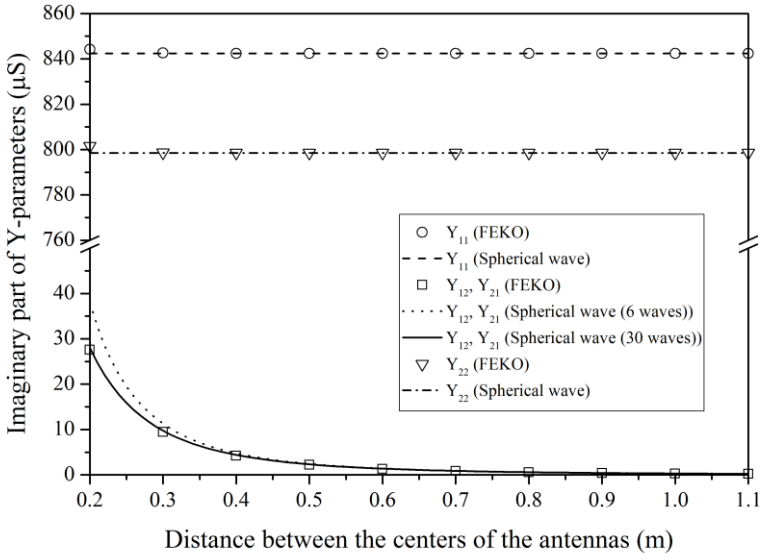

(b)

Figure 4.5 Y-parameters between antenna 3 and antenna 4. (a) real part (b) imaginary part.

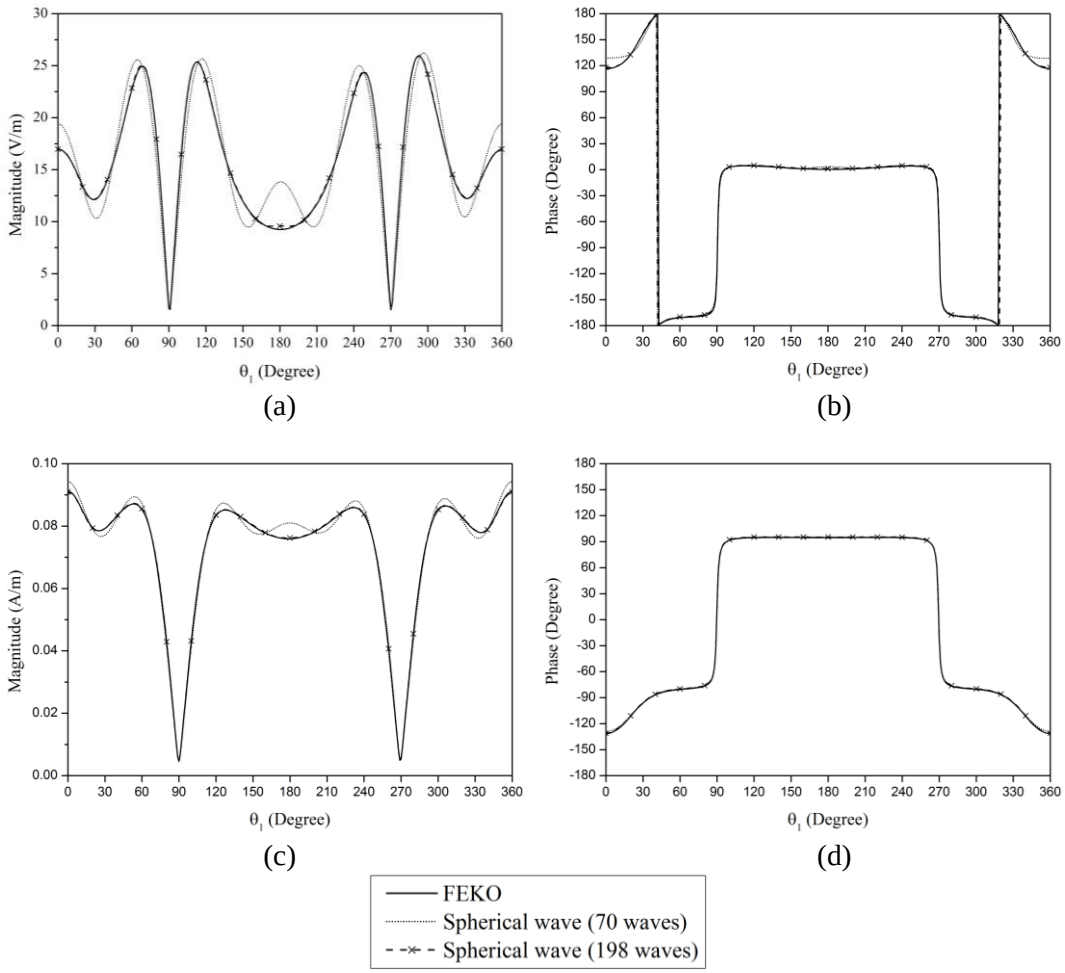

Figure 4.6 Electric and magnetic fields for configuration 1. (a) Magnitude of *r* component of the E-field (b) Phase of *r* component of the E-field (c) Magnitude of *r* component of the H-field (d) Phase of *r* component of the H-field.

ϕ_1 = 270°. When the fields were computed using spherical waves, 70 waves (maximum *n* of 5) and 198 waves (maximum *n* of 9) were used for configuration 1, and 30 waves (maximum *n* of 3) and 126 waves (maximum *n* of 7) were used for configuration 2. Figure 4.6 and Figure 4.7 show the *r* components of the E-field and the H-field calculated using

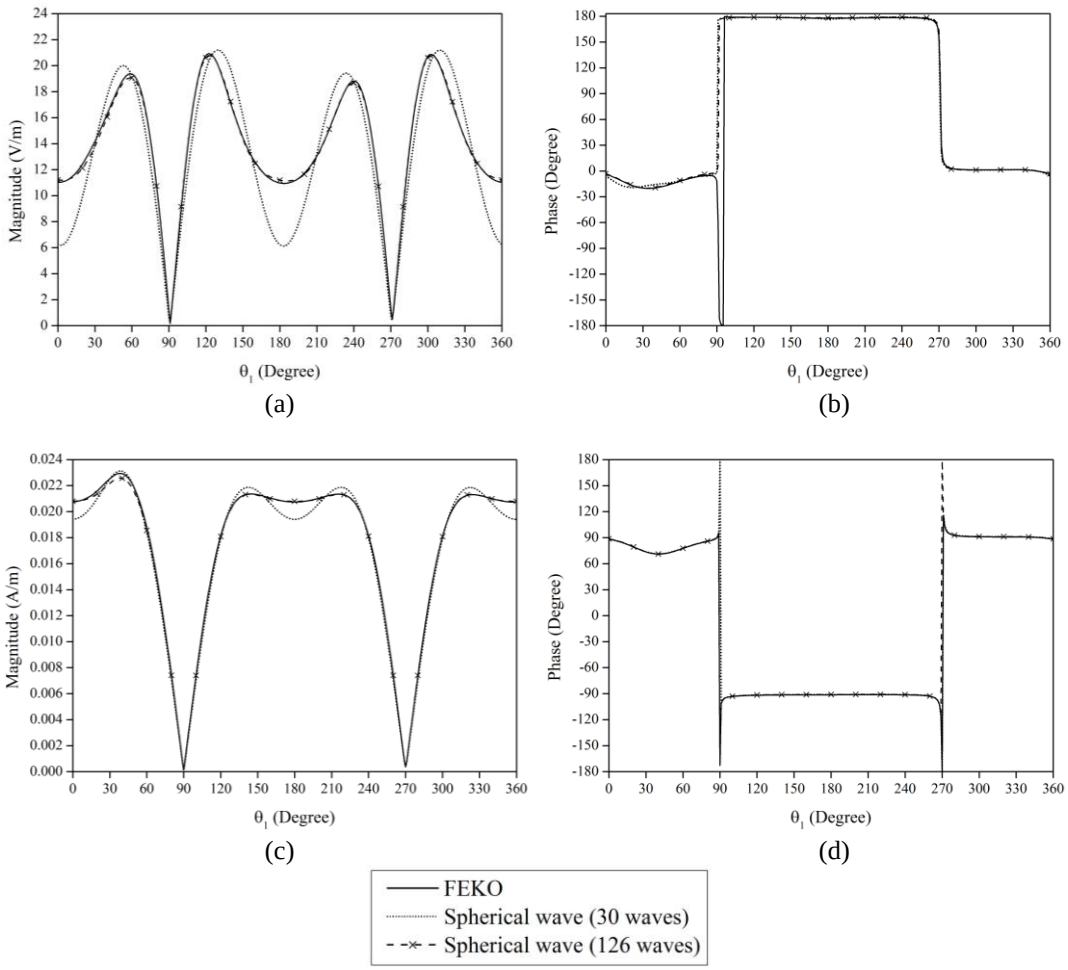

Figure 4.7 Electric and magnetic fields for configuration 2. (a) Magnitude of *r* component of the E-field (b) Phase of *r* component of the E-field (c) Magnitude of *r* component of the H-field (d) Phase of *r* component of the H-field.

spherical waves and using FEKO. For configuration 1, the graph for the fields calculated using 198 waves and the graph for the fields calculated using FEKO coincide, and for configuration 2, the graph for the fields calculated using 126 waves and the graph for the fields calculated using FEKO coincide. The θ component and the ϕ component of the

fields calculated using spherical waves and using FEKO also agree well. The author omits the graphs for the θ component and ϕ component.

4.1.2 Analysis of Coupling among Antennas in an Environment

In Section 4.1.1, the author determined the impedance and admittance parameters between two antennas in free space and the electromagnetic fields generated by two antennas in free space using a generalized scattering matrix. In practice, objects such as the ground, wall, and desks exist around antennas. Moreover, there may be more than two antennas. In this section, the author derives the impedance, admittance, and scattering parameters among multiple antennas and the electromagnetic field generated by antennas when objects are present near the antennas using a generalized scattering matrix.

A. Conversion of Spherical Wave Coefficients

When extraneous objects are present, the relation between the spherical wave coefficients with respect to one coordinate system and that with respect to another coordinate system is different from equation (4.13), which is used for free space. In this section, the relation between spherical wave coefficients for different coordinate systems in the presence of extraneous objects is determined.

Let current $\mathbf{J}_{s,m,n}^{(p)}$ generate only an outgoing spherical wave $\mathbf{E}_{s,m,n}^{(4)}$ with a coefficient of one with respect to coordinate system p when $\mathbf{J}_{s,m,n}^{(p)}$ is present alone in free space. p is a natural number. Let $\Sigma_{\min}^{(p)}$ be a surface of a minimum sphere among spheres that is centered on the origin of coordinate system p and encloses $\mathbf{J}_{s,m,n}^{(p)}$. Let $\Sigma_{\max}^{(p)}$ be a

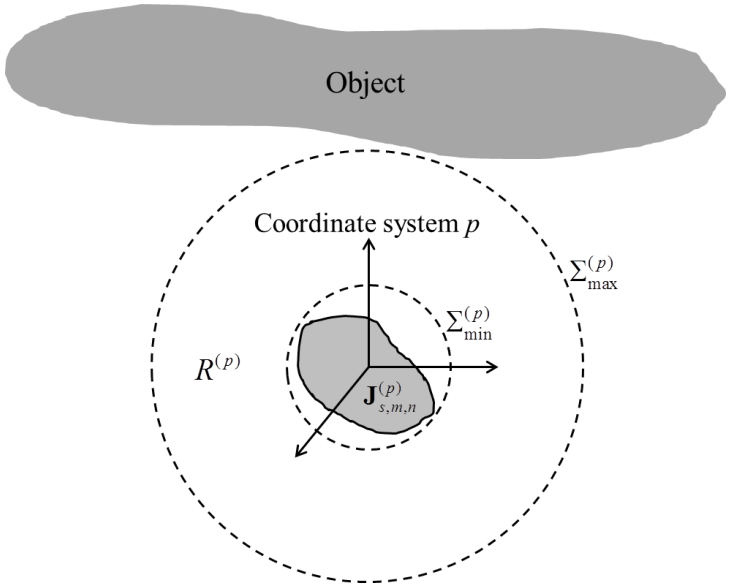

Figure 4.8 Current, minimum sphere, and maximum sphere.

surface of a maximum sphere among spheres that is centered on the origin of coordinate system p and does not contain part of objects or a current except for $\mathbf{J}_{s,m,n}^{(p)}$. Any objects or currents besides $\mathbf{J}_{s,m,n}^{(p)}$ are not inside $\Sigma_{\max}^{(p)}$. Let $R^{(p)}$ be a region between $\Sigma_{\min}^{(p)}$ and $\Sigma_{\max}^{(p)}$. Suppose that if objects are present near $\mathbf{J}_{s,m,n}^{(p)}$, the current distribution of $\mathbf{J}_{s,m,n}^{(p)}$ does not change from that of $\mathbf{J}_{s,m,n}^{(p)}$ in free space.

When objects are present near $\mathbf{J}_{s,m,n}^{(p)}$, the electromagnetic fields generated by $\mathbf{J}_{s,m,n}^{(p)}$ are scattered by objects, and the scattered fields are incident on $\mathbf{J}_{s,m,n}^{(p)}$. In region $R^{(p)}$, the field scattered by objects (i.e., the field generated by objects) can be expanded into standing spherical waves with respect to coordinate system p, because the scattered field is finite at the origin of coordinate system p. In region $R^{(p)}$, the coefficients of the incoming

spherical waves with respect to coordinate system p are purely attributable to objects because $\mathbf{J}_{s,m,n}^{(p)}$ cannot generate incoming spherical waves with respect to coordinate system p.

Let $\mathbf{a}_{s,m,n}^{(q,p)}$ be a column matrix whose entries are the coefficients of incoming spherical waves in $R^{(q)}$ with respect to coordinate system q when $\mathbf{J}_{s,m,n}^{(p)}$ and objects are present and no other currents are present. q may be the same as p or may be different from p. $\mathbf{a}_{s,m,n}^{(q,p)}$ can be calculated using equation (2.8) or the formula in [2, eq. (4.16)]. Let

$$\mathbf{J}^{(p)} = \sum_{s,m,n} b_{s,m,n}^{(p)} \mathbf{J}_{s,m,n}^{(p)} . \tag{4.29}$$

Let $\mathbf{a}^{(q,p)}$ be a column matrix containing the coefficients of the incoming spherical waves in $R^{(q)}$ with respect to coordinate system q when $\mathbf{J}^{(p)}$ and objects are present and no current besides $\mathbf{J}^{(p)}$ is present. By the superposition principle, $\mathbf{a}^{(q,p)}$ is represented by

$$\mathbf{a}^{(q,p)} = \sum_{s,m,n} b_{s,m,n}^{(p)} \mathbf{a}_{s,m,n}^{(q,p)} \tag{4.30}$$

Equation (4.30) can be written in matrix form as

$$\mathbf{a}^{(q,p)} = \mathbf{G}^{q,p} \mathbf{b}_t^{(p)} \tag{4.31}$$

where the ith column of $\mathbf{G}^{q,p}$ is $\mathbf{a}_{s,m,n}^{(p,p)}$, with $\{s, m, n\}$ satisfying equation (2.5), and the ith entry of $\mathbf{b}_t^{(p)}$ is $b_{s,m,n}^{(p)}$, with $\{s, m, n\}$ satisfying equation (2.5). Note that $\mathbf{b}_t^{(p)}$ is the same as the column matrix containing the coefficients of the outgoing spherical waves generated by $\mathbf{J}^{(p)}$ in free space.

Let $\mathbf{a}_p$ be a column matrix containing the coefficients of the incoming spherical waves

in $R^{(p)}$ with respect to coordinate system p. Let $\mathbf{J}^{(1)}$, $\mathbf{J}^{(2)}$, $\mathbf{J}^{(3)}$, $\cdots$, $\mathbf{J}^{(N)}$, and objects exist. In this case, $\mathbf{a}_p$ can be determined from (4.31) using the superposition principle:

$$\mathbf{a}_p = \sum_{n=1}^{N} \mathbf{G}^{p,n} \mathbf{b}_t^{(n)} \qquad (1 \le p \le N) \tag{4.32}$$

Let $\mathbf{b}_n$ be a column matrix containing the coefficients of outgoing spherical waves in $R^{(n)}$ with respect to coordinate system n. The coefficients of the outgoing spherical waves with respect to coordinate system n generated by $\mathbf{J}^{(n)}$ alone is $\mathbf{b}_n - \mathbf{a}_n$. Therefore, equation (4.32) can be written as

$$\mathbf{a}_p = \sum_{n=1}^{N} \mathbf{G}^{p,n} (\mathbf{b}_n - \mathbf{a}_n) \qquad (1 \le p \le N) \tag{4.33}$$

Suppose that two different currents $\mathbf{J}^{(p)}$ and $\mathbf{J}$ are inside the $\Sigma_{\min}^{(p)}$. Suppose that the electromagnetic field outside $\Sigma_{\min}^{(p)}$ when $\mathbf{J}^{(p)}$ is present alone in free space and the electromagnetic field outside $\Sigma_{\min}^{(p)}$ when $\mathbf{J}$ is present alone in free space are the same. Suppose that the current distribution of $\mathbf{J}$ in free space and the current distribution of $\mathbf{J}$ near objects are the same. In this case, the electromagnetic field outside $\Sigma_{\min}^{(p)}$ when only $\mathbf{J}^{(p)}$ is near objects and the electromagnetic field outside $\Sigma_{\min}^{(p)}$ when only $\mathbf{J}$ is near objects are the same (objects exist outside $\Sigma_{\min}^{(p)}$). Therefore, equation (4.33) is valid for an arbitrary current distribution.

The current distribution that generates the ith spherical wave is not unique. One of $\mathbf{J}_{s,m,n}^{(p)}$ is presented in [29]. This $\mathbf{J}_{s,m,n}^{(p)}$ flows on the surface of a sphere. In [29], $\mathbf{J}_{s,m,n}^{(p)}$ was derived using the equivalence principle.

B. Mutual Coupling among Antennas in an Environment

Suppose that N antennas are present near extraneous objects. Electromagnetic fields may or may not be incident on an antenna array. It is assumed that a minimum sphere enclosing an antenna does not touch extraneous objects or the minimum sphere of other antennas. Each antenna has its own coordinate system. Let the nth antenna be antenna n. Let the generalized-scattering-matrix equation of antenna n (n = 1, 2, 3, ⋯, N) be

$$\left[\begin{array}{c} \mathbf{w}_n \\ \hline \mathbf{b}_n \end{array}\right] = \left[\begin{array}{c|c} \boldsymbol{\Gamma}_n & \mathbf{R}_n \\ \hline \mathbf{T}_n & \mathbf{S}_n \end{array}\right] \left[\begin{array}{c} \mathbf{v}_n \\ \hline \mathbf{a}_n \end{array}\right]. \tag{4.34}$$

Equation (4.34) refers to the coordinate system of antenna n. From equation (4.34), we have

$$\mathbf{w}_n = \boldsymbol{\Gamma}_n \mathbf{v}_n + \mathbf{R}_n \mathbf{a}_n \tag{4.35}$$

$$\mathbf{b}_n = \mathbf{T}_n \mathbf{v}_n + \mathbf{S}_n \mathbf{a}_n . \tag{4.36}$$

Let $\mathbf{g}_n$ be the column matrix whose entries are the coefficients of the incoming spherical waves for the incident field with respect to the coordinate system of antenna n. That is, $\mathbf{g}_n$ is the column matrix containing the coefficients of the incoming spherical waves with respect to the coordinate system of antenna n when objects and antennas do not exist and the incident field exists in free space. The coefficients of the incoming spherical waves with respect to coordinate system of antenna n can be represented by the following, from (4.33):

$$\mathbf{a}_n = \sum_{m=1}^{N} \left(\mathbf{G}^{nm} (\mathbf{b}_m - \mathbf{a}_m) \right) + \mathbf{g}_n \tag{4.37}$$

Let

$$\mathbf{v}_n = \mathbf{A}_n\mathbf{x}_n + \mathbf{B}_n\mathbf{y}_n \tag{4.38}$$

$$\mathbf{w}_n = \mathbf{C}_n\mathbf{x}_n + \mathbf{D}_n\mathbf{y}_n . \tag{4.39}$$

where $\mathbf{x}_n$ and $\mathbf{y}_n$ are column matrices that have the same number of rows as $\mathbf{v}_n$ (or $\mathbf{w}_n$). Substituting (4.38) and (4.39) into (4.35) and rearranging, we obtain

$$\mathbf{x}_n = (\mathbf{C}_n - \boldsymbol{\Gamma}_n\mathbf{A}_n)^{-1}(\boldsymbol{\Gamma}_n\mathbf{B}_n - \mathbf{D}_n)\mathbf{y}_n + (\mathbf{C}_n - \boldsymbol{\Gamma}_n\mathbf{A}_n)^{-1}\mathbf{R}_n\mathbf{a}_n . \tag{4.40}$$

Equation (4.36) can be written in another form:

$$\mathbf{z}_n = \mathbf{T}_n\mathbf{v}_n + (\mathbf{S}_n - \mathbf{I}_n)\mathbf{a}_n \tag{4.41}$$

where

$$\mathbf{z}_n = \mathbf{b}_n - \mathbf{a}_n \tag{4.42}$$

In equation (4.41), $\mathbf{I}_n$ is the identity matrix for which the number of rows (or columns) is the same as the number of rows in $\mathbf{v}_n$ (or $\mathbf{w}_n$). Setting $\mathbf{A}_n = \mathbf{I}_n$, $\mathbf{B}_n = \mathbf{0}$, $\mathbf{C}_n = \boldsymbol{\chi}_n$, and $\mathbf{D}_n = \boldsymbol{\delta}_n$, equation (4.42) becomes

$$\mathbf{v}_n = -(\boldsymbol{\chi}_n - \boldsymbol{\Gamma}_n)^{-1}\boldsymbol{\delta}_n\mathbf{y}_n + (\boldsymbol{\chi}_n - \boldsymbol{\Gamma}_n)^{-1}\mathbf{R}_n\mathbf{a}_n . \tag{4.43}$$

Substituting (4.43) into (4.41) and rearranging, we obtain

$$\mathbf{P}_n\mathbf{a}_n - \mathbf{z}_n = \mathbf{H}_n\mathbf{y}_n \tag{4.44}$$

where

$$\mathbf{P}_n = \mathbf{T}_n(\boldsymbol{\chi}_n - \boldsymbol{\Gamma}_n)^{-1}\mathbf{R}_n + \mathbf{S}_n - \mathbf{I}_n \tag{4.45}$$

$$\mathbf{H}_n = \mathbf{T}_n(\boldsymbol{\chi}_n - \boldsymbol{\Gamma}_n)^{-1}\boldsymbol{\delta}_n . \tag{4.46}$$

Substituting (4.37) into (4.44),

$$\mathbf{P}_n\sum_{m=1}^{N}\left(\mathbf{G}^{nm}\mathbf{z}_m\right) + \mathbf{P}_n\mathbf{g}_n - \mathbf{z}_n = \mathbf{H}_n\mathbf{y}_n . \tag{4.47}$$

There are N equations whose form is the same as that of equation (4.47). Equation (4.47) can be expressed by one matrix equation as follows:

$$(\mathbf{PG}-\mathbf{I})\mathbf{z}=\mathbf{Hy}-\mathbf{Pg} \tag{4.48}$$

where

$$\mathbf{P}=\begin{bmatrix}\mathbf{P}_1 & \mathbf{0} & \mathbf{0} & \cdots & \mathbf{0}\\ \mathbf{0} & \mathbf{P}_2 & \mathbf{0} & \cdots & \mathbf{0}\\ \mathbf{0} & \mathbf{0} & \mathbf{P}_3 & \cdots & \mathbf{0}\\ \vdots & \vdots & \vdots & \ddots & \vdots\\ \mathbf{0} & \mathbf{0} & \mathbf{0} & \cdots & \mathbf{P}_N\end{bmatrix},\quad \mathbf{G}=\begin{bmatrix}\mathbf{G}^{11} & \mathbf{G}^{12} & \mathbf{G}^{13} & \cdots & \mathbf{G}^{1N}\\ \mathbf{G}^{21} & \mathbf{G}^{22} & \mathbf{G}^{23} & \cdots & \mathbf{G}^{2N}\\ \mathbf{G}^{31} & \mathbf{G}^{32} & \mathbf{G}^{33} & \cdots & \mathbf{G}^{3N}\\ \vdots & \vdots & \vdots & \ddots & \vdots\\ \mathbf{G}^{N1} & \mathbf{G}^{N2} & \mathbf{G}^{N3} & \cdots & \mathbf{G}^{NN}\end{bmatrix}$$

$$\mathbf{H}=\begin{bmatrix}\mathbf{H}_1 & \mathbf{0} & \mathbf{0} & \cdots & \mathbf{0}\\ \mathbf{0} & \mathbf{H}_2 & \mathbf{0} & \cdots & \mathbf{0}\\ \mathbf{0} & \mathbf{0} & \mathbf{H}_3 & \cdots & \mathbf{0}\\ \vdots & \vdots & \vdots & \ddots & \vdots\\ \mathbf{0} & \mathbf{0} & \mathbf{0} & \cdots & \mathbf{H}_N\end{bmatrix},\quad \mathbf{z}=\begin{bmatrix}\mathbf{z}_1\\ \mathbf{z}_2\\ \mathbf{z}_3\\ \vdots\\ \mathbf{z}_N\end{bmatrix},\quad \mathbf{g}=\begin{bmatrix}\mathbf{g}_1\\ \mathbf{g}_2\\ \mathbf{g}_3\\ \vdots\\ \mathbf{g}_N\end{bmatrix},\quad \mathbf{y}=\begin{bmatrix}\mathbf{y}_1\\ \mathbf{y}_2\\ \mathbf{y}_3\\ \vdots\\ \mathbf{y}_N\end{bmatrix} \tag{4.49}$$

From equation (4.48), we obtain

$$\mathbf{z}=(\mathbf{PG}-\mathbf{I})^{-1}(\mathbf{Hy}-\mathbf{Pg})\,. \tag{4.50}$$

Using equation (4.50) and spherical wave functions, the electromagnetic fields can be calculated.

Let

$$\mathbf{K}_n=(\mathbf{C}_n-\mathbf{\Gamma}_n\mathbf{A}_n)^{-1}(\mathbf{\Gamma}_n\mathbf{B}_n-\mathbf{D}_n) \tag{4.51}$$

$$\mathbf{M}_n=(\mathbf{C}_n-\mathbf{\Gamma}_n\mathbf{A}_n)^{-1}\mathbf{R}_n\,. \tag{4.52}$$

Then, equation (4.40) is written as

$$\mathbf{x}_n=\mathbf{K}_n\mathbf{y}_n+\mathbf{M}_n\mathbf{a}_n\,. \tag{4.53}$$

Equation (4.53) can be written as one matrix equation:

$$\mathbf{x} = \mathbf{K}\mathbf{y} + \mathbf{M}\mathbf{a} \tag{4.54}$$

where

$$\mathbf{K} = \begin{bmatrix} \mathbf{K}_1 & \mathbf{0} & \mathbf{0} & \cdots & \mathbf{0} \\ \mathbf{0} & \mathbf{K}_2 & \mathbf{0} & \cdots & \mathbf{0} \\ \mathbf{0} & \mathbf{0} & \mathbf{K}_3 & \cdots & \mathbf{0} \\ \vdots & \vdots & \vdots & \ddots & \vdots \\ \mathbf{0} & \mathbf{0} & \mathbf{0} & \cdots & \mathbf{K}_N \end{bmatrix}, \ \mathbf{M} = \begin{bmatrix} \mathbf{M}_1 & \mathbf{0} & \mathbf{0} & \cdots & \mathbf{0} \\ \mathbf{0} & \mathbf{M}_2 & \mathbf{0} & \cdots & \mathbf{0} \\ \mathbf{0} & \mathbf{0} & \mathbf{M}_3 & \cdots & \mathbf{0} \\ \vdots & \vdots & \vdots & \ddots & \vdots \\ \mathbf{0} & \mathbf{0} & \mathbf{0} & \cdots & \mathbf{M}_N \end{bmatrix}, \ \mathbf{x} = \begin{bmatrix} \mathbf{x}_1 \\ \mathbf{x}_2 \\ \mathbf{x}_3 \\ \vdots \\ \mathbf{x}_N \end{bmatrix}, \ \mathbf{a} = \begin{bmatrix} \mathbf{a}_1 \\ \mathbf{a}_2 \\ \mathbf{a}_3 \\ \vdots \\ \mathbf{a}_N \end{bmatrix} \tag{4.55}$$

From (4.37), we have

$$\mathbf{a} = \mathbf{G}\mathbf{z} + \mathbf{g}. \tag{4.56}$$

Substituting (4.56) into (4.54),

$$\mathbf{x} = \mathbf{K}\mathbf{y} + \mathbf{M}\mathbf{G}\mathbf{z} + \mathbf{M}\mathbf{g}. \tag{4.57}$$

Substituting (4.50) into (4.57) and rearranging, we obtain

$$\mathbf{x} = \left(\mathbf{K} + \mathbf{M}\mathbf{G}(\mathbf{P}\mathbf{G} - \mathbf{I})^{-1}\mathbf{H}\right)\mathbf{y} + \left(\mathbf{M} - \mathbf{M}\mathbf{G}(\mathbf{P}\mathbf{G} - \mathbf{I})^{-1}\mathbf{P}\right)\mathbf{g}. \tag{4.58}$$

When an electromagnetic field is incident on an antenna array or sources are applied to the feed ports of antennas, the voltages and currents at the feed ports can be calculated using equation (4.58).

When there is no incident field, $\mathbf{g} = \mathbf{0}$. In this case, equation (4.58) becomes

$$\mathbf{x} = \mathbf{T}\mathbf{y} \tag{4.59}$$

where

$$\mathbf{T} = \mathbf{K} + \mathbf{M}\mathbf{G}(\mathbf{P}\mathbf{G} - \mathbf{I})^{-1}\mathbf{H}. \tag{4.60}$$

If $\mathbf{x}_n$ represents the voltages at the feed ports of antenna n and $\mathbf{y}_n$ represents the currents at

the feed ports of antenna n, $\boldsymbol{\chi}_n = \mathbf{I}_n$, $\boldsymbol{\delta}_n$ is a diagonal matrix whose ith element (entry in ith row and ith column) is $-\sqrt{\mathrm{Re}(Z_{n,i}^R)}$, $\mathbf{A}_n$ and $\mathbf{C}_n$ are diagonal matrices whose ith element is $1\Big/\left(2\sqrt{\mathrm{Re}(Z_{n,i}^R)}\right)$, $\mathbf{B}_n$ is a diagonal matrix whose ith element is $Z_{n,i}^R\Big/\left(2\sqrt{\mathrm{Re}(Z_{n,i}^R)}\right)$, and $\mathbf{D}_n$ is a diagonal matrix whose ith element is $-\left(Z_{n,i}^R\right)^*\Big/\left(2\sqrt{\mathrm{Re}(Z_{n,i}^R)}\right)$, where $Z_{n,i}^R$ is the reference impedance of the ith power wave for antenna n. In this case, $\mathbf{T}$ is the impedance matrix. If $\mathbf{x}_n$ represents the currents at the feed ports of antenna n and $\mathbf{y}_n$ represents the voltages at the feed ports of antenna n, $\boldsymbol{\chi}_n$ is a diagonal matrix whose ith element is $-\left(Z_{n,i}^R\right)^*\Big/Z_{n,i}^R$, $\boldsymbol{\delta}_n$ is a diagonal matrix whose ith element is $\sqrt{\mathrm{Re}(Z_{n,i}^R)}\Big/Z_{n,i}^R$, $\mathbf{A}_n$ is a diagonal matrix whose ith element is $Z_{n,i}^R\Big/\left(2\sqrt{\mathrm{Re}(Z_{n,i}^R)}\right)$, $\mathbf{C}_n$ is a diagonal matrix whose ith element is $-\left(Z_{n,i}^R\right)^*\Big/\left(2\sqrt{\mathrm{Re}(Z_{n,i}^R)}\right)$, and $\mathbf{B}_n$ and $\mathbf{D}_n$ are diagonal matrices whose ith element is $1\Big/\left(2\sqrt{\mathrm{Re}(Z_{n,i}^R)}\right)$. In this case, $\mathbf{T}$ is an admittance matrix. If $\mathbf{x}_n$ represents $\mathbf{v}_n$ and $\mathbf{y}_n$ represents $\mathbf{w}_n$, $\boldsymbol{\chi} = \mathbf{B} = \mathbf{C} = \mathbf{0}$ and $\boldsymbol{\delta} = \mathbf{A} = \mathbf{D} = \mathbf{I}_n$. In this case, $\mathbf{T}^{-1}$ is a scattering matrix. If $\mathbf{x}_n$ represents $\mathbf{w}_n$ and $\mathbf{y}_n$ represents $\mathbf{v}_n$, $\mathbf{T}$ is not a scattering matrix, because equation (4.43) is not valid in this case.

C. Discussion

The methods for calculating network parameters and electromagnetic fields using a generalized scattering matrix and spherical wave present advantages. One advantage is that they can be calculated using the properties of an isolated antenna, so we do not need to

solve a boundary value problem in the presence of all antennas. Moreover, we do not need to know the detailed geometry of the antennas to calculate the network parameters and electromagnetic field[10]. When the antennas are canonical-minimum-scattering antennas, only the field pattern, radiation efficiency and input impedance of the antennas are required. The disadvantage of this method is that the network parameters and electromagnetic field cannot be calculated when the minimum sphere enclosing an antenna overlaps objects or the minimum sphere of another antenna. That is, when an antenna is very close to objects or other antennas, the network parameters and electromagnetic field cannot be calculated using a generalized scattering matrix and spherical wave (except in the case where a minimum sphere does not overlap). If we use another basis that is different from the spherical wave, this problem may be solved.

[10] In fact, we should know the detailed geometry of an antenna to determine a generalized scattering matrix. The above sentence means that if a generalized scattering matrix is given without knowing the geometry of the antenna, we can calculate the network parameters and electromagnetic fields.

4.2 Determination of Impedance Parameters among Antennas Using Their Current Distributions

4.2.1 Equivalent Circuit for Transmitting and Receiving Antennas

When the feed port of an antenna are excited with a source and there is no incident field (i.e., the antenna operates in a transmitting mode), the current and the voltage at the feed port can be calculated using the equivalent circuits shown in Figure 4.9 and Figure 4.10. A source can be represented as a Thevenin equivalent circuit or a Norton equivalent circuit. Figure 4.9 represents a Thevenin equivalent circuit, and Figure 4.10 represents a Norton equivalent circuit. In Figures 4.9 and 4.10, Z_A is the input impedance of an antenna seen at the feed port. In Figure 4.9, V_g is a voltage that a voltage source generates, and Z_g is the source impedance of the voltage source. In Figure 4.10, I^s is the current that a current source generates, and Z_{cg} is the source impedance of the current source. The current at Z_A and the voltage across Z_A in the equivalent circuits are the same as the current and the voltage at the feed port of a transmitting antenna, respectively.

When an electromagnetic field is incident on an antenna terminated in a load (i.e., the antenna operates in receiving mode), the current flowing at the load and the voltage across the load can be calculated by using the Thevenin or Norton equivalent circuit, as shown in Figure 4.11 and Figure 4.12. In Figures 4.11 and 4.12, Z_A is the input impedance of an antenna in transmitting mode, and Z_L is a load impedance. In Figure 4.11, V^{oc} represents the open-circuit voltage, and in Figure 4.12, I^{sc} represents a short-circuit current. In Section 4.2, it is assumed that a source or a load is connected to an infinitesimal gap on the

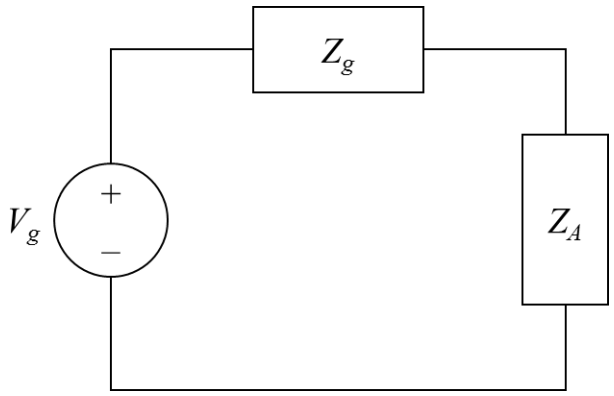

Figure 4.9 Thevenin equivalent circuit for a transmitting antenna.

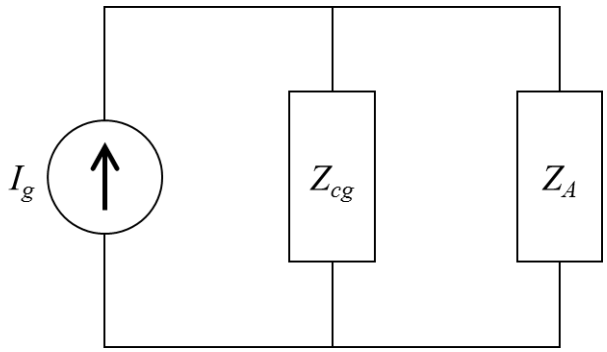

Figure 4.10 Norton equivalent circuit for a transmitting antenna.

conducting wire. Then, the open-circuit voltage V^{oc} is determined using [30, equation (13-46)]

$$V^{oc} = -\frac{1}{I^t}\int_G \mathbf{E}^i(\mathbf{r}') \cdot \mathbf{J}^t(\mathbf{r}')dv \tag{4.61}$$

where $\mathbf{E}^i$ is the incident electric field, $\mathbf{J}^t$ is the current density of a transmitting antenna, I^t is the total current flowing at the input terminals (feed port) of a transmitting antenna when the current density of the transmitting antenna is $\mathbf{J}^t$, $\mathbf{r}'$ is the position of a point in the current, and G is a region containing all currents. The short-circuit current I^{sc} is determined

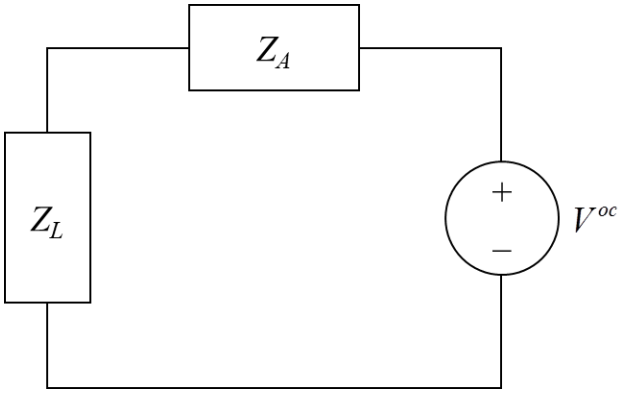

Figure 4.11 Thevenin equivalent circuit for a receiving antenna.

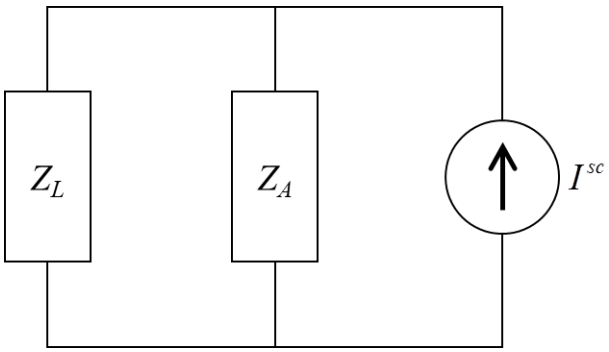

Figure 4.12 Norton equivalent circuit for a receiving antenna.

using [30, equation (13-45)]

$$I^{sc} = \frac{1}{V^t} \int_G \mathbf{E}^i(\mathbf{r}') \cdot \mathbf{J}^t(\mathbf{r}') dv \tag{4.62}$$

where V^t is the voltage difference between the input terminals of a transmitting antenna when the current density of the transmitting antenna is $\mathbf{J}^t$. Let I^s be the total current flowing at the input terminals of the short-circuited antenna when electric field $\mathbf{E}^i$ is incident. Then, $I^s = -I^{sc}$. The short-circuit current in the Norton equivalent circuit, I^{sc}, can be calculated by using either equation (4.62) or current I^s.

An analytical formula for the input impedance of an antenna near objects and the self-impedance and mutual-impedance of coupled antennas can be derived by exploiting the Thevenin or Norton equivalent circuit for a transmitting and receiving antenna. In this dissertation, we use the Thevenin equivalent circuit to determine the input impedance of an antenna near objects and self- and mutual-impedance of coupled antennas.

4.2.2 Input Impedance of an Antenna near Objects

When an antenna that is present alone in free space is excited with a source at its feed port, an electromagnetic field propagates outward, and there is no field that is incident on the antenna. When an antenna that is present near objects is excited with a source at its feed port, the electromagnetic field transmitted from the antenna is scattered by objects, and the scattered field is incident on the antenna. In this case, the voltage due to the incident field as well as the voltage due to a source is produced at the feed port. By the superposition principle, a voltage source due to an incident field is connected to Z_A in the Thevenin equivalent circuit for a transmitting antenna, as shown in Figure 4.13. The voltage generated by this voltage source is the same as the open-circuit voltage V^{oc} in the Thevenin equivalent circuit for a receiving antenna and is calculated using equation (4.61). When V^{oc} is calculated using equation (4.61), an electric field generated by only objects is used instead of $\mathbf{E}^i$.

The voltage at a feed port is denoted by V^p. Solving the circuit in Figure 4.13, the current flowing at Z_A is obtained. Letting the current flowing at Z_A be I^p,

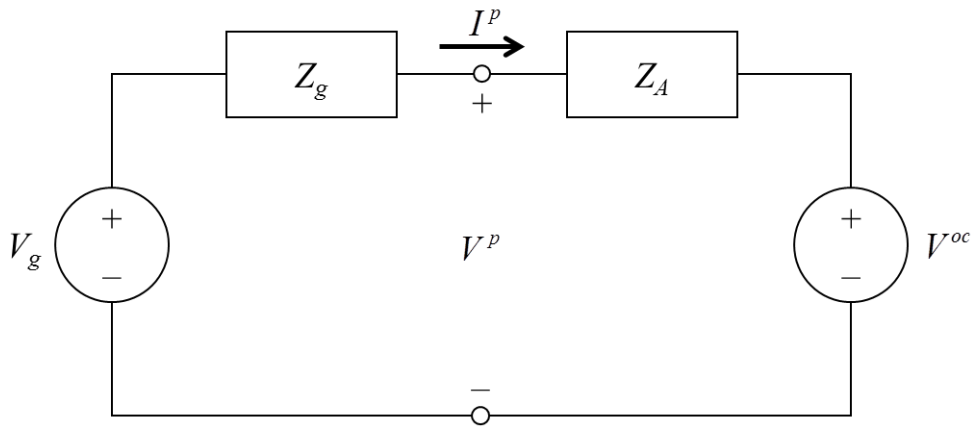

Figure 4.13 Equivalent circuit for an antenna near objects.

$$I^p = \frac{V^p - V^{oc}}{Z_A}. \tag{4.63}$$

The input impedance of an antenna is the ratio of the voltage at a feed port to the current at a feed port. Therefore, the impedance of an antenna near objects, Z_A^e, is

$$Z_A^e = \frac{V^p}{I^p} = \frac{V^p Z_A}{V^p - V^{oc}}. \tag{4.64}$$

Note that Z_A is the input impedance of an isolated antenna in free space and is not the input impedance of an antenna near objects. Let us calculate $Z_A^e - Z_A$.

$$Z_A^e - Z_A = \frac{V^p Z_A}{V^p - V^{oc}} - Z_A = \frac{V^{oc} Z_A}{V^p - V^{oc}} = \frac{V^{oc}}{I^p} \tag{4.65}$$

Let the electric field that objects generate be $\mathbf{E}^e$. Substituting (4.61) with $\mathbf{E}^i$ replaced by $\mathbf{E}^e$ into (4.65), a formula for the difference between the input impedance of an antenna in free space and the input impedance of an antenna near objects is obtained as follows:

$$Z_A^e - Z_A = -\frac{1}{I^p I^t}\int_G \mathbf{E}^e(\mathbf{r}')\cdot\mathbf{J}^t(\mathbf{r}')dv \tag{4.66}$$

Note that $\mathbf{E}^e$ is proportional to I^p and $\mathbf{J}^t$ is proportional to I^t. Note that I^p and $\mathbf{E}^e$ are independent of I^t and $\mathbf{J}^t$. $\mathbf{E}^e$ can be considered an electric field generated by objects when a current source of I^p without source impedance is applied to the input terminals of an antenna. Before calculating the input impedance of an antenna near objects (Z_A^e), the input impedance of an antenna that is present alone in free space (Z_A) should be calculated using a numerical or analytical method.

4.2.3 Self Impedance for Coupled Antennas

The impedance parameters can be determined as

$$Z_{mn} = \frac{V_m}{I_n} \quad \text{when } I_i = 0 \text{ for } i \neq n. \tag{4.67}$$

When $m = n$, Z_{mn} is called a self-impedance. The self-impedance Z_{mm} is the same as the impedance seen looking into an antenna at the feed port of antenna m when all other antennas are open-circuited. A self-impedance can be calculated using the same method as used in the calculation of the input impedance of an antenna near objects. All antennas except antenna m are open-circuited, and the input impedance of antenna m is calculated using (4.66) to obtain Z_{mm}. Z_{mm} is given by

$$Z_{mm} = Z_A^m - \frac{1}{I_m I_m^t}\int_G \mathbf{E}^{(m,m)}(\mathbf{r}')\cdot\mathbf{J}_m^t(\mathbf{r}')dv \tag{4.68}$$

where Z_A^m is the input impedance of antenna m that is alone in free space (i.e., in the

absence of other antennas and objects); $\mathbf{J}_m^t$ is the current density of transmitting antenna m that is alone in free space; I_m^t is the current flowing at the input terminals of transmitting antenna m when the current density is $\mathbf{J}_m^t$; and $\mathbf{E}^{(m,m)}$ is the electric field generated by open-circuited antennas and objects (except antenna m) when antenna m is excited with a current of I_m at its input terminals. Note that to calculate a self-impedance, we should know the input impedance of an isolated antenna.

Using a reciprocity theorem (Equation (3-36) in [8]), equation (4.68) can be written in another form as follows:

$$Z_{mm} = Z_A^m - \frac{1}{I_m I_m^t} \int_G \mathbf{E}_m^t(\mathbf{r}') \cdot \mathbf{J}^{(m,m)}(\mathbf{r}') dv \tag{4.69}$$

where $\mathbf{E}_m^t$ is the electric field generated by transmitting antenna m that is alone in free space (i.e., in the absence of other antennas and objects) and $\mathbf{J}^{(m,m)}$ is the current density of objects and antennas except for antenna m when all antennas except for antenna m are open-circuited and antenna m is excited with a current of I_m, i.e., $\mathbf{J}^{(m,m)}$ generates $\mathbf{E}^{(m,m)}$.

The self-impedance is calculated in a situation where all antennas except one are open-circuited. An open-circuited canonical-minimum-scattering antenna is invisible. Therefore, when all antennas are canonical-minimum-scattering antennas, the self-impedance Z_{mm} is equal to the input impedance of antenna m in the presence of objects and in the absence of all other antennas.

4.2.4 Mutual Impedance for Coupled Antennas

When $m \neq n$, Z_{mn} in equation (4.67) is called a mutual-impedance. In (4.67), V_m is the

same as the open-circuit voltage in the Thevenin equivalent circuit for antenna m in receiving mode. From (4.61) and (4.67), the mutual-impedance, Z_{mn}, is as follows:

$$Z_{mn} = -\frac{1}{I_n I_m^t} \int_G \mathbf{E}^{(m,n)}(\mathbf{r}') \cdot \mathbf{J}_m^t(\mathbf{r}') dv \quad \text{for } m \neq n \tag{4.70}$$

where $\mathbf{E}^{(m,n)}$ is the electric field generated by objects and antennas except for antenna m when all antennas except for antenna n are open-circuited and antenna n is excited with a current of I_n at its input terminals. Note that $\mathbf{E}^{(m,n)}$ is proportional to I_n and $\mathbf{J}_m^t$ is proportional to I_m^t. Note that I_n and $\mathbf{E}^{(m,n)}$ are independent of I_m^t and $\mathbf{J}_m^t$.

Using a reciprocity theorem (Equation (3-36) in [8]), equation (4.70) can be written in another form as follows:

$$Z_{mn} = -\frac{1}{I_n I_m^t} \int_G \mathbf{E}_m^t(\mathbf{r}') \cdot \mathbf{J}^{(m,n)}(\mathbf{r}') dv \quad \text{for } m \neq n \tag{4.71}$$

where $\mathbf{J}^{(m,n)}$ is the current density of objects and antennas except antenna m when all antennas except antenna n are open-circuited and antenna n is excited with current of I_n, i.e., $\mathbf{J}^{(m,n)}$ generates $\mathbf{E}^{(m,n)}$. If the antennas are dipole antennas and the number of antennas is two, equation (4.71) is the same as equation (7.135) in [6].

To calculate the self and mutual impedances using the method presented in Section 4.2, we should know the current distributions of antennas and objects. In general, the current distribution is calculated using a numerical method in the presence of all antennas and objects. However, in some cases, we can predict the current distributions of antennas without calculating the currents in the presence of all antennas and objects. From Section 4.1.2, we know that the impedance parameters of canonical-minimum-scattering antennas

can be determined from the modal transmitting patterns and $\boldsymbol{\Gamma}$ in (2.13) alone. From this result, we know that when calculating the impedance parameters among CMS antennas, only the current distributions of isolated transmitting antennas are required. Therefore, we can assume that the current distribution of a CMS antenna near objects and open-circuited CMS antennas is similar to the current distribution of an isolated transmitting CMS antenna in free space. In addition, if the antennas and objects are sufficiently far apart, the shape of the current of an antenna near objects and open-circuited antennas are similar to the shape of the current of an isolated transmitting antenna in free space. Therefore, in this case, the impedance parameters among antennas can be calculated using only the current distributions of the isolated transmitting antennas in free space.

When calculating the impedance parameters, all antennas are open-circuited except one. An open-circuited canonical-minimum-scattering antenna is invisible. Therefore, when all antennas are canonical-minimum-scattering antennas, $\mathbf{E}^{(m,n)}$ is the same as the electric field when antenna n and objects exist and all other antennas do not exist and antenna n is excited with I_n.

4.3 Determination of Impedance Parameters among Antennas using Equivalent Currents

4.3.1 Calculation of Impedance Parameters among Antennas Using Equivalent Currents

This section studies a simple method to calculate the impedance parameters. From Section 4.1, we know that the impedance parameters between two canonical-minimum-scattering antennas depend only on their modal transmitting patterns, reflection coefficients, and their positions. Consider two systems comprising two canonical-minimum-scattering antennas. In one system, one antenna is called antenna 1 and the other is called antenna 2, and in the other system, one antenna is called antenna 3 and the other is called antenna 4. Let the modal transmitting patterns, reflection coefficients, and positions of antenna 1 and antennas 3 be the same, and let the modal transmitting patterns, reflection coefficients, and positions of antenna 2 and antenna 4 be the same. Let the shapes of antennas 1, 2, 3, and 4 be different. Then, the impedance parameters for the two systems are the same. From this fact, we can guess that if we calculate the impedance parameters using an equivalent current that generates the same field as that generated by the original antennas, the result is equal to those calculated using the original antennas. In this case, the equivalent current should have a fictitious feed port and fictitious network that makes the reflection coefficient and modal transmitting pattern be the same as those of the original antennas. In this section, we investigate the method for calculating the impedance parameters among antennas using an equivalent current.

Let $\mathbf{J}_m^{eq}$ be the equivalent current that generates the same field as that generated by

an isolated transmitting antenna m in free space. That is, $\mathbf{J}_m^{eq}$ produces $\mathbf{E}_m^t$. Applying a reciprocity theorem to equation (4.71), the following equation is obtained:

$$Z_{mn} = -\frac{1}{I_n I_m^t}\int_G \mathbf{E}_m^t(\mathbf{r}')\cdot\mathbf{J}^{(m,n)}(\mathbf{r}')dv = -\frac{1}{I_n I_m^t}\int_G \mathbf{E}^{(m,n)}(\mathbf{r}')\cdot\mathbf{J}_m^{eq}(\mathbf{r}')dv \quad \text{for } m \neq n \qquad (4.72)$$

$\mathbf{E}^{(m,n)}$ can be calculated using the equivalent current. Likewise, the self-impedance can be calculated using the equivalent current:

$$Z_{mm} = Z_A^m - \frac{1}{I_m I_m^t}\int_G \mathbf{E}^{(m,m)}\cdot\mathbf{J}_m^{eq}dv \qquad (4.73)$$

Here, $\mathbf{E}^{(m,m)}$ can be calculated using the equivalent current.

The equivalent current is composed of infinitesimal electric dipoles or infinitesimal electric loops. Let I be the current value of an electric dipole and l be the length of the electric dipole. Let **p** be a vector whose direction is the same as the direction of the flow of current in the electric dipole and whose magnitude is $|Il|$. In this dissertation, we shall call **p** the electric moment vector. Let I be the current value of the electric loop (current value of the loop is different from the current value of the dipole) and A be the area of the circle in the electric loop. Let **m** be a vector whose direction is perpendicular to the plane in which a loop lies and whose magnitude is $|IA|$. In this dissertation, we shall call **m** the magnetic moment vector.

Suppose that $\mathbf{J}_m^{eq}$ in equations (4.72) and (4.73) is composed of one infinitesimal electric dipole that is located at $\mathbf{r}^e$. Calculating the integral in equations (4.72) and (4.73), we obtain

$$\int_G \mathbf{E}^{(m,i)}(\mathbf{r}')\cdot\mathbf{J}_m^{eq}(\mathbf{r}')dv = \mathbf{E}^{(m,i)}(\mathbf{r}^e)\cdot\mathbf{p} \qquad (4.74)$$

where i is either m or n. Suppose that $\mathbf{J}_m^{eq}$ in equations (4.72) and (4.73) is composed of one infinitesimal electric loop that is located at $\mathbf{r}^h$. Calculating the integral in equations (4.72) and (4.73), we obtain

$$\begin{aligned}\int_G \mathbf{E}^{(m,i)}(\mathbf{r}')\cdot\mathbf{J}_m^{eq}(\mathbf{r}')dv &= I\oint_G \mathbf{E}^{(m,i)}(\mathbf{r}')\cdot d\mathbf{l} = -j\omega\mu I\iint_G \mathbf{H}^{(m,i)}\cdot d\mathbf{s} \\ &= -j\omega\mu IA\mathbf{H}^{(m,i)}(\mathbf{r}^h)\cdot\frac{\mathbf{m}}{|\mathbf{m}|} = -j\omega\mu\mathbf{H}^{(m,i)}(\mathbf{r}^h)\cdot\mathbf{m}\end{aligned} \tag{4.75}$$

where $\mathbf{H}^{(m,i)}$ is the magnetic field when the electric field is $\mathbf{E}^{(m,i)}$.

If $\mathbf{J}_m^{eq}$ is composed of multiple infinitesimal electric dipoles and infinitesimal electric loops, the result is obtained by the superposition of all currents. Therefore, the impedance parameters are as follows:

$$Z_{nn} = Z_A^n - \frac{1}{I_n^t I_n}\left(\sum_{p=1}^{N_e^n}\left(\mathbf{E}^{(n,n)}(\mathbf{r}_{p,n}^e)\cdot\mathbf{p}_p^n\right) - \sum_{p=1}^{N_h^n}\left(\mathbf{H}^{(n,n)}(\mathbf{r}_{p,n}^h)\cdot j\omega\mu\mathbf{m}_p^n\right)\right) \tag{4.76}$$

$$Z_{mn} = -\frac{1}{I_m^t I_n}\left(\sum_{p=1}^{N_e^m}\left(\mathbf{E}^{(m,n)}(\mathbf{r}_{p,m}^e)\cdot\mathbf{p}_p^m\right) - \sum_{p=1}^{N_h^m}\left(\mathbf{H}^{(m,n)}(\mathbf{r}_{p,m}^h)\cdot j\omega\mu\mathbf{m}_p^m\right)\right) \quad \text{for } m\neq n \tag{4.77}$$

$\mathbf{p}_p^n$ is the electric moment vector of the pth infinitesimal dipole for antenna n, and $\mathbf{m}_p^n$ is the magnetic moment vector of the pth infinitesimal loop for antenna n; N_e^n and N_h^n are the number of infinitesimal dipoles and infinitesimal loops for antenna n, respectively; $\mathbf{r}_{p,n}^e$ is the position of the pth infinitesimal dipole for antenna n, and $\mathbf{r}_{p,n}^h$ is the position of the pth infinitesimal loop for antenna n. A collection of all $\mathbf{p}_p^n$ and all $\mathbf{m}_p^n$ (n is fixed to one value) generates the same field as that generated by an isolated transmitting antenna n with current at input terminals I_n^t. $\mathbf{E}^{(n,n)}$, $\mathbf{E}^{(m,n)}$, $\mathbf{H}^{(n,n)}$, and $\mathbf{H}^{(m,n)}$ in equations (4.76) and

(4.77) are calculated using equivalent sources.

The method for calculating impedance parameters using an equivalent current has advantages. If the antennas are canonical-minimum-scattering antennas, the impedance parameters can be calculated from only field patterns and the input impedances of antennas using the method presented in this section. If field pattern is given and the geometry of an antenna is not known, the equivalent current that generates the given field pattern can be found.

If equivalent current is simple, the time needed to calculate the impedance parameters is small. Therefore, we can quickly guess the impedance parameters if we can guess a simple equivalent current for an antenna.

If the equivalent current is complex, the time needed to calculate the impedance parameters using an equivalent current is larger than time needed to calculate the impedance parameters using the method in Section 4.2. Therefore, in this case, the method using an equivalent current does not have an advantage over the method in Section 4.2 from the perspective of the computation.

4.3.2 Example: Two Helical Antennas in Half Space

The author calculates the impedance parameters between two helical antennas over half space using equivalent currents. Half of the space was free space, and half of the space was a dielectric. The dielectric constant of the dielectric was 10, and the loss tangent was 0.1. One helical antenna will be termed antenna 1, and the other will be termed antenna 2. For antenna 1, the radius was 8 cm, the height was 10 cm, the number of turns was 8, and

the diameter of the cross-section of the wire was 1 mm. For antenna 2, the radius was 6.8 cm, the height was 12 cm, the number of turns was 10, and diameter of the cross-section of the wire was 1 mm. Both antenna 1 and antenna 2 were made of copper. The two antennas were both fed at the center of the wire. The resonant frequencies of antenna 1 and antenna 2 were 29.4 MHz and 30 MHz, respectively. The axes of the helical antennas were perpendicular to the dielectric surface. The shortest distance between the center of the helical antenna and the surface of the dielectric was 20 cm. The distance between the centers of the two helical antennas was 30 cm (Figure 4.14).

In this dissertation, equivalent currents were found from spherical wave coefficients generated by an isolated transmitting antenna in free space. Figure 4.15 shows point, dipole, and quadrupole sources. One point electric source in Figure 4.15 (a) generates only the TM_{01} mode, and one point magnetic source in Figure 4.15 (d) generates only the TE_{01}

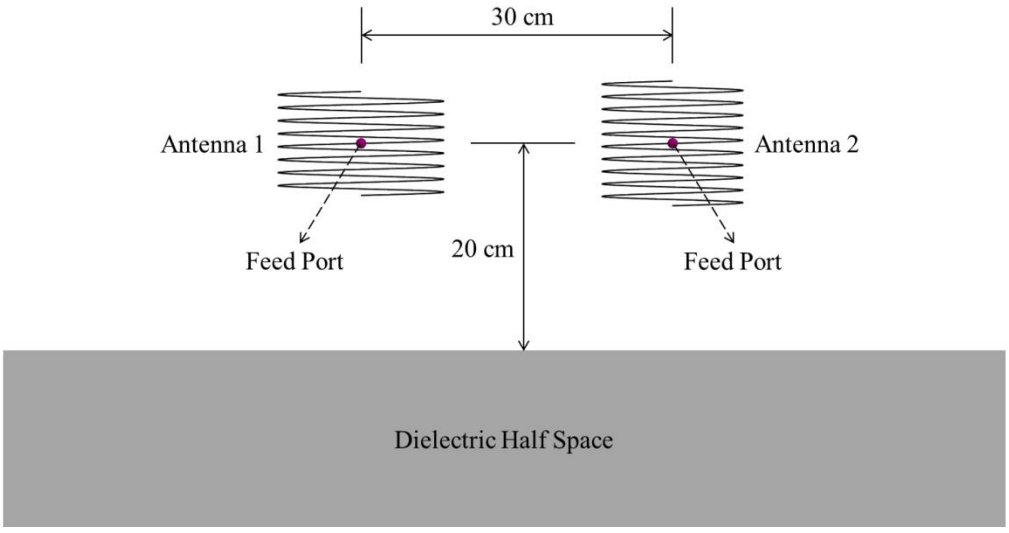

Figure 4.14 Antenna configuration in half space.

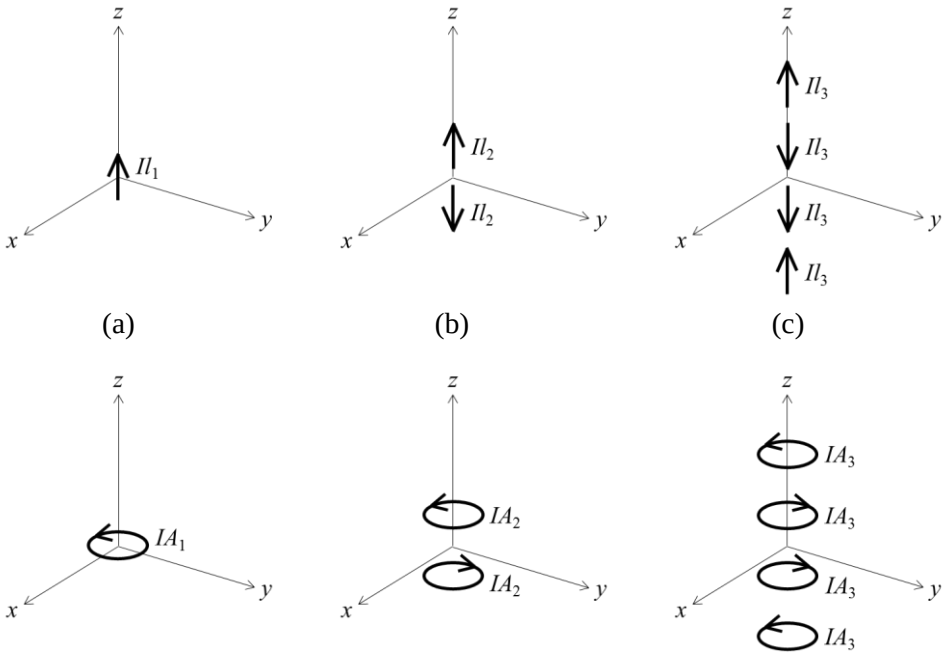

Figure 4.15 (a) Point electric source (b) Dipole electric source (c) Quadrupole electric source (d) Point magnetic source (e) Dipole magnetic source (f) Quadrupole magnetic source. The infinitesimal electric dipoles are aligned with the *z*-axis and the infinitesimal electric loops lie in the *xy*-plane. The centers of the sources are located at the coordinate origin. Il_n is the electric moment of an infinitesimal electric dipole and IA_n is the magnetic moment of an infinitesimal electric loop (n = 1, 2, 3).

mode [8, p. 287] (a point electric source is the same as an infinitesimal electric dipole, and a point magnetic source is the same as an infinitesimal electric loop). A dipole electric source in Figure 4.15 (b) generates only TM_{02} mode, and a dipole magnetic source in Figure 4.15 (e) generates only TE_{02} mode [8, p. 288]. A quadrupole electric source in Figure 4.15 (c) generates TM_{01} mode and TM_{03} mode, and a quadrupole magnetic source in Figure 4.15 (f) generates TE_{01} mode and TE_{03} mode [8, p. 314]. The parameters of the electric and magnetic sources were determined by equating the field for spherical waves and the field generated by the sources. Besides this method using spherical waves, an

equivalent current can be found by an algorithm, such as the algorithm described in [31].

The author applied 1 V to isolated antenna 1 in free space and calculated the spherical wave coefficients generated by antenna 1 when the center of the helix was located at the origin of the coordinate system and the axis of the helix coincided with the *z*-axis. The author applied 1 V to isolated antenna 2 in free space and calculated the spherical wave coefficients generated by antenna 2 when the center of the helix was located at the origin of the coordinate system and the axis of the helix coincided with the *z*-axis. The dominant spherical wave coefficients generated by antennas 1 and 2 are shown in Table 4.1 and Table 4.2, respectively. The sources that generate the same spherical wave coefficients as those generated by isolated transmitting helical antennas were found. Equivalent currents are composed of one point electric source, one magnetic point source, one quadrupole electric source, and one quadrupole magnetic source. Because the TM_{02} mode and TE_{02} mode are not produced by the helical antennas, there are no dipole sources in the equivalent current. The TM_{01} mode and TE_{01} mode generated by quadrupole electric and magnetic sources are very small compared with the TM_{01} mode and TE_{01} mode generated by the point electric and magnetic sources. Therefore, the TM_{01} and TE_{01} modes produced by the quadrupole electric and magnetic sources were ignored. The parameters of the equivalent sources for antenna 1 and antenna 2 are shown in Table 4.3 and Table 4.4, respectively.

The author calculated the impedance parameters using (4.76), (4.77) and equivalent sources. The electromagnetic fields were calculated using the Sommerfeld integral [32]–[34]. Self-impedances were calculated using only point electric and magnetic sources. The

mutual-impedance was calculated using point electric and magnetic sources and quadrupole electric and magnetic sources. Figure 4.16 shows the impedance parameters calculated using FEKO and using equivalent sources. There is good agreement between the two results.

Table 4.3 Coefficients of dominant spherical wave for antenna 1

	10 MHz	20 MHz	30 MHz
TE_{01}	$-7.683\times10^{-6}\,j$	$-1.023\times10^{-4}\,j$	$4.765\times10^{-3}\,j$
TM_{01}	$-2.299\times10^{-5}\,j$	$-1.531\times10^{-4}\,j$	$4.751\times10^{-3}\,j$
TE_{03}	$4.273\times10^{-11}\,j$	$2.193\times10^{-9}\,j$	$-2.143\times10^{-7}\,j$
TM_{03}	$2.991\times10^{-10}\,j$	$7.841\times10^{-9}\,j$	$-5.322\times10^{-7}\,j$

Table 4.4 Coefficients of dominant spherical wave for antenna 2

	10 MHz	20 MHz	30 MHz
TE_{01}	$-6.066\times10^{-6}\,j$	$-7.865\times10^{-5}\,j$	$-8.885\times10^{-2}-7.232\times10^{-2}\,j$
TM_{01}	$-2.422\times10^{-5}\,j$	$-1.570\times10^{-4}\,j$	$-1.182\times10^{-1}-9.625\times10^{-2}\,j$
TE_{03}	$1.594\times10^{-11}\,j$	$7.346\times10^{-10}\,j$	$1.451\times10^{-6}+1.182\times10^{-6}\,j$
TM_{03}	$1.934\times10^{-10}\,j$	$4.832\times10^{-9}\,j$	$7.634\times10^{-6}+6.216\times10^{-6}\,j$

Table 4.5 Parameters of equivalent sources for antenna 1

	10 MHz	20 MHz	30 MHz
IA_1	$3.912\times10^{-5}\,j$	$1.303\times10^{-4}\,j$	$-2.696\times10^{-3}\,j$
Il_1	$2.454\times10^{-5}\,j$	$8.169\times10^{-5}\,j$	$-1.690\times10^{-3}\,j$
IA_3	$-2.896\times10^{-5}\,j$	$-9.288\times10^{-5}\,j$	$1.793\times10^{-3}\,j$
Il_3	$-4.248\times10^{-5}\,j$	$-1.392\times10^{-4}\,j$	$2.800\times10^{-3}\,j$

Table 4.6 Parameters of equivalent sources for antenna 2

	10 MHz	20 MHz	30 MHz
IA_1	$3.089\times10^{-5}\,j$	$1.001\times10^{-4}\,j$	$5.027\times10^{-2}+4.092\times10^{-2}\,j$
Il_1	$2.585\times10^{-5}\,j$	$8.380\times10^{-5}\,j$	$4.207\times10^{-2}+3.424\times10^{-2}\,j$
IA_3	$-1.081\times10^{-5}\,j$	$-3.112\times10^{-5}\,j$	$-1.214\times10^{-2}-9.894\times10^{-3}\,j$
Il_3	$-2.748\times10^{-5}\,j$	$-8.580\times10^{-5}\,j$	$-4.016\times10^{-2}-3.270\times10^{-2}\,j$

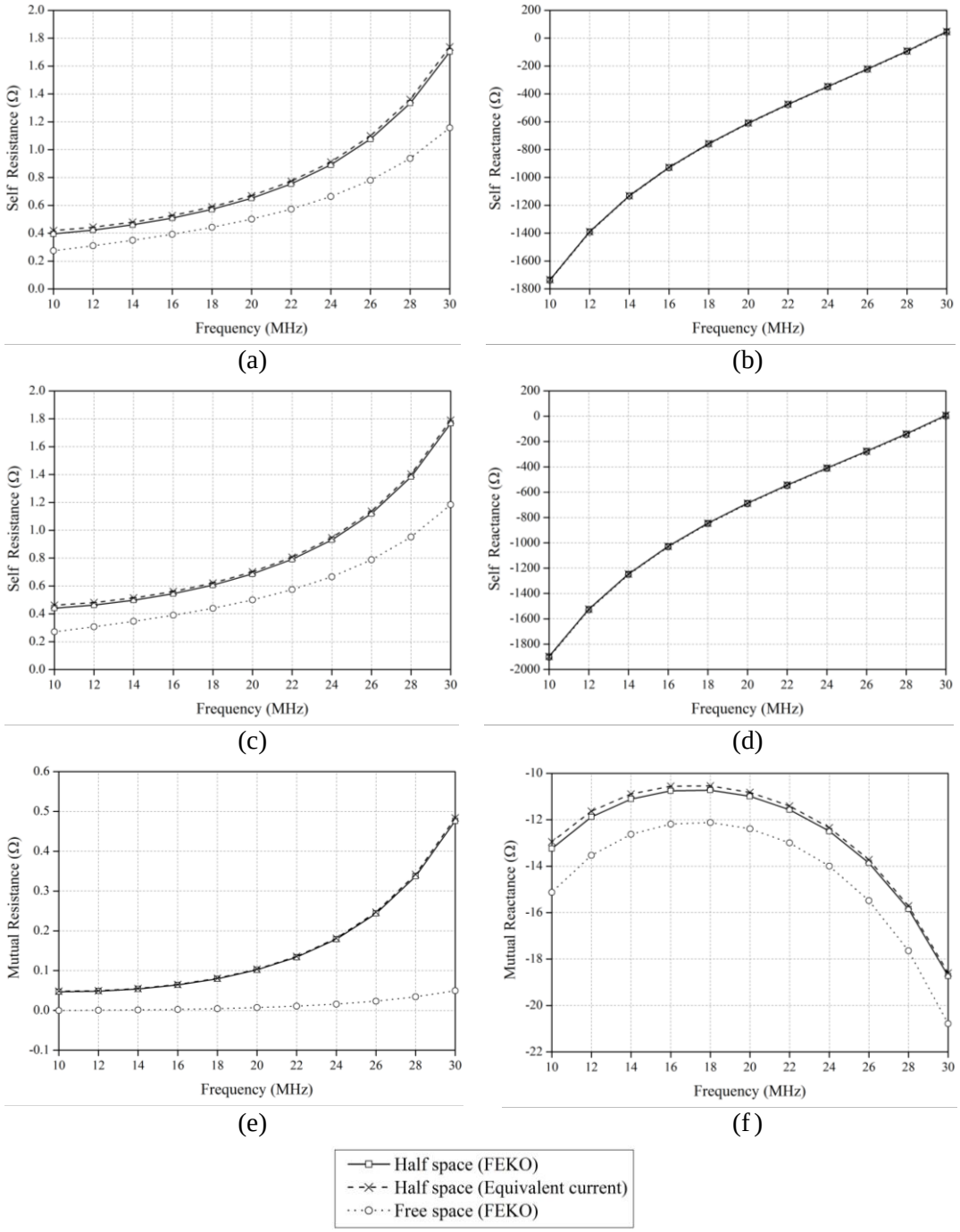

Figure 4.16 Impedance parameters between antenna 1 and antenna 2 in half space and free space. (a) real part of Z_{11} (b) imaginary part of Z_{11} (c) real part of Z_{22} (d) imaginary part of Z_{22} (e) real part of Z_{21} and Z_{12} (f) imaginary part of Z_{21} and Z_{12}.

Chapter 5

Analysis of Wireless Energy Transfer

5.1 Introduction

Over the last century, many people have attempted to transmit electrical energy without wires. In the late 19th and early 20th centuries, Nikola Tesla devoted much effort to transmitting electrical energy wirelessly. He insisted that he succeeded in transferring electrical energy over a long distance [35], but no one was able to reproduce his experiment, to the best of our knowledge. In the 1960s, Brown studied the wireless transmission of energy using microwave [36]. This technology can be used for long-range energy transfer, but it requires that there is no obstacle between the source and the device receiving the energy, and the device is to be tracked in the case of mobile devices. For short-range energy transfer, these drawbacks can be overcome by using near-field. Therefore, wireless energy transfer via near-field has received a considerable amount of attention for short-range energy transfer.

Several analytical models for wireless energy transfer via near-field have been proposed. Two of the most frequently used models to analyze wireless energy transfer are coupled mode theory [37] and equivalent circuits [38], [39]. These models typically require a solution of a boundary value problem in the presence of the detailed geometry of all antennas. Using these models, we cannot comprehensively understand the factors that affect the behavior of wireless energy transfer. Furthermore, these models are approximate. It may be desirable to describe wireless energy transfer in terms of an equation of closed-form using parameters of an isolated antenna. This can help us understand the factors that affect wireless energy transfer and design an efficient wireless energy transfer system. The theory presented in the previous chapter is suitable for this purpose.

A wireless energy transfer system can be viewed as a coupled antenna system because energy is transferred from antenna to antenna through a coupling phenomenon. Coupled antennas can be considered a network which is described by the impedance parameters, admittance parameters, or scattering parameters. These parameters can be calculated using the methods presented in the previous chapter. In this chapter, methods for analyzing wireless energy transfer are studied.

5.2 Maximum Power Transfer Efficiency and Optimum Load Impedance

One of the most important parameters in wireless energy transfer is the power transfer efficiency. The power transfer efficiency depends on the load impedance. In this section, formulas for calculating the load impedance for which the power transfer efficiency is maximized and the maximum power transfer efficiency from the impedance parameters are

derived.

Consider a wireless energy transfer system consisting of two antennas. Let one antenna be called antenna 1 and the other be called antenna 2. Let a load impedance Z_L be connected to the feed port of antenna 2, and let a source be connected to the feed port of antenna 1. In this dissertation, the power transfer efficiency (*PTE*) is defined as

$$PTE = \frac{P_L}{P_{in}} = \frac{\mathrm{Re}(Z_L)}{\mathrm{Re}(Z_i)}\left|\frac{Z_{21}}{Z_{22}+Z_L}\right|^2 \tag{5.1}$$

where P_L is the power delivered to a load, P_{in} is the power that enters the network, and Z_i is the impedance seen looking into an antenna at the feed port of antenna 1 in the presence of antenna 2. The power transfer efficiency is maximized at Z_L^{opt}, which satisfies the following equations:

$$\left.\frac{\partial PTE}{\partial \mathrm{Re}(Z_L)}\right|_{Z_L=Z_L^{opt}} = 0 \tag{5.2a}$$

$$\left.\frac{\partial PTE}{\partial \mathrm{Im}(Z_L)}\right|_{Z_L=Z_L^{opt}} = 0 \tag{5.2b}$$

$\mathrm{Re}(Z_L^{opt})$ and $\mathrm{Im}(Z_L^{opt})$ that satisfy the above equations are as follows:

$$\mathrm{Re}(Z_L^{opt}) = \sqrt{\mathrm{Re}(Z_{22})^2 - \frac{\mathrm{Re}(Z_{22})}{\mathrm{Re}(Z_{11})}\mathrm{Re}(Z_{12}Z_{21}) - \frac{\mathrm{Im}(Z_{12}Z_{21})^2}{4\,\mathrm{Re}(Z_{11})^2}} \tag{5.3a}$$

$$\mathrm{Im}(Z_L^{opt}) = \frac{\mathrm{Im}(Z_{12}Z_{21})}{2\,\mathrm{Re}(Z_{11})} - \mathrm{Im}(Z_{22}) \tag{5.3b}$$

where $\mathrm{Re}(Z_{11}) \neq 0$. Z_L^{opt} is called the optimum load impedance.

The maximum power transfer efficiency (PTE^{max}) is obtained by substituting (5.3a)

and (5.3b) into (5.1). The maximum power transfer efficiency is given by the following:

$$PTE^{max} = \frac{|X_2|^2}{2 - \mathrm{Re}(X_1 X_2) + \sqrt{4 - 4\,\mathrm{Re}(X_1 X_2) - \mathrm{Im}(X_1 X_2)^2}} \tag{5.4}$$

where

$$X_1 = \frac{Z_{12}}{\sqrt{\mathrm{Re}(Z_{11})\,\mathrm{Re}(Z_{22})}} \tag{5.5a}$$

$$X_2 = \frac{Z_{21}}{\sqrt{\mathrm{Re}(Z_{11})\,\mathrm{Re}(Z_{22})}} \tag{5.5b}$$

If a system is reciprocal, $Z_{12} = Z_{21}$. Therefore, equation (5.5) can be written as

$$PTE^{max} = \frac{|X|^2}{2 - \mathrm{Re}(X^2) + \sqrt{4 - 4\,\mathrm{Re}(X^2) - \mathrm{Im}(X^2)^2}} \tag{5.6}$$

where

$$X = \frac{Z_{21}}{\sqrt{\mathrm{Re}(Z_{11})\,\mathrm{Re}(Z_{22})}}\,. \tag{5.7}$$

5.3 Example

The author calculates the maximum power transfer efficiency and optimum load impedance of wireless energy transfer systems comprising two helical antennas. The antennas used in this section are the same as those used in Section 4.1.1.E. In one system, antenna 1 and antenna 2 were used. In this case, r varied from 60 cm to 150 cm, and θ, ϕ, ϕ_0, θ_0, and χ_0 were all equal to 0. In the other system, antenna 3 and antenna 4 were used. In this case, θ and ϕ were fixed at 40° and 90°, respectively, and r varied from 20 cm to

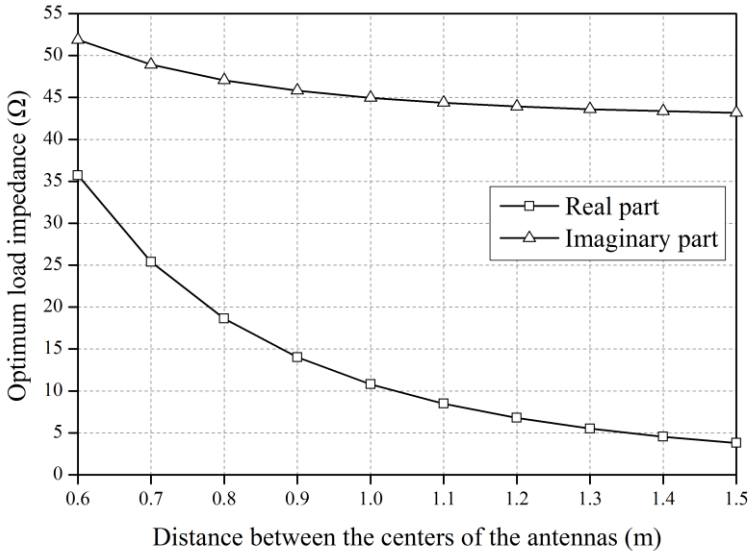

(a)

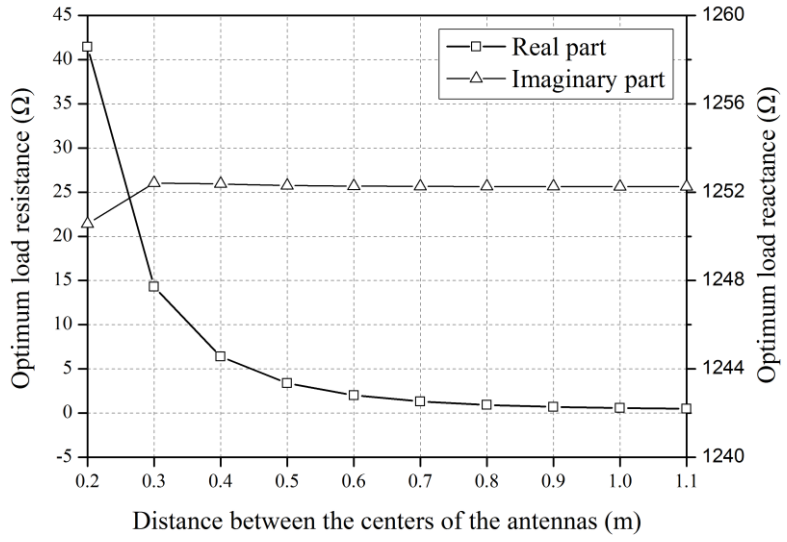

(b)

Figure 5.1 Optimum load impedance. (a) system comprising antenna 1 and antenna 2 (b) system comprising antenna 3 and antenna 4.

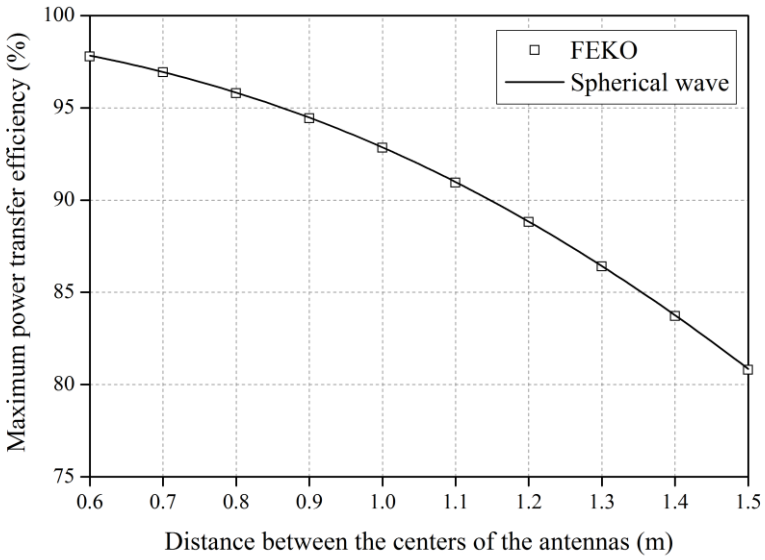

(a)

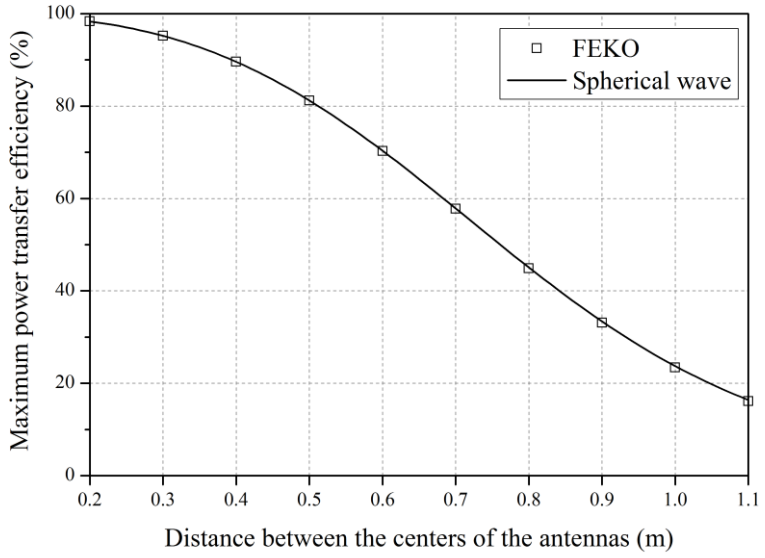

(b)

Figure 5.2 Maximum power transfer efficiency. (a) system comprising antenna 1 and antenna 2 (b) system comprising antenna 3 and antenna 4.

110 cm. $\phi_0 = 90°$, $\theta_0 = \theta$, and $\chi_0 = -90°$. Both systems operated at a frequency of 13.56 MHz.

Using equation (5.4), the author calculated the optimum load impedance from the Z-parameters obtained with FEKO for the two systems. Figure 5.1 shows the optimum load impedances. The author terminated the feed ports of antennas 2 and 4 with the optimum load impedance in the FEKO simulation and calculated the power transfer efficiency for the two systems. The author also computed the maximum power transfer efficiency using (5.6) and the Z-parameters obtained with (4.18) for the two systems. Figure 5.2 shows the maximum power transfer efficiency. The maximum power transfer efficiencies calculated using the two methods agree well.

5.4 Properties of Wireless Energy Transfer

In this section, we consider a reciprocal system. Let X in equation (5.7) be $X = x + iy$, where x and y are real. For PTE^{max} to be real, $-1 \le x \le 1$. Therefore, in the real world, the absolute value of x cannot be larger than one. When $x = \pm 1$, PTE^{max} becomes one. PTE^{max} is an even function of x and y.

Differentiate PTE^{max} with respect to x and y. Then,

$$\frac{\partial PTE^{\max}}{\partial x} = \frac{2x\sqrt{\frac{1+y^2}{1-x^2}}}{2-x^2+y^2+\sqrt{4\left(1-x^2\right)\left(1+y^2\right)}} \tag{5.8a}$$

$$\frac{\partial PTE^{\max}}{\partial y} = \frac{2y\sqrt{\frac{1-x^2}{1+y^2}}}{2-x^2+y^2+\sqrt{4\left(1-x^2\right)\left(1+y^2\right)}}. \tag{5.8b}$$

$\partial PTE^{max}/\partial x$ is positive when $x > 0$ and is negative when $x < 0$. Therefore, PTE^{max} increases as the absolute value of x increases if y is fixed ($|x| > 1$ is not considered). $\partial PTE^{max}/\partial y$ is positive when $y > 0$ and is negative when $y < 0$. Therefore, PTE^{max} increases as the absolute value of y increases if x is fixed.

The operating frequency for wireless energy transfer via near-field is usually below or near the lowest resonant frequency of the antennas. As explained in Chapter 3, at a frequency that is much smaller than the lowest resonant frequency, antennas can be modeled as canonical-minimum-scattering antennas. Moreover, some classes of antennas such as the helical antenna in Section 5.3 can be modeled as canonical-minimum-scattering antennas at the lowest resonant frequency. Therefore, we can assume that the antennas used in near-field wireless energy transfer are canonical-minimum-scattering antennas.

Impedance parameters between two canonical-minimum-scattering antennas in free space are represented by equation (4.18). The reference impedance is arbitrary. Here, the reference impedance is chosen so that the reflection coefficient is zero (i.e., the reference impedance is equal to the complex conjugate of the input impedance of an antenna). Then, the Z-parameters are as follows:

$$Z_{11} = Z_{A1} \tag{5.9a}$$

$$Z_{22} = Z_{A2} \tag{5.9b}$$

$$Z_{21} = Z_{12} = \sqrt{\mathrm{Re}(Z_{A1})\,\mathrm{Re}(Z_{A2})}\,\mathbf{R}_2\mathbf{G}^{+}\mathbf{T}_1 \tag{5.9c}$$

From (5.9) and (5.7), X in (5.6) becomes

$$X = \mathbf{R}_2\mathbf{G}^{+}\mathbf{T}_1 . \tag{5.10}$$

To increase the maximum power transfer efficiency, we should make the absolute value of X large by choosing $\mathbf{R}_2$ and $\mathbf{T}_1$ accordingly.

Intuitively, one would expect that the maximum power transfer increases as the radiation efficiency of an antenna increases if the field patterns and positions of the antennas are fixed. This is because the loss in the antenna decreases as the radiation efficiency increases. Here, the author will show this property using a mathematical method. Let the ith entry of the modal transmitting pattern $\mathbf{T}$ of an antenna be T_i. When an incident power wave with a coefficient of one is excited at a feed port of an antenna, the time-average power radiated by the antenna is $\frac{1}{2}\sum_i |T_i|^2$ from equation (2.6). Hence, if the reflection coefficient is zero, the radiation efficiency of the antenna is $\sum_i |T_i|^2$. The modal receiving pattern $\mathbf{R}$ can be determined from $\mathbf{T}$ using (2.14). Therefore, if the shape of the field pattern is fixed[11], the absolute values of the entries of $\mathbf{T}$ and $\mathbf{R}$ increase with the radiation efficiency of the antenna. If the positions of the antennas are fixed, the entries in $\mathbf{G}^{+}$ are constant. Therefore, if the shape of the field patterns and positions of the antennas are fixed, the maximum power transfer efficiency increases as the radiation efficiency increases.

[11] This means that the magnitude and phase of the normalized electromagnetic field do not change when the electromagnetic field is normalized so that the maximum magnitude of the electromagnetic field is constant.

Fig. 6 in reference [40] shows a graph of the maximum power transfer efficiency between two identical CMS antennas that generate TE_{01} mode or TM_{01} mode as a function of the wavelength for various radiation efficiencies. In this figure, we can identify that the maximum power transfer efficiency increases with the radiation efficiency. Using equations (5.6) and (5.10), we can find the relation among the maximum power transfer efficiency, radiation efficiency and distance between two antennas for general CMS antennas that generate arbitrary spherical waves. One key factor for increasing the maximum power transfer efficiency is the radiation efficiency of the antenna. Therefore, to design an efficient wireless energy transfer system, we should attempt to design an antenna with a high radiation efficiency.

From equation (5.10), we know that only the modal transmitting pattern of an antenna is required to calculate the maximum power transfer efficiency. The modal transmitting pattern contains information about the shape of the field pattern and the radiation efficiency of an antenna but does not contain information about the shape of the antenna. Therefore, we do not need to know the shapes of the antennas to investigate the maximum power transfer efficiency of a wireless energy transfer system. In fact, to calculate a modal transmitting pattern, we need the shape of the antenna. However, we can guess the approximate shape of the field pattern of many small antennas.

Chapter 6

Conclusion

This dissertation proposed analytical models for scattering by an antenna and coupling among antennas. The scattering properties of an antenna were analyzed using the theory of characteristic modes. The current of a loaded antenna was expanded into characteristic currents of a short-circuited antenna. When an antenna is very small compared with the wavelength of the incident electromagnetic field, the antenna rarely scatters unless the load reactance is close to the negative of the input reactance because the absolute values of all eigenvalues are very large. Therefore, such an antenna can be modeled as a minimum scattering antenna. When the current and the input impedance of an antenna are determined using only one characteristic mode, the open-circuited antenna rarely scatters the electromagnetic field because the current component of a transmitting antenna cancels the component of a short-circuited antenna. Therefore, such an antenna can be modeled as a canonical minimum scattering antenna. When one or several

eigenvalues are close to zero, a short-circuited antenna scatters well. When an antenna is not dominated by a single characteristic mode and the absolute value of the input impedance is very large, an open-circuited antenna scatters well.

In this dissertation, several methods for analyzing mutual coupling among antennas were proposed. First, a method for calculating the impedance parameters, admittance parameters, and electromagnetic field using a generalized scattering matrix was proposed. This method can be applied to antennas near objects as well as in free space. Using this method, only the parameters of an isolated antenna are required. Moreover, we do not need to know the detailed geometries of the antennas. If a minimum sphere enclosing an antenna overlaps with objects or a minimum sphere enclosing another antenna, this method cannot be used to calculate the impedance parameters, admittance parameters, and electromagnetic field. Second, a method for calculating the impedance parameters among antennas near objects using the current distribution of the antennas was proposed. For this method, when antennas are canonical minimum scattering antennas, only the current distributions of isolated transmitting antennas are required to calculate the impedance parameters. Third, a method for calculating the impedance parameters using equivalent currents that generate the same field as that generated by an antenna was proposed. If the equivalent currents are simple, the impedance parameters can be simply calculated using this method.

The models for scattering and coupling proposed in this dissertation were applied to the analysis of wireless energy transfer via the near field. Many antennas used in wireless energy transfer systems via the near field can be modeled as minimum scattering antennas

because such systems operate at a frequency below or near the lowest resonant frequency of the antennas. The maximum power transfer efficiency of a wireless energy transfer system and the load impedance that maximizes the power transfer efficiency were derived from the impedance parameters. A method to increase the maximum power transfer efficiency was explained. If the shapes of the field patterns and the positions of the antennas are fixed, the maximum power transfer efficiency increases with the radiation efficiency of the antennas. Using the method presented in this dissertation, we can calculate the maximum power transfer efficiency using only the field patterns and radiation efficiency of the antennas (if the antennas are canonical minimum scattering antennas). Therefore, we do not need to know the detailed shapes of the antennas to calculate the maximum power transfer efficiency. The theory presented in this dissertation may be helpful to understanding the characteristics of wireless energy transfer.

Appendix

An addition theorem expresses wave functions in one coordinate system in terms of wave functions in another coordinate system. Coordinate system 2 is translated from coordinate system 1 by **r**, as shown in Figure 4.1. $\mathbf{r}_1$ and $\mathbf{r}_2$ are position vectors with respect to coordinate system 1 and coordinate system 2, respectively. The wave functions in coordinate system 1 and the wave functions in coordinate system 2 are related through the following equation:

$$\mathbf{M}_{mn}^{(c)}(\mathbf{r}_1) = \sum_{\nu=1}^{\infty} \sum_{\mu=-\nu}^{\nu} \left[A_{\mu\nu,mn}^{(c)}(\mathbf{r}) \mathbf{M}_{\mu\nu}^{(1)}(\mathbf{r}_2) + B_{\mu\nu,mn}^{(c)}(\mathbf{r}) \mathbf{N}_{\mu\nu}^{(1)}(\mathbf{r}_2) \right] \tag{A.1a}$$

$$\mathbf{N}_{mn}^{(c)}(\mathbf{r}_1) = \sum_{\nu=1}^{\infty} \sum_{\mu=-\nu}^{\nu} \left[A_{\mu\nu,mn}^{(c)}(\mathbf{r}) \mathbf{N}_{\mu\nu}^{(1)}(\mathbf{r}_2) + B_{\mu\nu,mn}^{(c)}(\mathbf{r}) \mathbf{M}_{\mu\nu}^{(1)}(\mathbf{r}_2) \right] \tag{A.1b}$$

for $|\mathbf{r}_2| < |\mathbf{r}|$ and

$$\mathbf{M}_{mn}^{(c)}(\mathbf{r}_1) = \sum_{\nu=1}^{\infty} \sum_{\mu=-\nu}^{\nu} \left[A_{\mu\nu,mn}^{(1)}(\mathbf{r}) \mathbf{M}_{\mu\nu}^{(c)}(\mathbf{r}_2) + B_{\mu\nu,mn}^{(1)}(\mathbf{r}) \mathbf{N}_{\mu\nu}^{(c)}(\mathbf{r}_2) \right] \tag{A.2a}$$

$$\mathbf{N}_{mn}^{(c)}(\mathbf{r}_1) = \sum_{\nu=1}^{\infty} \sum_{\mu=-\nu}^{\nu} \left[A_{\mu\nu,mn}^{(1)}(\mathbf{r}) \mathbf{N}_{\mu\nu}^{(c)}(\mathbf{r}_2) + B_{\mu\nu,mn}^{(1)}(\mathbf{r}) \mathbf{M}_{\mu\nu}^{(c)}(\mathbf{r}_2) \right] \tag{A.2b}$$

for $|\mathbf{r}_2| > |\mathbf{r}|$, where

$$A_{\mu\nu,mn}^{(c)}(\mathbf{r}) = (-1)^{\mu}\left(\frac{m-\mu}{|m-\mu|}\right)^{m-\mu}\frac{j^{\nu-n}}{2}\sqrt{\frac{(2n+1)(2\nu+1)}{n(n+1)\nu(\nu+1)}}e^{j(m-\mu)\phi}$$
$$\sum_{p=|n-\nu|}^{n+\nu}\left\{j^{p}(2p+1)\left[n(n+1)+\nu(\nu+1)-p(p+1)\right]\cdot\right.$$
$$\sqrt{\frac{(p-|m-\mu|)!}{(p+|m-\mu|)!}}\begin{pmatrix} n & \nu & p \\ 0 & 0 & 0\end{pmatrix}\begin{pmatrix} n & \nu & p \\ m & -\mu & \mu-m\end{pmatrix}\cdot \tag{A.3a}$$
$$\left.\mathrm{z}_{p}^{(c)}(kr)\mathrm{P}_{p}^{|m-\mu|}(\cos\theta)\right\}$$

$$B_{\mu\nu,mn}^{(c)}(\mathbf{r}) = (-1)^{\mu}\left(\frac{m-\mu}{|m-\mu|}\right)^{m-\mu}\frac{j^{\nu-n}}{2}\sqrt{\frac{(2n+1)(2\nu+1)}{n(n+1)\nu(\nu+1)}}e^{j(m-\mu)\phi}$$
$$\sum_{p=|n-\nu|+1}^{n+\nu-1}\left\{j^{p}(2p+1)\cdot\right.$$
$$\sqrt{(n+\nu+1+p)(n+\nu+1-p)(n-\nu+p)(\nu-n+p)}\cdot \tag{A.3b}$$
$$\sqrt{\frac{(p-|m-\mu|)!}{(p+|m-\mu|)!}}\begin{pmatrix} n & \nu & p-1 \\ 0 & 0 & 0\end{pmatrix}\begin{pmatrix} n & \nu & p \\ m & -\mu & \mu-m\end{pmatrix}\cdot$$
$$\left.\mathrm{z}_{p}^{(c)}(kr)\mathrm{P}_{p}^{|m-\mu|}(\cos\theta)\right\}$$

Here, $\left((m-\mu)/|m-\mu|\right)^{m-\mu}$ is defined as 1 when $m-\mu=0$, and $\begin{pmatrix} j_1 & j_2 & j_3 \\ m_1 & m_2 & m_3\end{pmatrix}$ is the Wigner 3-j symbol [41]. Function $A_{l'm',lm}$ in [33, p. 595] was modified to obtain $A_{\mu\nu,mn}^{(c)}$, and function $B_{\mu\nu}^{mn}$ in [42] was modified to obtain $B_{\mu\nu,mn}^{(c)}$.

Coordinate system 3 is rotated from coordinate system 2 (Figure 4.1). The rotation of the coordinate system is expressed using the Euler angles (χ_0, θ_0, ϕ_0) [2, Appendix A2]. Let $\mathbf{r}_3$ be the position vector with respect to coordinate system 3. The relation between the wave functions in coordinate system 2 and the wave functions in coordinate system 3 is expressed as follows:

$$\mathbf{M}_{mn}^{(c)}(\mathbf{r}_2) = \sum_{\mu=-n}^{n} D_{\mu m}^{n}(\chi_0, \theta_0, \phi_0)\mathbf{M}_{\mu n}^{(c)}(\mathbf{r}_3) \tag{A.4a}$$

$$\mathbf{N}_{mn}^{(c)}(\mathbf{r}_2) = \sum_{\mu=-n}^{n} D_{\mu m}^{n}(\chi_0, \theta_0, \phi_0)\mathbf{N}_{\mu n}^{(c)}(\mathbf{r}_3) \tag{A.4b}$$

where

$$D_{\mu m}^{n}(\chi_0, \theta_0, \phi_0) = (-1)^{m-\mu} e^{jm\phi_0} d_{\mu m}^{n}(\theta_0) e^{j\mu\chi_0} \tag{A.5}$$

with $d_{\mu m}^{n}(\theta_0)$ defined as in [2, p. 345]. The reason that the sign of $D_{\mu m}^{n}$ in (A.5) is different from the sign of $D_{\mu m}^{n}$ in [2] is that the wave functions used in this dissertation and [2] are different.

Bibliography

[1] D. M. Kerns, *Plane-Wave Scattering-Matrix Theory of Antennas and Antenna-Antenna Interactions*, Washington, USA: U.S. Government Printing Office 1981.

[2] J. E. Hansen, *Spherical Near-field Antenna Measurements*, London, U.K.: Peregrinus, 1988

[3] J. Rubio, M. A. Gaonzalez, and J. Zapata, "Generalized-scattering-matrix analysis of a class of finite arrays of coupled antennas by using 3-D FEM and spherical mode expansion," *IEEE Trans. Antennas Propag*., vol. 53, no. 3, pp. 1133–1144, Mar. 2005.

[4] R. J. Pirkl, "Spherical wave scattering matrix description of antenna coupling in arbitrary environments," *IEEE Trans. Antennas and Propag*., vol. 60, no.12, pp. 5654–5662, Dec. 2012.

[5] W. Wasylkiwskyj and W. K. Kahn, "Scattering properties and mutual coupling of antennas with prescribed radiation pattern," *IEEE Trans. Antennas Propag*., vol. 18, no. 6, pp. 741-752, Nov. 1970.

[6] R.S. Elliott, *Antenna theory and design*, Revised Edition, Hoboken, N.J., USA: A John Wiley & Sons, 2003, ch. 7.

[7] W. Wasylskyj and W. K. Kahn, "Theory of mutual coupling among minimum-scattering antennas," *IEEE Trans. Antennas and Propag*., vol. 18, no. 2, pp. 204–216, Mar. 1970.

[8] R. F. Harrington, *Time-Harmonic Electromagnetic Fields*, New York, USA: McGraw-Hill, 1961.

[9] L.-W. Li, X.-K. Kang, and M.-S. Leong, *Spheroidal Wave Functions in Electromagnetic Theory*, New York, USA: John Wiley & Sons, 2002.

[10] M. Abramowitz and I. A. Stegun, *Handbook of Mathematical Functions*, New York, USA: Dover, 1965, ch. 8.

[11] J. A. Stratton, *Electromagnetic Theory*, New York, USA: McGraw-Hill, 1941, ch. 7.

[12] R. B. Marks and D. F. Williams, "A general waveguide circuit theory," *J. Res. Nat. Inst. Standards Technol.*, vol. 97, no. 5, pp. 533–562, Sep.–Oct. 1992.

[13] J. Rahola, "Power waves and conjugate matching," *IEEE Trans. Circuit and sys-II.*, vol. 55, no. 1, pp. 92–96, Jan. 2008.

[14] D. M. Pozar, *Microwave Engineering*, 4th ed., New York, USA: John Wiley & Sons, 2012, p. 186

[15] A. Z. Elsherben, and A. A. Kishk, "Modeling of cylindrical objects by circular dielectric and conducting cylinders," *IEEE Trans. Antennas Propag.*, vol. 40, no. 1, pp. 96–99, Jan. 1992.

[16] E. Martini, G. Carli, and S. Maci, "A domain decomposition method based on a generalized scattering matrix formalism and a complex source expansion," *Progress Electromagn. Res. B*, vol. 19, pp. 445–473, 2010.

[17] R. J. Garbacz, "Modal expansions for resonance scattering phenomena," *Proc. IEEE*, vol. 53, pp. 856–864, Aug. 1965.

[18] R. F. Harrington and J. R. Mautz, "Theory of characteristic modes for conducting bodies," *IEEE Trans. Antennas Propag.*, vol. 19, no. 5, pp. 622–628, Sep. 1971.

[19] R. F. Harrington and J. R. Mautz, "Computation of characteristic modes for conducting bodies," *IEEE Trans. Antennas Propag.*, vol. 19, no. 5, pp. 629–639, Sep. 1971.

[20] J. Demmel, “Generalized Hermitian Eigenproblems (Section 2.3),” In Z. Bai, J. Demmel, J. Dongarra, A. Ruhe, and H. van der Vorst, editors, *Templates for the Solution of Algebraic Eigenvalue Problems: A Practical Guide*, p. 15, SIAM, Philadelphia, 2000

[21] Z. Bai, T. Ericsson, and T. Kowalski, “Symmetric Indefinite Lanczos Method (Section 8.6),” In Z. Bai, J. Demmel, J. Dongarra, A. Ruhe, and H. van der Vorst, editors, *Templates for the Solution of Algebraic Eigenvalue Problems: A Practical Guide*, p. 250, SIAM, Philadelphia, 2000

[22] R. F. Harrington, J. R. Mautz, and Y. Chang, “Characteristic modes for dielectric and magnetic bodies,” *IEEE Trans. Antennas Propag.*, vol. 20, no. 2, pp. 194–198, Mar. 1972.

[23] R. E. Collin and F. J. Zucker, *Antenna Theory, Volume I*, New York, USA: McGraw-Hill Book Company, 1969, Chapter 4.

[24] R. E. Collin, “Limitations of the Thevenin and Norton Equivalent Circuits for a Receiving Antenna,” *IEEE Antennas Propagat. Mag.*, vol. 45, no. 2, pp. 119–124, Apr. 2013.

[25] A. Alu, “Power relations and a consistent analytical model for receiving wire antennas,” *IEEE Trans. Antennas Propag.*, vol. 58, no. 5, pp. 1436–1448, May. 2010.

[26] R. F. Harrington, *Field Computation by Moment Methods*, New York, USA: MacMillan, 1968.

[27] W. K. Kahn and H. Kurss, “Minimum-scattering antennas,” *IEEE Trans. Antennas Propag.*, vol. 13, no.5, pp. 671–675, Sep. 1965.

[28] S. M. Rao, D. R. Wilton, and A. W. Glisson, “Electromagnetic Scattering by Surfaces of Arbitrary Shape,” *IEEE Trans. Antennas Propagat*, vol. 30, no. 3, pp. 409–418, May. 1982.

[29] E. Martini, G. Carli, and S. Maci, "An equivalence theorem based on the use of electric currents radiating in free space," *IEEE Antennas Wireless Propag. Lett.*, vol. 7, pp. 421–424, 2008.

[30] E. C. Jordan and K.G. Balmain, *Electromagnetic Waves and Radiating Systems*, 2nd ed., Englewood Cliffs, USA: Prentice-Hall, 1968.

[31] S. M. Mikki and A. A. Kishk, "Quantum particle swarm optimization for electromagnetics," *IEEE Trans. Antennas Propag.*, vol. 54, no. 10, pp. 2764–2775, Oct. 2006.

[32] A. Ishimaru, *Electromagnetic Wave Propagation, Radiation, and Scattering*, Englewood Cliffs, USA: Prentice-Hall, 1991, Ch. 15.

[33] W. C. Chew, *Waves and Fields in Inhomogeneous Media*, New York, USA: IEEE Press, 1995.

[34] J. R. Wait, *Electromagnetic Waves in Stratified Media*, New York, USA: IEEE Press, 1996.

[35] N. Tesla, *The problem of Increasing Human Energy*, New York, USA: Cosimo, 2007.

[36] W. C. Brown, "The history of power transmission by radio waves," *IEEE Trans. Microw. Theory Techn.*, vol. 32, no. 9, pp. 1230-1242, Sep. 1984.

[37] A. Karalis, J. D. Joannopoulos, and M. Soljacic, "Efficient wireless non-radiative mid-range energy transfer," *Ann. Phys.*, vol. 323, no. 1, pp. 34-48, Jan. 2008.

[38] P. Sample, T. Meyer, and R. Smith, "Analysis, experimental result, and range adaptation of magnetically coupled resonators for wireless power transfer," *IEEE Trans. Ind. Electron.*, vol. 58, no. 2, pp. 544-554, Feb. 2011

[39] T. Imura and Y. Hori, "Maximizing air gap and efficiency of magnetic resonant coupling for wireless power transfer using equivalent circuit and Neumann formula," *IEEE Trans. Ind. Electron.*, vol. 58, no. 10, pp. 4746–4752, Oct. 2011.

[40] J. Lee and S. Nam “Fundamental aspects of near-field coupling small antennas for wireless power transfer,” *IEEE Trans. Antennas Propag*., vol. 58, no. 11, pp. 3442-3449, Nov. 2010.

[41] A. R. Edmonds, *Angular Momentum in Quantum Mechanics*, 2nd ed., Princeton: Princeton University Press, 1974, ch. 3.

[42] L. Tsang and J. A. Kong, “Effective propagation constants for coherent electromagnetic wave propagation in media embedded with dielectric scatters,” *J. Appl. Phys*, vol. 53, no. 11, pp. 7162–7173, Nov. 1982.

한글 초록

본 논문은 안테나에 의한 산란과 안테나들 사이의 결합을 해석하는 방법을 제안한다. 특성 모드 이론을 이용하여 안테나의 산란 특성을 해석한다. 부하가 달린 안테나에 흐르는 전류는 단락된 안테나의 특성 전류의 선형 조합으로 표현된다. 안테나의 크기가 입사 전자기장의 파장에 비해 매우 작을 때, 부하 리액턴스가 안테나의 입력 리액턴스의 음수 값에 가깝지 않으면 안테나가 거의 산란하지 않는다. 따라서 파장에 비해 작은 안테나를 최소 산란 안테나로 가정할 수 있다. 안테나의 전류와 입력 임피던스를 하나의 특성 전류만을 사용하여 계산할 수 있을 때, 개방된 안테나는 거의 산란하지 않는다. 따라서 이러한 안테나를 표준 최소 산란 안테나로 가정할 수 있다.

결합된 안테나들의 포트들에 있는 전압과 전류는 임피던스 파라미터를 사용하여 계산할 수 있다. 본 논문은 결합된 안테나들 사이의 임피던스 파라미터를 계산하는 세 가지 방법을 제안한다. 첫 번째 방법은 일반 산란 행렬을 이용하여 계산하는 방법이고, 두 번째 방법은 안테나에 흐르는 전류 분포를 이용하여 계산하는 방법이고, 세 번째 방법은 안테나가 만드는 전자기장과 똑같은 전자기장을 만드는 등가 전류를 이용하여 계산하는 방법이다. 또한 결합된 안테나들에 전자기장이 입사하거나 안테나들의 포트들에 전원이 인가될 때, 일반 산란 행렬을 이용하여 결합된 안테나들이 만드는 전자기장을 계산하는 방법을

제안한다. 이 방법들은 안테나가 자유 공간에 있을 때뿐만 아니라 안테나 주변에 물질이 있을 때에도 사용될 수 있다. 만약에 안테나가 최소 산란 안테나이면 임피던스 파라미터와 전자기장의 계산이 간단해진다.

본 논문에서 제안된 안테나의 산란과 결합 이론을 무선 에너지 전송을 해석하는데 적용한다. 근접장을 이용한 무선 에너지 전송에 사용되는 많은 안테나들을 최소 산란 안테나로 가정할 수 있다. 왜냐하면 대부분의 근접장을 이용한 무선 에너지 전송은 안테나들의 공진주파수보다 작은 주파수 또는 공진주파수 근처의 주파수에서 동작하기 때문이다. 본 논문에서는, 임피던스 파라미터로부터 무선 에너지 전송 시스템의 에너지 전송 효율의 최대값과 에너지 전송 효율이 최대가 되는 부하 임피던스를 계산하는 공식을 유도한다.

주요어 : 안테나 결합, 안테나 산란, 일반 산란 행렬, 특성 모드 이론,
무선 에너지 전송

학번 : 2011－30221